October 2019

Metabolic cost of asymmetrical walking: preferred step time asymmetry optimizes metabolic cost of walking

Jan Stenum

Recommended Citation

Stenum, Jan, "Metabolic cost of asymmetrical walking: preferred step time asymmetry optimizes metabolic cost of walking" (2019). *Doctoral Dissertations*. 1766.
https://scholarworks.umass.edu/dissertations_2/1766

Metabolic cost of asymmetrical walking:
preferred step time asymmetry optimizes metabolic cost of walking

A Dissertation Presented

by

JAN STENUM

Submitted to the Graduate School of the
University of Massachusetts Amherst in partial fulfillment
of the requirements for the degree of

DOCTOR OF PHILOSOPHY

September 2019

Kinesiology

Metabolic cost of asymmetrical walking:
preferred step time asymmetry optimizes metabolic cost of walking

A Dissertation Presented

by

JAN STENUM

Approved as to style and content by:

Julia T. Choi, Chair

Brian R. Umberger, Member

Richard E. A. van Emmerik, Member

Young-Hui Chang, Member

Jane Kent, Department Chair
Department of Kinesiology

ACKNOWLEDGEMENTS

I am grateful to my doctoral advisor Dr Julia T. Choi for supporting me and letting me pursue some questions for the present dissertation that I thought were interesting and that she challenged me to try to make more interesting. Throughout the last 5 years it has been an exciting undertaking to absorb from Julia as much knowledge as I have had the capacity to acquire.

I am thankful for the advise and suggestions that I have received from my dissertation committee members Drs Brian R. Umberger, Richard E. A. van Emmerik and Young-Hui Chang which I believe have improved this work a lot. Apart from his role on my dissertation committee, I also want to thank Richard for putting me in contact with Julia back in 2014 which allowed me to come to Amherst and pursue a doctoral degree.

Members of the Locomotion Neuromechanics Laboratory Dr Gabriella Borin, Daniel Gregory, Sumire Sato and Dane Napoli have kindly listened to me talk ad naseum about this research and I have benefited by them allowing me to do so.

I owe a special thanks to Jacob Banks for keeping me company in the sometimes otherwise deserted room 6 in the basement of Totman; most importantly for the work I am presenting here, I am grateful to Jake for generously spending his time and using his expertise to help me with a crucial piece of my project by setting up the real-time feedback that allowed me to enforce step time asymmetry—thanks Jake!

My experiments were quite demanding and required that the volunteers who enrolled came to the laboratory for several visits with many hours of treadmill walking. I am therefore thankful for the commitment of all the volunteers that enrolled in my studies. Similarly, I am grateful for the many hours that the undergraduate students Cameron Vigliotta and Peter Murphy spent volunteering as pilot subjects while I refined the experimental protocols.

I am grateful to the UMASS Graduate School, the School of Public Health and Health Sciences, the Department of Kinesiology and the American Society of Biomechanics for providing various types of funding for this project.

Last, but certainly not least, I would like to thank the staff at the Department of

Kinesiology's main office—especially Charlene Galica and Meredith Kern—for working hard to help me and the other graduate students navigate the administrative milestones from enrollment to graduation.

ABSTRACT

METABOLIC COST OF ASYMMETRICAL WALKING:
PREFERRED STEP TIME ASYMMETRY
OPTIMIZES METABOLIC COST OF WALKING

SEPTEMBER 2019

JAN STENUM, BSC, UNIVERSITY OF COPENHAGEN
MSC, UNIVERSITY OF COPENHAGEN
PHD, UNIVERSITY OF MASSACHUSETTS AMHERST
Directed by: Professor Julia T. Choi

Hemiparetic and amputee walking often has asymmetrical step lengths and step times, and it is metabolically costlier than symmetrical able-bodied walking. Consequently, asymmetry has been suggested to account for the greater energy expenditure, but the metabolic cost of asymmetrical walking is poorly understood. Conversely, even though symmetry is metabolically optimal in able-bodied walking, it is also possible that *asymmetrical* gait parameters may be selected if they are optimal under imposed constraints. First, to understand the metabolic cost of asymmetry, we performed experiment 1 in which we recruited 10 able-bodied subjects to walk with a range of different combinations of asymmetrical step lengths and step times on a normal treadmill at 1.25 m s^{-1}. We found that the metabolic cost of step time asymmetry was more than twice the cost of step length asymmetry, but that the costs were not additive. Rather, the metabolic cost of walking with concurrent asymmetry in step lengths and step times was best explained by the cost of step time asymmetry alone. Second, to understand if asymmetrical gait parameters may be selected if they are energetically optimal, we performed experiment 2 in which we recruited 10 able-bodied subjects to walk with a range of different combinations of asymmetrical step lengths and step times on a split-belt treadmill in 3 conditions with speed-differences of 0.5 m s^{-1}, 1.0 m s^{-1} and 1.5 m s^{-1} at an average speed of 1.25 m s^{-1}. Across all speed-difference conditions, we found that subjects preferred to use asymmetrical step times that were energetically optimal, but that the preferred asymmetry in step lengths was sub-optimal. Overall, our results suggest that step time asymmetry is more effective than step length asymmetry to induce changes to metabolic cost and that symmetry is not necessarily energetically optimal. Instead, *asymmetry* in step times may be preferred when it is energetically optimal. Our results are based on asymmetry imposed on able-bodied walking and future research may test how the results generalize to other types of gait asymmetry in order to understand the implications for gait rehabilitation in which the goal often is to achieve a more symmetrical walking pattern.

CONTENTS

Page

CHAPTER

APPENDICES

LIST OF TABLES

Table **Page**

LIST OF FIGURES

CHAPTER 1

INTRODUCTION

1.1 Background and motivation

1.1.1 Optimization of human movement

The control of human movement is redundant: we can complete a task using an uncountable number of movement patterns and combinations of muscles (Bernstein, 1967). But what explains why a single action is performed from the many available? Theoretically, redundancy can be solved by selection based on optimality principles (Scott, 2004; Todorov, 2004). Optimality principles rely on an optimal control law based on state estimation of the system. This computational approach can predict many different types of behaviors and motor actions, for example: arm movement trajectories (Todorov & Jordan, 2002), saccadic eye movements (Harris & Wolpert, 1998), muscle activity following standing perturbations (Lockhart & Ting, 2007), kinematics, kinetics and muscle activity for walking (Anderson & Pandy, 2001) and running (Miller et al., 2012) and the transition between walking and running (Srinivasan & Ruina, 2006).

Within optimal control theory, it is not clear what is being optimized to select the appropriate muscle activations. For human locomotion, there is evidence that people exploit the redundancy of the locomotor system to minimize metabolic cost. Characteristic locomotor behaviors such as preferred walking speed (Ralston, 1958), the combination of stride length and time (Cavanagh & Williams, 1982; Zarrugh & Radcliffe, 1978) and the walk-run transition speed (Margaria et al., 1963) appear to coincide with the energetically optimal solutions. It is, however, debatable whether minimizing metabolic cost is the primary goal, or whether energy optimization is a byproduct of other processes which happen to be energetically optimal. Furthermore, it is not clear how optimality is implemented for the flexibility required of the locomotor system as it contends with everchanging environments, tasks and physiology.

1.1.2 Metabolic cost of human locomotion

Humans prefer to walk at slow speeds and transition to running at a speed around 2.0 m s^{-1} (Thorstensson & Roberthson, 1987). Although humans can use a range of walking speeds (Bornstein & Bornstein, 1976) people often choose a preferred speed of around 1.25 m s^{-1} (Ralston, 1958).

In a complete stride cycle, each leg is either in contact with the ground, during the stance phase, or swings forward, in the swing phase. In walking, the stance phase is about 60% of the stride cycle, so that at least one foot is in contact with the ground at any time (Perry & Burnfield, 2010). The stance phase begins and ends with a double support period, in which both feet contact the ground, that each comprise about 10% of the stride cycle.

Center of mass mechanics in walking can be described by pendular dynamics in which kinetic and potential energy oscillate out-of-phase. Therefore, changes in mechanical energy are minimized which reduces the need for mechanical work performed on the center of mass (Cavagna et al., 1977). During level walking, the net mechanical work performed on the center of mass across the stride cycle is zero. Even so, the center of mass loses mechanical energy at the legs' collisions with the ground (Ruina et al., 2005; Donelan et al., 2002b). The collisional losses must be compensated by positive mechanical work throughout the stride cycle, which, in turn, exacts a metabolic cost in walking (Donelan et al., 2002a).

Basic kinematic parameters, such as speed, stride length and stride time, can predict the metabolic cost of walking. Metabolic energy rate increases quadratically with speed (Ralston, 1958), but if metabolic cost is expressed as the metabolic cost per distance traveled, the relationship between cost and walking speed is U-shaped (Fig. 1.1A). Furthermore, at a given speed, metabolic cost can be predicted from the

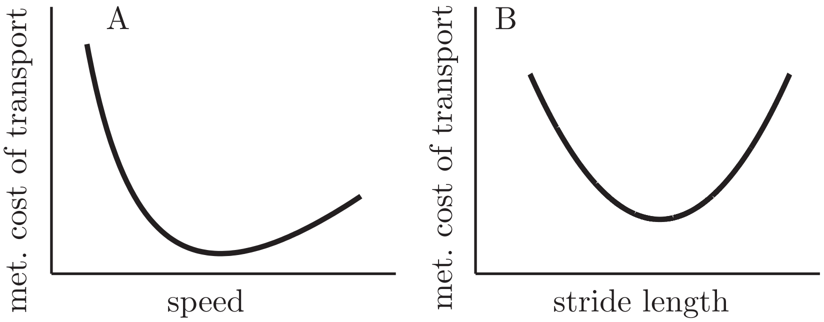

Figure 1.1: Metabolic cost and basic kinematics of walking. Metabolic costs of transport (cost per distance traveled) has a U-shaped relationship with walking speed (A) and stride length when walking at a fixed speed (B).

combinations of stride length and stride time, so that the relationship is U-shaped (Zarrugh & Radcliffe, 1978) (Fig. 1.1B).

What determines the metabolic cost of walking? The cost can be partitioned into costs of the stance and swing phase (Umberger, 2010). Costs incurred during the stance phase comprise the majority of the cost of the stride cycle (Marsh et al., 2004; Doke et al., 2005; Gottschall & Kram, 2005; Umberger, 2010). During step-to-step transitions (periods of the stride cycle that correspond to double support), the leading leg performs negative work on the center of mass (Donelan et al., 2002b). This negative work is termed a collisional loss of center of mass energy and has been proposed as the dominant loss of center of mass energy throughout the stride cycle (Ruina et al., 2005). Consequently, positive mechanical work must be performed to compensate for the losses, and, furthermore, the positive work has been proposed as a major determinant of the metabolic cost of walking (Donelan et al., 2002a). Even though positive center of mass work can be performed throughout the entire stance phase, in normal walking it is primarily performed by ankle plantarflexors of the trailing leg during step-to-step transitions (Kuo et al., 2005). From a simple walking model (Fig. 1.2A), the collisional losses of center of mass energy (W^{-}_{CO}) has been proposed to be proportional to the product of squared step length (l) and squared pre-transition velocity (instantaneous center of mass velocity at the onset of the step-to-step transition; v_{pre}) (Adamczyk & Kuo, 2009):

$$W^{-}_{CO} \propto l^2 * v^2_{pre}\,. \tag{1.1}$$

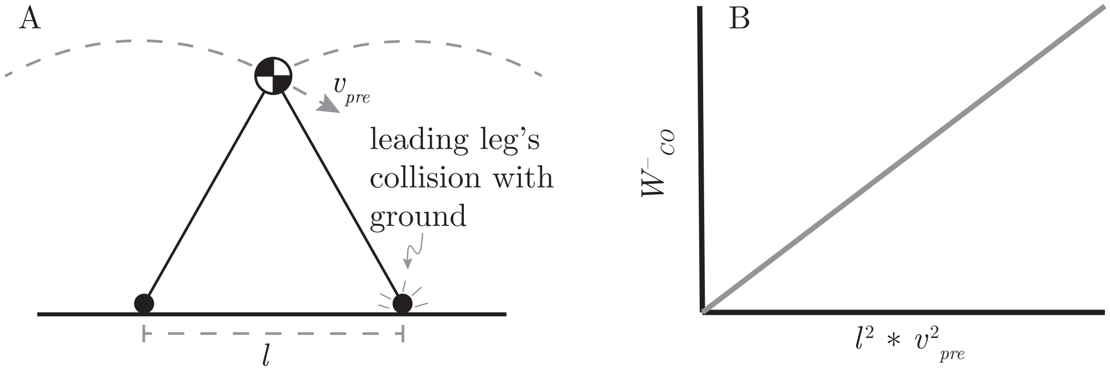

Figure 1.2: Relationship between collision loss and basic kinematics. A simple walking model (A) predicts that collisional losses of center of mass energy (W^{-}_{CO}) is determined by step length (l) and pre-transition velocity (v_{pre}) (B).

For a complete stride the total collisional loss is the sum of both transitions:

$$\Sigma W^{-}_{CO} \propto \Sigma l^2 * v^2_{pre}\,, \tag{1.2}$$

where Σ denotes the sum of the 2 step-to-step transitions of a complete stride. Positive mechanical work (W^{+}) is performed during the stance phases (to make up for collisional losses in center of mass energy) and in proportion to the losses:

$$\Sigma W^{+} \propto \Sigma W^{-}_{CO}\,. \tag{1.3}$$

The positive mechanical work performed on the center of mass during stance has been shown to exact a metabolic cost (Donelan et al., 2002a). Using Equations 1.2 and 1.3, we therefore express stance cost as:

$$stance\,cost \propto \Sigma l^2 * v^2_{pre}\,. \tag{1.4}$$

The cost of swinging the legs (Fig. 1.3A) makes up the costs of the swing phase and has been estimated to account for about a third of the cost of the stride cycle (Marsh et al., 2004; Doke et al., 2005; Umberger, 2010). Both the mechanical work performed on the leg and production of muscle force have been suggested to account for the cost of leg swing (Doke et al., 2005). However, the rate of force production by hip muscles has been

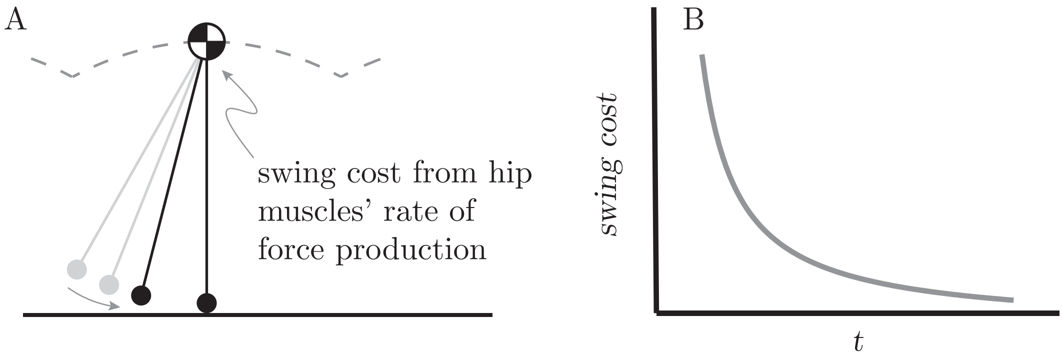

Figure 1.3: Relationship between swing cost and step time. A simple walking model (A) predicts that swing costs are derived from rate of force production of hip muscles and depends on step time (t) (B).

proposed to dominate the cost of the swing phase, especially when swinging the legs rapidly (Kuo, 2001; Doke & Kuo, 2007). Rate of force production captures the cost of recruiting less economical fast-twitch muscle fibers for large forces at brief durations (Kuo, 2001). Since swing time is proportional to step time, swing cost can be expressed using step times (Fig. 1.3B). From a rate of force production cost, the cost of swinging the legs can be modeled as being proportional to t^{-3} (Doke & Kuo, 2007), where t is step time. We therefore model total swing cost of a complete stride as:

$$swing\ cost \propto \Sigma t^{-3}\,, \tag{1.5}$$

where Σ denotes the sum of the 2 swing phases of a complete stride.

Human treadmill walking is largely symmetrical between left and right legs (Gundersen et al., 1989; Hamill et al., 1984; Hannah et al., 1984; Seeley et al., 2008; Ankaralı et al., 2015). Indeed, most research on the energetics of locomotion has been done in symmetrical gaits. It is not clear if basic kinematic parameters (such as step lengths and step times) determine the metabolic cost of locomotor asymmetry. Based on collisional losses of center of mass energy, it has been predicted, but not tested, that asymmetrical step lengths increase metabolic cost of walking (Srinivasan, 2011). Ellis et al. (2013) had people walk with increasing step time asymmetry while step length asymmetry was free to vary. With increasing step time asymmetry, Ellis et al. (2013) found increased collisional losses, increased positive work performed on the center of mass and increased metabolic cost. But since step lengths were free to vary, the effects of either asymmetrical step lengths or step times on the added metabolic cost of asymmetry are difficult to delineate.

Through which mechanisms could asymmetry affect metabolic cost of walking? Step length and step time asymmetry could increase metabolic cost through their combined effect on collisional losses (Equation 1.2): step length asymmetry directly influences the predictor ($l^2 * v_{pre}^2$) of collisional losses, whereas it is unknown how specific combinations of asymmetrical step lengths and step times determine pre-transition velocity. Asymmetry could increase collisional losses: for example, at constant v_{pre}, the collisional loss increases with step length squared (Equation 1.1; Fig. 1.4A). Since the extra cost of a long step length ($+\Delta l$) exceeds the reduced cost of a short step length ($-\Delta l$), total collisional losses increase with step length asymmetry when compared to 2 symmetrical step lengths (l_*) (Fig. 1.4B). In this proposed mechanism, asymmetrical step lengths and step times exact an added metabolic cost through increased collisional losses and, in turn, increased positive mechanical work in the stance phase. An alternative mechanism depends on swing costs. Because swing times are proportional to step times, swing cost increases sharply with short step times (Fig. 1.5A). Step time asymmetry could lead to an added metabolic cost because the increased cost of a brief step time ($-\Delta t$) exceeds the decreased cost of a long step time ($+\Delta t$) which would increase swing costs compared to 2 symmetrical step times (t_*) (Fig. 1.5B). However, since swing costs account for only about a third of the cost of the stride cycle, the added metabolic cost from the influence of step time asymmetry on swing cost is likely negligible at small step time asymmetries. Thus, we identify 2 potential mechanisms by which kinematic asymmetry could increase metabolic cost of walking. One mechanism is associated with stance costs and is derived from the influence of asymmetry in step lengths and step times on collisional losses and, in turn, the positive mechanical work performed to make up for the losses. The other mechanism is associated with swing costs and is derived from the observation that at a large step time asymmetry, the increased cost of swinging one leg rapidly likely exceeds the reduced cost of swinging the other leg slowly. We propose that kinematic asymmetry primarily incurs an added metabolic cost from these mechanisms.

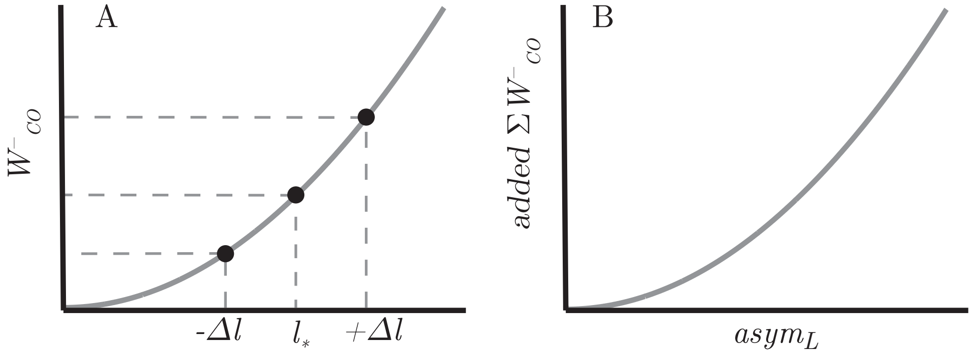

Figure 1.4: Asymmetry can increase cost through collision losses. If v_{pre} is constant, collision losses depend only on step length squared (A). Since the increased cost of a longer step length ($+\Delta l$) exceeds the reduced cost of a shorter step length ($-\Delta l$), total cost is increased with step length asymmetry ($asym_{\mathrm{L}}$) compared to the cost of 2 symmetrical step lengths (l_*) (B).

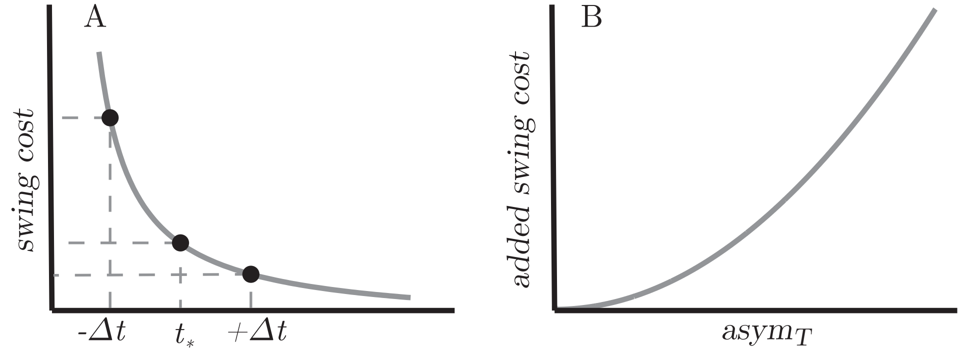

Figure 1.5: Asymmetry can increase swing cost. Since the increased cost of a shorter step time ($-\Delta t$) exceeds the reduced cost of a longer step time ($+\Delta t$) (A), total cost is increased with step time asymmetry ($asym_{\mathrm{T}}$) compared to the cost of 2 symmetrical step times (t_*) (B).

Understanding what determines metabolic cost of asymmetry is useful for understanding the energetic cost of gait asymmetry. Many gait pathologies result in asymmetrical gait and an increased metabolic cost of walking (Waters & Mulroy, 1999). The increased metabolic cost is commonly interpreted as a direct result of asymmetry, but the mechanism is unclear. With a more detailed understanding of how kinematic asymmetry influences metabolic cost, we should be able to characterize how we can alleviate the (hypothesized) detrimental effects of asymmetry on metabolic cost. This could also have implications for rehabilitation, in which the explicit goal often is to make people walk more symmetrically (Bastian, 2008).

1.1.3 Do humans exploit asymmetry to minimize metabolic cost?

Adaptation of locomotor control has been studied by walking on a split-belt treadmill (Choi & Bastian, 2007; Reisman et al., 2005). A split-belt treadmill consists of 2 treadmill belts of which speed can be controlled independently. As such, walking on a split-belt treadmill can introduce an asymmetrical environment in which one leg moves faster than the other. Humans can adapt walking in the split-belt treadmill environment: at the start of split-belt treadmill locomotion, the locomotor pattern is perturbed, but after a couple of minutes the locomotor pattern adapts a new steady-state pattern (Reisman et al., 2005). In steady-state split-belt treadmill walking, people prefer to use symmetrical step lengths and asymmetrical step times (Finley et al., 2013). Even though it is not, a priori, clear why symmetry should be preferred in an asymmetrical environment, convergence to symmetrical step lengths has been proposed to drive the changes in the locomotor pattern in split-belt treadmill walking (Malone et al., 2012).

Furthermore, convergence to symmetrical step lengths has been proposed to minimize metabolic cost during the adaptation period to split-belt treadmill walking. Finley et al. (2013) measured metabolic cost during the adaptation period to split-belt treadmill walking and found that cost was reduced during the adaptation period. Based on the correlation between the reduced cost and changes in step length asymmetry across the adaptation period, Finley et al. (2013) concluded that convergence to symmetrical step lengths was minimizing metabolic cost. To test this idea, Sánchez et al. (2017) had people walk on a split-belt treadmill with a range of different step length asymmetries, in steady-state, while stride time and step time asymmetry were free to vary. Contrary to their expectations, Sánchez et al. (2017) found that metabolic cost was not different across the range of step length asymmetries that they tested. Even though this suggests that step length symmetry is not minimizing metabolic cost during the adaptation period, the effects of uncontrolled stride time and step time asymmetry could have confounded the results.

Recent studies show that humans can adapt their locomotor pattern to optimize metabolic cost when they are put into an unusual environment wearing resistive knee-braces (Selinger et al., 2015). This suggests that humans can readily change the locomotor pattern to find economical ways to walk. It is, however, not clear if humans exploit locomotor asymmetry to minimize the metabolic cost of locomotion. Anatomical and kinematic asymmetries in human runners have been found to have no effect on measured running economy (Seminati et al., 2013). This suggests that the locomotor system may have adapted to an asymmetrical constraint to optimize metabolic cost of locomotion. This idea, however, remains to be tested.

1.2 Problem statement and purpose

The determinants of the metabolic cost of locomotor asymmetry are not well understood. Asymmetry increases metabolic cost (Ellis et al., 2013), however, it is unknown if asymmetrical step lengths and step times can explain the added metabolic cost of asymmetry in walking. Recent studies suggest that humans can adapt their locomotor pattern to optimize metabolic cost (Selinger et al., 2015). But it is unclear if humans exploit locomotor asymmetry to optimize metabolic cost when adapting to an asymmetrical constraint.

The purpose of the proposed work is to address 2 aims. First, what are the kinematic determinants of the added cost of asymmetrical walking? Second, is locomotor asymmetry in split-belt treadmill walking adapted to optimize metabolic cost? To address the first aim, metabolic energy expenditure will be measured in healthy people walking on a treadmill with either asymmetrical step lengths, asymmetrical step times or concurrent asymmetry in step lengths and step times. To address the second aim, metabolic energy expenditure will be measured in healthy people walking on a split-belt treadmill with experimentally controlled step length and step time asymmetry to determine if they adapt and exploit asymmetry to optimize metabolic cost.

1.3 Specific aims

1.3.1 Aim 1: Determine the mechanisms for the added metabolic cost of asymmetry in walking

Asymmetry increases metabolic cost (Ellis et al., 2013), but it is unknown if basic kinematic parameters predict the added cost. We propose that the added cost of asymmetry primarily is attributed to the effects of step length and time asymmetries on collisional losses of center of mass energy.

We will assess the effects of asymmetrical step lengths and step times on metabolic cost of walking on a normal treadmill. At a given speed and stride time, we will systematically constrain increasing levels of asymmetry in 4 conditions: only step length asymmetry, only step time asymmetry and 2 conditions with concurrent step length and step time asymmetry (since asymmetry is directional, there are 2 permutations of concurrent asymmetry). To constrain subjects' asymmetry, we will use real-time asymmetry feedback. We will measure metabolic cost using expired air analysis and calculate work performed on the center of mass by individual legs from ground reaction forces.

Hypothesis 1.1: Total collisional losses are proportional to the summed product of squared step length and squared pre-transition velocity for all asymmetry conditions (Fig. 1.6A).

Hypothesis 1.2: Total positive mechanical work performed on the center of mass is proportional to total collisional losses for all asymmetry conditions (Fig. 1.6B).

Hypothesis 1.3: Net metabolic cost is proportional to total positive mechanical work rate performed on the center of mass for all asymmetry conditions (Fig. 1.6C).

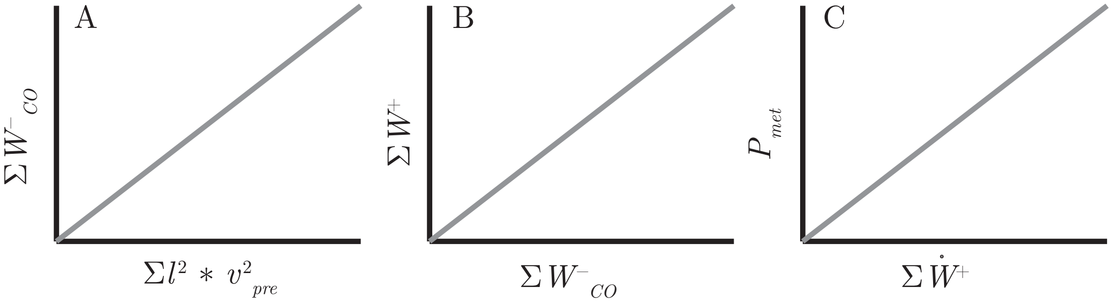

Figure 1.6: Predictions for aim 1. Total collisional losses (ΣW^-_{CO}) will be proportional to the product of squared step length (l) and squared pre-transition velocity (v_{pre}) summed across both transitions of a stride cycle (A). Total positive work (ΣW^+) will be proportional to total collisional losses (B). Metabolic cost (P_{met}) will be proportional to total positive work rate ($\Sigma \dot{W}^+$) (C).

1.3.2 Aim 2: Determine whether humans exploit asymmetry to optimize metabolic cost

The locomotor pattern must constantly adapt to changes in the environment in which we move. Adaptations of walking to speed-asymmetry between the legs on a split-belt treadmill have suggested a general adaptation strategy: people choose a steady-state locomotor pattern with asymmetrical step times and symmetrical step lengths, while they reduce metabolic cost during the adaptation period (Finley et al., 2013). The proposed experiment will test whether people exploit asymmetry to minimize metabolic cost in walking.

In split-belt treadmill locomotion, at a given stride time, stride length (sum of 2 consecutive step lengths) linearly decreases with step time asymmetry according to the constraint of the split-belt treadmill environment (see Appendix A for derivation and interpretation):

$$l_{stride} = (\overline{v} - \frac{\Delta v}{2} asym_{\mathrm{T}}) * t_{stride} \,, \tag{1.6}$$

where l_{stride} is stride length, t_{stride} is stride time, $\overline{v}$ is averaged belt speed, Δv is belt speed-difference and $asym_{\mathrm{T}}$ is step time asymmetry. Since collisional losses must decrease with a shorter stride length (Equation 1.2), step time asymmetry must, in turn, decrease stance costs in split-belt treadmill walking. We model stance costs at increasing step time asymmetry for 3 speed-difference conditions (speed-differences at 0.5 m s^{-1}, 1.0 m s^{-1} and

1.5 m s^{-1} at an average speed of 1.25 m s^{-1}) using Equation 1.4. Modeled stance costs decrease with step time asymmetry (Fig. 1.7A). The relationship between stride length and step time asymmetry depends on speed-difference between the belts: as Δv increases, the same $asym_{\mathrm{T}}$ will lead to a shorter l_{stride} (Equation 1.6). Therefore, $asym_{\mathrm{T}}$ decreases stance costs faster at a greater Δv (stance costs have steeper decreasing slopes for greater speed-differences; Fig. 1.7A). However, a greater Δv introduce more asymmetrical pre-transition velocities, v_{pre}, which increases collisional losses and, in turn, stance costs (at $asym_{\mathrm{T}} = 0$, Δv increases stance costs; Fig. 1.7A). At the same time, step time asymmetry must increase swing costs (Equation 1.5) for all speed-difference conditions (Fig. 1.7A).

Summing the modeled stance and swing costs to give total cost yields 3 distinct cost curves for each speed-difference condition (Fig. 1.7B). The effects of step time asymmetry on reduced stance costs and increased swing costs leads to 3 distinct step time asymmetries that are energetically optimal trade-offs of the stance and swing costs for each speed-difference condition. The energetically optimal step time asymmetries increase with greater speed-differences. We predict that step time asymmetry in split-belt treadmill walking is adapted to optimize metabolic cost. Furthermore, we predict that the effects of step time asymmetry on reduced stance costs and increased swing costs explain the existence of energetic optima. Last, we predict that the energetically optimal step time asymmetry increases with speed-differences between the belts.

Hypothesis 2.1: Self-selected step time asymmetry will increase with belt speed-difference during split-belt treadmill locomotion.

Hypothesis 2.2: The self-selected step time asymmetry will minimize metabolic cost of split-belt treadmill locomotion across speed-difference conditions.

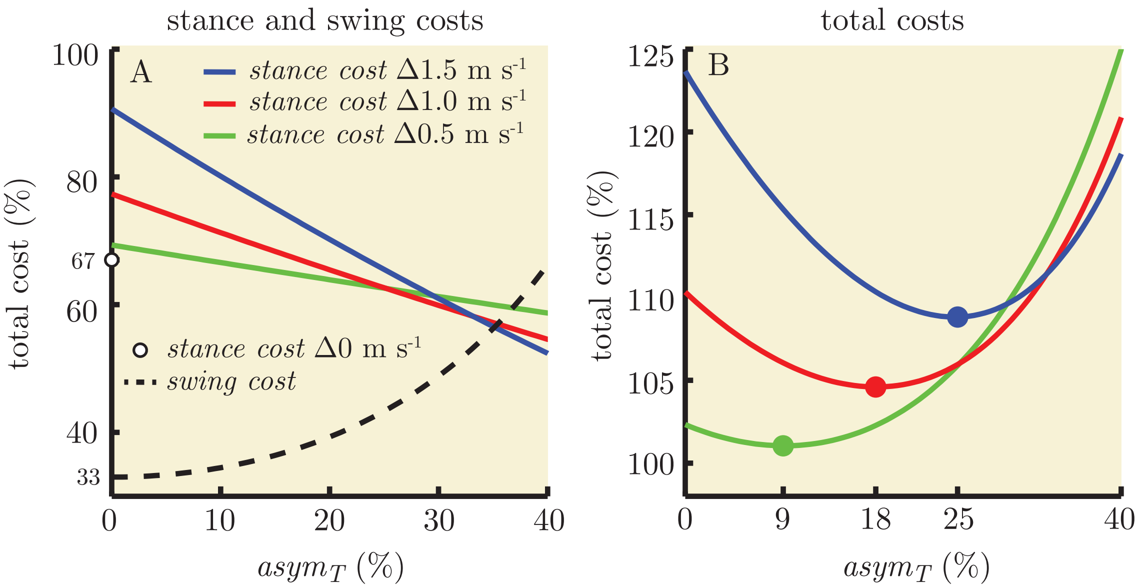

Figure 1.7: Predictions for aim 2. (A) Modeled stance and swing costs as a function of step time asymmetry ($asym_{\mathrm{T}}$) in split-belt treadmill walking at 3 different speed-differences, 0.5 m s^{-1}, 1.0 m s^{-1}, 1.5 m s^{-1}, at an averaged speed of 1.25 m s^{-1}. Within each speed-difference condition, $asym_{\mathrm{T}}$ decreases stance costs (Equation 1.4) because stride lengths are shortened (Equation 1.6). Between speed-difference conditions, stance costs decrease at different rates because $asym_{\mathrm{T}}$ interacts with Δv to shorten stride length (Equation 1.6). At $asym_{\mathrm{T}} = 0$, stance costs increase with Δv because of more asymmetrical pre-transition velocities (Equation 1.4). Additionally, step time asymmetry increases swing costs (Equation 1.5). Based on experimental and modeling studies (Doke et al., 2005; Umberger, 2010; Marsh et al., 2004), stance costs are weighted so that the stance cost of walking without a speed-difference ($\Delta 0$ m s^{-1}) make up 74% of the total cost, while swing cost is weighted to make up 26% of the total cost at $asym_{\mathrm{T}} = 0$. (B) Modeled total costs (sum of stance and swing) of split-belt treadmill walking at increasing $asym_{\mathrm{T}}$. The energetically optimal step time asymmetry increases with speed-differences between the belts.

CHAPTER 2

LITERATURE REVIEW

2.1 Walking

2.1.1 The stride cycle

Walking is a cyclic movement of which the stride cycle is the unit of movement: after one stride cycle another repeats. During the stride cycle each leg either contacts the ground in the stance phase or is off the ground during the swing phase. In walking, the stance phase is about 60% of the stride cycle (Perry & Burnfield, 2010). This means that each stance phase is bookended by double support periods in which both legs contact the ground. Each double support period is about 10% of the stride cycle so that the single support phase, in which only a single leg contacts the ground, is about 40% of the stride cycle. During double support phases, the leg that ends its stance phase is named the trailing leg, whereas the leg that starts its stance phase is named the leading leg.

2.1.2 Center of mass mechanics

The pattern of mechanical energy fluctuations in walking prescribe a gait-specific strategy to conserve mechanical energy. In walking, the center of mass moves in an up-and-down sinusoidal pattern: during single support, the center of mass moves up in the early part, attains its highest position about mid-stance and moves down in late stance; while during a period that corresponds with double support, the center of mass is redirected from down-to-up, and, therefore, reaches its lowest position (Saunders et al., 1953). By stepping on force platforms, the potential and kinetic energy of the center of mass has been examined (Cavagna, 1975). Potential and kinetic energy were found to oscillate out-of-phase in walking (Cavagna & Margaria, 1966). Out-of-phase oscillations of potential and kinetic energy of the center of mass implies that changes in mechanical energy over the stride cycle are minimized, and, in turn, that the mechanical work performed on the center of mass is minimized. The exchange between potential and kinetic energy of the center of mass, and, ultimately, conservation of mechanical energy, has been proposed as a major defining feature of the mechanics of walking (Cavagna et al., 1977). Furthermore, the exchange of potential and kinetic energy supports the idea that the defining characteristic of walking mechanics can be captured by dynamic walking models with inverted pendulum mechanics (Garcia et al., 1998; Kuo, 2002; McGeer, 1990). An inverted pendulum captures the notion that during single support, the stance leg behaves like an inverted pendulum: the center of mass vaults over a relatively straight stance leg that pivots around the ankle. Dymamic walking models focus on collisional losses of center of mass energy and have yielded predictions about the energetics of walking which have stimulated the scientific discourse on walking energetics in recent years (Kuo, 2001; Kuo et al., 2005; Ruina et al., 2005).

2.1.3 Symmetry

Bilateral symmetry is an important evolutionary trait and has been credited for the success of many modern animals, including humans (Collins & Valentine, 2001; Finnerty et al., 2004). Even so, locomotor asymmetry could arise from structural asymmetry (Gurney, 2002), asymmetrical neural input (Arsenault et al., 1986) or complex interactions of the motor system (Collins & Stewart, 1993; Gregg et al., 2012).

Walking is, as an idealized gait form, bilaterally symmetrical. This is contrary to asymmetrical gaits such as skipping, in which the legs serve different roles (Minetti, 1998; Whitall & Caldwell, 1992). But even though walking is bilaterally symmetrical, do humans actually walk symmetrically?

Bilateral symmetry in locomotion is commonly quantified by comparing a single gait variable across the legs (Sadeghi et al., 2000). There is, however, no consensus on which gait variables capture asymmetry most appropriately. Asymmetry has been reported from basic kinematics (such as step lengths and step times, Kodesh et al. (2012)), joint angle kinematics and kinetics (Forczek & Staszkiewicz, 2012; Seeley et al., 2010), ground reaction forces (Hamill et al., 1984) and muscle activity (Arsenault et al., 1986). Furthermore, asymmetry has also been assessed using more complex techniques such as frequency analyses (Bellanca et al., 2013), coordination analyses (Haddad et al., 2006) and composite scores (Exell et al., 2012). Not only is there no standard asymmetry measure, but it is unclear how different asymmetry variables are related (Hsiao-Wecksler et al., 2010).

Healthy human gait has often been assumed to be bilaterally symmetrical (Sadeghi et al., 2000). Studies that have directly tested bilateral symmetry in healthy human locomotion have reported that human gait is symmetrical while others have reported that it is asymmetrical. Lower limb joint kinematics (Gundersen et al., 1989; Hannah et al., 1984) and ground reaction forces in walking (Hamill et al., 1984; Seeley et al., 2008) have been concluded to be bilaterally symmetrical. On the other hand, bilateral asymmetry in walking has also been concluded from kinematics (Chodera, 1974; Du Chatinier & Rozendal, 1970) and kinetics (Herzog et al., 1989). Persistent bilateral asymmetry has been proposed to arise from functionally different roles of the legs (each for propulsion and support) possibly explained by leg dominance (Sadeghi et al., 2000). However, this idea has limited support from experimental studies (Brown et al., 2014; Polk et al., 2017; Seeley et al., 2008; Strike & Taylor, 2009; Wang & Watanabe, 2012). This suggests that, despite the reported statistically significant asymmetries, healthy human locomotion is largely symmetrical (Ankaralı et al., 2015).

All studies that have assessed asymmetry has done so by having people walk on smooth and even surfaces overground or on a treadmill. Less is known about walking in environments that are rough or uneven. In theses environments people could be more inclined to walk asymmetrically. Indeed, humans are fully capable of walking asymmetrically or use asymmetrical gait forms. This suggests that, even though symmetry appears to be preferred in normal settings, asymmetry could be preferred under other circumstances.

2.2 Energetics of walking

The metabolic energy expended during healthy human locomotion can amount to a considerable portion of the energy budget (Passmore & Durnin, 1955; Waters & Mulroy, 1999). Metabolic energy expenditure is usually measured by indirect calorimetry using expired air analysis. To assess the net metabolic cost of locomotion, that is, the cost of locomotion per se, basal metabolic rate is subtracted from gross metabolic energy expenditure. Although easy to implement, indirect calorimetry cannot account for anaerobic contributions to metabolism.

Energy is used by muscle tissue during locomotion. Metabolic energy is expended when a muscle produces mechanical work (Hill, 1938); both positive (shortening contractions) and negative (lengthening contractions) mechanical work. Muscle work is performed at different efficiencies (about 25% for positive work and −120% for negative work) so that the metabolic cost of performing positive work is much greater than negative work (Abbott et al., 1952; Margaria et al., 1963). But even if a muscle does not produce mechanical work, metabolic energy is expended when the muscle produces force in a static contraction (Hill, 1958). Consequently, the division of metabolic energy expenditure from muscle work or force, provides the framework in which locomotor energetics is commonly analyzed.

2.2.1 Energetics of stance

The energetic cost of locomotion can be divided into costs incurred during stance and during swing (Umberger, 2010). During the stance phase in walking, the center of mass vaults over a relatively straight stance leg. Inverted pendulum models predict that no mechanical work is needed during the stance phase: potential and kinetic energy are perfectly exchanged so that there are no changes in mechanical energy, and, in turn, no mechanical work. In contrast to pendular dynamics, dynamic walking models include collisions with the ground in which center of mass energy decreases (Ruina et al., 2005; Bertram & Hasaneini, 2013). The collisional loss is incurred by the leading leg during double support periods as the leg performs negative work on the center of mass (Donelan et al., 2002b). This interval, in which the center of mass velocity is redirected, is referred to as a step-to-step transition. In human walking, the step-to-step transition corresponds to the double support phase (Adamczyk & Kuo, 2009). Losses in center of mass energy must be compensated by positve work as the net work on the center of mass is zero in overground or treadmill walking on the level. While the negative work performed on the center of mass can be performed by both muscle tissue (at a high efficiency) and by passive soft-tissue (Zelik & Kuo, 2010), positive work must primarily be performed by muscle tissue and, therefore, exacts a substantial metabolic cost. Since collisional losses in center of mass energy imposes metabolic costs, coordination strategies that reduce losses are energetically favourable as they reduce the need to counteract the loss with positive muscle work. Strategies that reduce collisional losses include: to perform positive work during the step-to-step transition rather than during single support (Kuo, 2002; Soo & Donelan, 2012), to perform equal amounts of negative collision work and positive push-off work during step-to-step transitions (Kuo et al., 2005), and to perform push-off work before collision work (Ruina et al., 2005; Adamczyk & Kuo, 2009). Dynamic walking models and collisional losses have yielded predictions about the energetic cost of walking that have implications for walking energetics in a broader framework (Kuo, 2007; Kuo & Donelan, 2010). Furthermore, collisional losses have provided insights into the energetics of hemiparetic walking (Farris et al., 2015), push-off deficiency following trans-tibial amputation (Adamczyk & Kuo, 2015; Huang et al., 2015) and locomotor adaptation (Selgrade et al., 2017a,b).

2.2.2 Energetics of swing

During the swing phase, the leg swings forward to advance progression and prepare for another stance phase (Perry & Burnfield, 2010). The movement of the leg during swing has previously been suggested to be governed by pendular dynamics (Mochon & McMahon, 1980). Pendular leg swing implies that the leg is swung at no metabolic cost, which, however, is not the case (Doke et al., 2005; Gottschall & Kram, 2005; Marsh et al., 2004; Umberger, 2010). The cost of swinging the leg during walking has been estimated to be about a third of the total metabolic cost of the stride cycle, which is a non-trivial contribution (Doke et al., 2005; Marsh et al., 2004; Umberger, 2010). Not only is pendular leg swing not supported by the energetic demands, pendular leg swing is not supported from several considerations of normal walking such as muscle activity, joint moments and stride time (Whittlesey et al., 2000). However, it has been suggested that bursts of muscle activity from hip muscles at the beginning and end of the swing phase control swing duration (Doke et al., 2005; Doke & Kuo, 2007; Kuo, 2001), which allows the possibility that much of the intervening swing period is dictated by pendular dynamics at a low metabolic cost.

At the leg's natural swing period, the metabolic cost of leg swing is minimal (Doke et al., 2005; Holt et al., 1991). For short swing periods, the cost of swinging the leg appears to increase sharply; for swing periods longer than the natural period, the cost only increases moderately (Doke et al., 2005; Doke & Kuo, 2007). Both mechanical work performed on the swing leg and muscle force production have been proposed to contribute to the metabolic cost of leg swing (Doke et al., 2005; Doke & Kuo, 2007). Each term (mechanical work or force) has been proposed to dominate at different swing periods relative to the leg's natural swing period. For swinging the leg at periods longer than natural, mechanical work has been proposed to dominate (Doke et al., 2005); while the high metabolic cost of short swing periods is dominated by the cost of producing muscle force (Doke & Kuo, 2007).

2.2.3 Energetics of locomotor asymmetry

Generally, asymmetry increases metabolic cost of locomotion. Enforcing asymmetrical step times in walking in healthy humans increases metabolic cost (Ellis et al., 2013). Furthermore, imposing an inertial asymmetry between the legs, by applying an added mass to a single leg, increases metabolic cost of healthy walking (Martin et al., 1997). It is also true that asymmetrical, pathological gait is metabolically costlier than healthy gait (Finley & Bastian, 2017; Waters & Mulroy, 1999). In pathological gait, however, it is inconclusive if asymmetry is an economical compensation or if asymmetry contributes to a costlier gait (Lai et al., 2001; Mattes et al., 2000; Sánchez & Finley, 2018).

Moreover, it is not clear what determines the metabolic cost of asymmetry in healthy human locomotion. Based on collisional losses, it has been hypothesized that step length asymmetry incurs an added metabolic cost (Srinivasan, 2011). This, however, remains to be tested in normal walking. Ellis et al. (2013) had people walk with increasing step time asymmetry while step length asymmetry was free to vary. With increasing step time asymmetry, Ellis et al. (2013) found increased collisional losses, increased positive work performed on the center of mass and increased metabolic cost. But since step lengths were free to vary, that makes it difficult to delineate the effects of either asymmetrical step lengths or step times on the added metabolic cost of asymmetry.

2.3 Optimal control of locomotion

A fundamental question in the study of locomotion is how movement is controlled and organized. Because the locomotor system is redundant, we can perform the same action using multiple strategies (Bernstein, 1967). Redundancy could, theoretically, be solved by optimality principles (Nubar & Contini, 1961; Scott, 2004; Todorov, 2004). It has been hypothesized that movement patterns adapt in a manner that minimizes metabolic cost (Sparrow & Newell, 1998). This suggests that metabolic energy expenditure is a likely optimality objective. Indeed, many hallmarks of normal locomotion can be explained by energetic optima.

The transition between walking and running occurs at a speed around 2.0 m s^{-1} (Hreljac, 1993; Thorstensson & Roberthson, 1987). Walking at speeds slower than the transition speed or running at speeds faster than the transition speed minimizes metabolic cost of transport (the metabolic cost to travel a given distance) (Margaria et al., 1963; Minetti et al., 1994). An optimal effort strategy from the legs' muscle activity even generalizes to adapted gaits on a split-belt treadmill (Stenum & Choi, 2016). This suggests that gaits may be selected to minimize metabolic cost of transport.

In walking, a speed of around 1.25 m s^{-1} minimizes metabolic cost of transport (Farris & Sawicki, 2012; Ralston, 1958). When people are free to self-select their walking speed, it tends to coincide with the speed that minimizes metabolic cost of transport (Ralston, 1958). Classically, metabolic cost of transport in running has been described without an energetically optimal speed (Margaria et al., 1963). But newer studies contend that an optimal running speed does exist (Cher et al., 2015; Steudel-Numbers & Wall-Scheffler, 2009), and, furthermore, that people choose to run at their energetically optimal running speed (Rathkey & Wall-Scheffler, 2017). This suggests that people choose a walking speed, and possibly a running speed, to minimize metabolic cost of transport.

During walking or running at a given speed, there is a combination of stride length and stride time that minimizes metabolic cost. This has been observed for treadmill walking at intermediate speeds (Cotes & Meade, 1960; Umberger & Martin, 2007; Zarrugh & Radcliffe, 1978) and treadmill running at moderate speeds (Cavanagh & Williams, 1982; Högberg, 1952; Snyder & Farley, 2011). The combination of stride length and stride time that people naturally choose when walking or running at a given speed coincides with their energetically optimal combination (Cavanagh & Williams, 1982; Snyder & Farley, 2011; Umberger & Martin, 2007; Zarrugh & Radcliffe, 1978). This suggests that people choose combinations of stride length and stride time to minimize metabolic cost.

Further evidence that humans tend to use energetically optimal locomotor patterns comes from a line of studies that constrain either walking speed, step length or step time separately, and independently, over a range of values (Bertram, 2005; Bertram & Ruina, 2001). Constraining either speed, step length or step time yielded distinctly different combinations of step length and step time. The constraint-dependent combinations were predicted from optimizing metabolic cost of transport within the possible combinations of each constraint. Furthermore, optimal metabolic cost of transport also predicted the constraint-dependent combinations of step length and step time in running (Gutmann et al., 2006). This suggests that people flexibly change the locomotor pattern to different task demands by minimizing metabolic cost of transport.

Inherent to optimality theory is state estimation of the system. Even though evidence suggests that locomotor behaviors are selected to optimize metabolic cost, that does not necessarily imply that people are energetically optimal from state estimation. For example, energetically optimal locomotion could be predisposed from evolutionary adaptations (Alexander, 2001) or from the propensity of self-organizing systems to minimize energy cost (Diedrich & Warren, 1995) without the need to estimate energetic cost. A recent study, however, suggests that humans adapt locomotion from a direct optimization of metabolic cost. When people walk on a treadmill wearing resistive knee braces, that impose an added metabolic penalty at either higher or lower step rates than preferred, they learn to adapt their step rate to optimize metabolic cost (Selinger et al., 2015). This has been interpreted to indicate that humans can adapt their locomotor pattern from a direct optimization of metabolic cost.

Two processes have been proposed to account for the selection of energetically optimal locomotor patterns (Snaterse et al., 2011). The first process is an iterative, slowly converging (>30 seconds), direct optimization of energy use that could drive locomotor patterns to optima. Direct optimization requires that the nervous system estimates energetic demand, from various sensations related to metabolism, and dynamically adapt locomotion to minimize energy use. Because sensations of expended energy are slowly conducted and because of its iterative nature, direct optimization is a relatively slow process. Physiological sensors of metabolic cost include blood gas receptors and local muscle afferents that are sensitive to muscle exertion. To test if blood gas receptors were responsible for driving movement patterns to energetic optima, Wong et al. (2017) manipulated the carbon dioxide content of inspired air as a function of step rate during treadmill walking to create simulated energtically optimal step rates. Wong et al. (2017) found that people did not adjust their step rate to the simulated energetically optimal step rates which suggests that blood gas receptors are not responsible for driving an energy optimization process. The second process is a quickly converging (∼2 seconds), energetically optimal, pre-programmed, locomotor pattern that could set locomotor patterns to optima. An optimal, pre-programmed pattern requires explicit, prior experience with the task and the constraints. Thus, pre-programmed patterns depend on prior direct optimization of energy use. Following perturbations, fast and slow convergences have been shown in selection of preferred walking speed (Pagliara et al., 2014) and preferred step rate in walking and running (Pagliara et al., 2014; Snyder et al., 2012). Thus, the time course in which locomotor patterns adjust to optimality have been suggested to reveal the processes that underlie energetic optimization.

Even though humans can adapt to minimize metabolic cost, that does not imply that humans only, always and instantly seek to optimize metabolic cost. Indeed, recent studies show that people can be instructed to walk downhill with a more relaxed gait that reduces metabolic cost compared to the preferred downhill walking pattern (Hunter et al., 2010; Monsch et al., 2012). This suggests that humans do not always and only optimize metabolic cost. Instead, metabolic cost is likely one of several task-dependent objectives of normal gait. Other locomotor objectives that are broadly acknowledged include stability (Bauby & Kuo, 2000; Holt et al., 1995; Kang & Dingwell, 2008), stepping accuracy (Matthis et al., 2017), movement time (Bornstein & Bornstein, 1976; Shadmehr et al., 2016), performance (Mero et al., 1992) and pain aversion (Hodges & Tucker, 2011). This suggests that locomotion has multiple task-dependent objectives, one of which is minimization of metabolic cost.

Stability has been proposed as an optimality objective (Holt et al., 1995). Stability of leg joint coordination has been proposed to be optimal at the preferred stride rate (Holt et al., 1995; Russell & Haworth, 2014). It is not clear how trunk stability, assessed using local divergence measures, changes with walking speed. At increasing speeds, both decreases in stability (Dingwell & Marin, 2006; England & Granata, 2007), increases in stability (Bruijn et al., 2009), and no changes have been reported (Hak et al., 2013), which is partly explained by the calculation methods used in each study (Stenum et al., 2014). A limitation to our understanding of stability is that several stability measures have been defined that capture different properties related to stability (Bruijn et al., 2013). Furthermore, the stability measures are not related in a straightforward manner which makes interpretation across different studies difficult (Bruijn et al., 2013). Based on analysis of a dynamic walking model (Kuo, 1999), human walking has been shown to require active lateral stabilization through control of foot placements and step widths (Bauby & Kuo, 2000). Active lateral stabilization exacts a (small) metabolic cost based on work performed on the center of mass (Donelan et al., 2004, 2001) or by controlling foot placement during swing (Rankin et al., 2014). While the relationship between stability and metabolic cost has been proposed as a trade-off, this idea has not been confirmed experimentally (Monsch et al., 2012).

2.4 Neural control of locomotion

Inputs from 3 major neural systems regulate locomotion by, directly or indirectly, controlling motor neurons to activate muscle: spinal interneurons coordinate movements within and across legs; sensory feedback continuously contributes to motor neuron activity and provide sensory information for motor adaptation; and, supraspinal centers exert direct volitional control of motor neuron activity and adapts locomotion from sensory information. Even though the neural systems contribute differently to locomotor control, the net effect of all input in healthy people is smooth, coordinated and rhythmic locomotion.

2.4.1 Spinal interneurons

Spinal interneurons coordinate agonist and antagonist muscles by reciprocal inhibition. Reciprocal inhibition involves inhibitory spinal interneurons that are activated by stretch-sensitive afferents from agonist muscles (Eccles et al., 1956). During human walking, reciprocal inhibition changes across the stride cycle: for example, reciprocal inhibition from dorsiflexors to plantarflexors is large in swing, but small in stance (Petersen et al., 1999); while reciprocal inhibition is silenced during static contractions (Crone et al., 1987). This suggests that reciprocal inhibition acts to prevent a stretch reflex in the antagonist muscle, when the agonist muscle is shortening during locomotion.

While reciprocal inhibition coordinates agonist and antagonist muscles around a joint, central pattern generators coordinate rhythmic stepping. In animal studies, direct evidence has provided insight into the organization of patterned control from central pattern generators (Kiehn, 2016; McLean et al., 2008). For example, 2 types of interneurons, that span the midline in the spinal cord of mice, mediates out-of-phase coordination at slow-to-fast, non-overlapping, locomotor frequencies (Talpalar et al., 2013). In humans, however, central pattern generators have only been demonstrated indirectly (Bussel et al., 1996; Calancie et al., 1994; Dimitrijevic et al., 1998). For example, involuntary stepping movements have been documented by tonic electrical stimulation of the lumbar spinal cord in people with complete spinal cord injury

(Dimitrijevic et al., 1998). Even though this suggests that central pattern generators exist in humans, it is unclear if, and, if so how, they contribute to locomotor coordination during movement (Nielsen, 2003).

In humans, pattern generation of stepping has been studied in split-belt treadmill walking. Pattern generation appears to be separately controlled within each leg in humans (Choi & Bastian, 2007; Prokop et al., 1995; Yang et al., 2005). For example, pattern generation before the maturation of direct control of supraspinal input has been studied in infants. Infants can complete 2–3 stride cycles on one leg during a single stride cycle on the other leg when they are stepping (and supported) on a split-belt treadmill (Yang et al., 2005). Furthermore, adaptable pattern generation has been shown to be separate for each leg (Choi & Bastian, 2007).

2.4.2 Sensory feedback

Sensory feedback contributes to locomotor control in 2 roles: to actively drive motor neuron activity (including via reflex pathways, Pearson (2004)) and to provide information for motor learning (Prokop et al., 1995). Sensory feedback has been shown to drive changes in muscle activity in the soleus muscle during walking. When plantarflexors were suddenly unloaded by an ankle orthosis during stance, soleus muscle activity decreased with a short latency (Sinkjær et al., 2000). The short latency suggests that sensory feedback contributes to muscle activity during locomotion. Sensory feedback also contributes to locomotor control in learning. When cutaneous sensory feedback was disrupted by repetitive electrical stimulation during locomotor adaptation to an ankle orthosis, adaptation was impeded (Choi et al., 2016). This suggests that sensory feedback contributes to locomotor control by continuously modulating motor neuron activity, and, furthermore, by changing motor neuron activity through motor learning.

2.4.3 Supraspinal centers

Possibly because of evolutionary adaptations to human bipedalism, the motor cortex exerts direct control of motor neurons to leg muscles through the corticospinal tract (Nielsen, 2003). Imaging and electrophysiological studies show that the motor cortex is actively involved in controlling locomotion. During cycling, cerebral blood flow increased to the motor cortex (Christensen et al., 2000), which suggests that the motor cortex is involved in controlling rhythmic movements. Changes in transmission in the corticospinal tract have been tested with transcranial magnetic stimulation of the motor cortex while the resulting leg muscle activity was detected concurrently as motor evoked potentials. Motor evoked potentials of the tibialis anterior, gastrocnemius and soleus muscles have been shown to be modulated during the stride cycle (Capaday et al., 1999; Petersen et al., 1998, 2001). This suggests that the motor cortex is directly contributing to muscle activity during locomotion.

The cerebellum, contrary to the motor cortex, does not exert direct control over motor neurons. However, the cerebellum is critically important for coordinating smooth movements and for the ability to adapt and retain sensory-driven motor adaptations (Lisberger & Thach, 2013; Martin et al., 1996; Morton & Bastian, 2006; Yanagihara & Kondo, 1996). For example, people with cerebellar damage are unable to adapt locomotion when they walk on a split-belt treadmill (Morton & Bastian, 2006). While sensory information is conveyed through several cells in the cerebellum, a critical part of motor adaptation is suggested to arise from sensory information through climbing fibers onto Purkinje cells. It is has been suggested that the cerebellum compares an expected sensory consequence of the intended motor action to the actual sensory information in order to calibrate the transformation between the intended and actual movement (Lisberger & Thach, 2013). The cerebellum therefore plays an integral part in locomotor adaptation.

2.5 Locomotor adaptation

Motor adaptation can be defined as the adjustment of a well-learned movement over trial-and-error practice when in a novel, perturbing environment (Reisman et al., 2010). Motor adaptation therefore refers to motor adjustment that occurs over a relatively short time-scale in a single training session. A hallmark of motor adaptation is that it requires active de-adaptation: when the perturbation is removed, the adapted movement shows an aftereffect that actively needs de-adaptation to return to a baseline level. This implies that the neural control of movement has adapted, and, importantly, retained the adaptation during the adaptation period.

Kinematic parameters that are related to coordination of the legs, such as step length asymmetry, step time asymmetry and foot placement difference, adapt predictively (that is, gradually across many strides) to split-belt treadmill walking (Malone et al., 2012; Reisman et al., 2005). On the other hand, kinematic parameters that are more closely related to coordination within a single leg, such as stance time asymmetry and timing of peak joint angles, adapt reactively (that is, immediately following a few strides) (Reisman et al., 2005). This likely reflects that split-belt treadmill locomotion primarily perturbs the control of coordination across the legs.

Locomotor adaptation has been proposed to be a sensory-driven process that relies on updating an internal model (Bastian, 2008; Malone et al., 2012). Internal models (inspired by engineering and computational motor control) predict the sensory consequences of muscle activations and, in turn, compare predicted sensory information to the actual sensory feedback (Franklin & Wolpert, 2011; Wolpert et al., 2013). The cerebellum has been proposed to perform this comparison. Most importantly, motor adaptation has been shown to depend critically on the cerebellum (Martin et al., 1996; Morton & Bastian, 2006; Yanagihara & Kondo, 1996).

Proprioceptive feedback about disrupted kinematic symmetry has been proposed as the sensory information that drives locomotor adaptation (Malone et al., 2012; Roemmich et al., 2016). It is often assumed, implicitly or explicitly, that humans adapt their locomotor pattern to symmetry when walking on a split-belt treadmill. This is based on the empirical finding that step lengths tend to be symmetrical following split-belt treadmill adaptation (Finley et al., 2013; Malone et al., 2012; Reisman et al., 2005). But, a priori, it is not clear why symmetry should be the preferred locomotor pattern in an asymmetrical environment.

Recently, minimization of metabolic cost has been proposed as a complementary mechanism that drives adaptation during split-belt treadmill locomotion (Finley et al., 2013). Convergence to step length symmetry during split-belt treadmill adaptation has been proposed to drive the observed reduction in metabolic cost. But when healthy people were instructed to walk at a range of step length asymmetries during steady-state split-belt treadmill locomotion, there was no change in metabolic cost with asymmetry (Sánchez et al., 2017). Even though this suggests that step length symmetry is not minimizing metabolic cost during the adaptation period, Sánchez et al. (2017) did not control subjects' stride time and step time asymmetry which could have confounded the results.

CHAPTER 3

METHODS

3.1 Definitions and constraints

3.1.1 The stride cycle

We define the stride cycle as the events occurring between successive ipsilateral foot contacts. The stride cycle consists of 2 steps: a step from left-to-right foot contacts ($\mathrm{L} \rightarrow \mathrm{R}$) and a step from right-to-left foot contacts ($\mathrm{R} \rightarrow \mathrm{L}$). Even though stride cycles can be defined on either left or right legs, we consider them to be identical because they comprise the same 2 steps.

3.1.2 Step and stride time

We define a step time as the duration between successive bilateral foot contacts with the ground. Because the stride cycle consists of 2 steps, we further define step times between left-to-right foot contacts ($t_{\mathrm{L}\rightarrow\mathrm{R}}$) and right-to-left foot contacts ($t_{\mathrm{R}\rightarrow\mathrm{L}}$). A stride time ($t_{stride}$) is defined as the sum of a pair of successive step times:

$$t_{stride} = t_{\mathrm{L}\rightarrow\mathrm{R}} + t_{\mathrm{R}\rightarrow\mathrm{L}} \,. \tag{3.1}$$

3.1.3 Step and stride length

We define a step length as the anterior-posterior distance between the same anatomical marker on either foot between successive bilateral foot contacts (Zatsiorky et al., 1994). We define 2 step lengths: a step length from left-to-right foot contacts ($l_{\mathrm{L}\rightarrow\mathrm{R}}$) and a step length from right-to-left foot contacts ($l_{\mathrm{R}\to\mathrm{L}}$). A stride length ($l_{stride}$) is defined as the sum of a pair of successive step lengths:

$$l_{stride} = l_{\mathrm{L}\to\mathrm{R}} + l_{\mathrm{R}\to\mathrm{L}}\,. \tag{3.2}$$

3.1.4 Locomotor pattern

We define the locomotor pattern as a specific combination of stride length and time (Zatsiorky et al., 1994).

3.1.5 Asymmetry

Even though humans are largely bilaterally symmetrical when they walk and run (Gundersen et al., 1989; Hamill et al., 1983; Hannah et al., 1984; Seeley et al., 2008), step lengths and step times could, independently, be asymmetrical. We use a standard definition of asymmetry to capture locomotor pattern asymmetry in either spatial (step lengths) or temporal (step times) domains (Ellis et al., 2013; Herzog et al., 1989). We define step length asymmetry ($asym_{\mathrm{L}}$) as:

$$asym_{\mathrm{L}} = \frac{l_{\mathrm{L}\to\mathrm{R}} - l_{\mathrm{R}\to\mathrm{L}}}{l_{\mathrm{L}\to\mathrm{R}} + l_{\mathrm{R}\to\mathrm{L}}} * 100\%\,, \tag{3.3}$$

and define step time asymmetry ($asym_{\mathrm{T}}$) as:

$$asym_{\mathrm{T}} = \frac{t_{\mathrm{L}\to\mathrm{R}} - t_{\mathrm{R}\to\mathrm{L}}}{t_{\mathrm{L}\to\mathrm{R}} + t_{\mathrm{R}\to\mathrm{L}}} * 100\%\,. \tag{3.4}$$

An asymmetry of zero means equal step lengths or step times. Our asymmetry measure is directional: positive asymmetry is step lengths or step times that are greater from left-to-right foot contacts than right-to-left foot contacts, and vice versa for negative asymmetry.

3.1.6 A note on stride length definition

Stride length is usually defined as the anterior-posterior distance between an anatomical marker on the same foot between successive foot contacts on the same leg (Zatsiorky et al., 1994). Here, we instead define stride length as the sum of a pair of successive step lengths. In the following paragraphs we show that the 2 definitions agree in overground and normal treadmill locomotion, but that they conflict in split-belt treadmill locomotion.

In overground locomotion or on a normal treadmill the 2 definitions agree. The usual definition, but not ours, subdivides stride lengths into left and right legs. But in forward locomotion (overground or on normal treadmill) left and right stride lengths must be the same; if they were unequal, that implies circular, turning locomotion (Hoogkamer et al., 2014). Consequently, in overground and normal treadmill locomotion, both definitions of stride length agree.

In split-belt treadmill locomotion, however, the 2 definitions conflict. During split-belt treadmill locomotion, with treadmill belts moving at different speeds, stride times of the left and right legs remain the same. If stride times were not the same, each leg would accumulate a different number of strides. Even though this phenomenon has been reported in human infants walking on a split-belt treadmill (Yang et al., 2005), human adults retain identical stride times even with large speed-differences between the treadmill belts (Reisman et al., 2005; Stenum & Choi, 2016). Because the legs have the same stride time, but move in separate local inertial reference frames (van Ingen Schenau, 1980) with different speeds, left and right stride lengths must be asymmetrical according to the usual definition of stride length, in which stride length must be defined in each belt's local reference frame. However, using our definition of stride length, as the sum of a pair of successive step lengths, only a single stride length is defined. Thus, in split-belt treadmill locomotion, the usual definition yields 2 unequal stride lengths, whereas we define only a single stride length.

3.1.7 Locomotor pattern constraint of normal treadmill locomotion

In normal treadmill locomotion, the treadmill belt runs at a given speed (v). In treadmill locomotion (when the center of mass remains stationary) the locomotor pattern must therefore, on average, satisfy the following constraint:

$$l_{stride} * t_{stride}^{-1} = v\,. \tag{3.5}$$

3.1.8 Locomotor pattern constraint of split-belt treadmill locomotion

A split-belt treadmill has 2 belts of which speed can be controlled independently. If the left belt speed (v_{L}) and the right belt speed (v_{R}) are different, that creates a speed-difference ($\Delta v = v_{\mathrm{R}} - v_{\mathrm{L}}$) between the belts. When humans locomote on a split-belt treadmill with a speed-difference, each leg is in contact with separate belts so that, during stance, each leg is moving at a different speed compared to stance on the other leg. In this way, each leg is moving in separate local inertial reference frames (van Ingen Schenau, 1980). It is not clear, a priori, how the locomotor pattern is constrained during split-belt treadmill locomotion with a speed-difference.

In Appendix A we derive the following equality constraint on the locomotor pattern during split-belt treadmill locomotion:

$$l_{stride} * t_{stride}^{-1} = \overline{v} - \frac{\Delta v}{2} * asym_{\mathrm{T}}\,, \tag{3.6}$$

where $\overline{v}$ is averaged belt speed and Δv is belt speed-difference.

From Equation 3.6, there is an inverse relationship between stride length and step time asymmetry: at a given stride time and averaged belt speeds, stride length decreases linearly with increasing step time asymmetry. The relationship depends on the belt speed-difference: at greater speed-differences there is a larger reduction in stride length for the same step time asymmetry (Fig. 3.1).

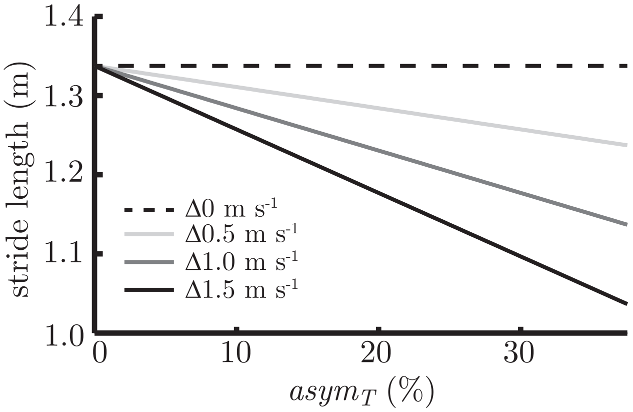

Figure 3.1: Example of relationship between stride length and step time asymmetry ($asym_\mathrm{T}$) on a split-belt treadmill. Split-belt treadmill locomotion without a speed-difference (Δ0 m s^{-1}) and at 3 different speed-differences (Δ0.5 m s^{-1}, Δ1.0 m s^{-1} and Δ1.5 m s^{-1}, in which right belt speed is faster than left belt speed), with the same averaged belt speeds (1.25 m s^{-1}) and at the same stride time (1.07 s). There is a linear decrease in stride length with increasing self-selected $asym_\mathrm{T}$ (i.e. step time is longer from left-to-right than from right-to-left). The rate of decrease in stride length with $asym_\mathrm{T}$ depends on the speed-difference between the treadmill belts: at larger speed-differences, the same $asym_\mathrm{T}$ leads to a shorter stride length.

3.2 Proposed studies

We will leverage the locomotor constraints of either a normal treadmill or a split-belt treadmill to address our aims. We will perform experiment 1 to address aim 1 and perform experiment 2 to address aim 2. In experiment 1 we will test whether kinematic parameters determine the metabolic cost of asymmetry in walking by having subjects walk on a normal treadmill. In experiment 2 we will test whether people exploit asymmetry in order to optimize metabolic cost by having subjects walk on a split-belt treadmill.

3.2.1 Subjects

For each experiment, we will recruit 10 healthy subjects between 18 and 30 years without orthopedic or neurological damage that adversely affects locomotion. Subjects can, but are not required to, participate in more than a single experiment. We will screen for leg length difference and baseline walking asymmetries during a familiarization visit to the laboratory. We justify our sample sizes based on the 10 subjects included in a study that tested the effect of step time asymmetry on metabolic cost (Ellis et al., 2013) and the

11 subjects included in a study that reported the changes in metabolic cost during the adaptation period in split-belt treadmill walking (Finley et al., 2013).

3.2.2 Experimental setup

For both experiments, subjects will come to the laboratory before data collection for a familiarization visit. During the visit, subjects will be screened for baseline asymmetries. To participate in the experiment, leg length difference must be less than 2 cm. Leg length differences less than 2 cm are estimated to have no effect on metabolic cost (Gurney, 2002). Leg lengths will be measured in the supine position as the distance between the anterior superior iliac spine and the lateral malleolus using a tape measure and averaged across 2 measurements (Gurney, 2002). Furthermore, subjects must walk with less than 5% step length and step time asymmetry. We consider kinematic asymmetries less than 5% acceptable because it is within a previously reported range of step length and step time asymmetries of healthy humans during treadmill walking (Kodesh et al., 2012).

Subjects will familiarize to walking on the treadmill with real-time asymmetry feedback. We will use visual feedback to enforce step length and step time asymmetry. To this end, we will use 2 simultaneous feedback systems: one feedback system concerns step time asymmetry and the other system concerns foot placement difference ($\alpha_{\mathrm{L}\to\mathrm{R}}$), both of which will be projected onto a screen in front of the treadmill. By simultaneously controlling step time asymmetry and foot placement difference, we are effectively controlling both step length and step time asymmetry according to the relationship (Finley et al., 2015):

$$l_{\mathrm{L}\to\mathrm{R}} - l_{\mathrm{R}\to\mathrm{L}} = 2\alpha_{\mathrm{L}\to\mathrm{R}} + v_{\mathrm{L}} * t_{\mathrm{L}\to\mathrm{R}} - v_{\mathrm{R}} * t_{\mathrm{R}\to\mathrm{L}}\,. \tag{3.7}$$

The feedback for step time asymmetry will be a bar graph. The height of the bar depends on the actual step time asymmetry (calculated in real-time according to Equation 3.4) that the subject performs. A horizontal line will represent the target step time asymmetry and the subject will be asked to keep the height of the bar graph at the target value. To enforce the target value, the color of the bar graph will turn from blue into green when the bar is within ±2% of the target value. The feedback for foot placement difference consists of 2 boxes that each represent the target positions for left and right foot contacts. The anterior-posterior distance between the boxes is $\alpha_{\mathrm{L}\to\mathrm{R}}$. $\alpha_{\mathrm{L}\to\mathrm{R}}$ will be calculated, from the desired step length and step time asymmetry for the trial, according to Equation 3.7. To guide foot contacts to the target boxes, reflective markers put on the fifth metatarsal on each foot will be represented as blue dots. At either foot contact, the dot will remain fixed at the contact position until the other foot's contact. To enforce successful foot placements, the dot will change color to green within ±1 cm of the target box's center or change to gray outside of the interval.

For the data collection visit, subjects must have fasted 4 hours before they come to the laboratory to ensure that foodstuffs have been absorbed. Furthermore, subjects will be asked not to drink coffee or energy drinks before data collection. Subjects will sit in a chair for 10 minutes and then stand quietly for 5 minutes to measure standing metabolism. Next, subjects will walk on the treadmill for 10 minutes to warm up. During the visit, subjects will walk at 1.25 m s^{-1}. Stride time will be determined after minute 7 of the warm-up period from the time to complete 50 strides (left foot contact to left foot contact) and averaged across 3 trials to get preferred stride time (Umberger & Martin, 2007). For all subsequent trials, stride time will be constrained to the individual subject's preferred stride time by timing either their left or right foot contact to the beat of a metronome. We choose to have subjects walk at a fixed speed of 1.25 m s^{-1} instead of a self-selected, preferred walking speed determined for each individual subject. We choose 1.25 m s^{-1} because it is an intermediate walking speed that is close to people's preferred walking speed and because we do not expect small deviations in this speed range to affect our conclusions regarding the relationship between kinematic asymmetry and metabolic cost.

3.2.3 Experimental design

Experiment 1: Subjects will walk at 1.25 m s^{-1} in 4 experimental conditions where asymmetry will be enforced in either the spatial domain (step lengths), the temporal domain (step times) or concurrently in both domains (Fig. 3.2). Each condition will consist of 4 trials with asymmetry constrained to 5%, 10%, 15% and 20%. In the

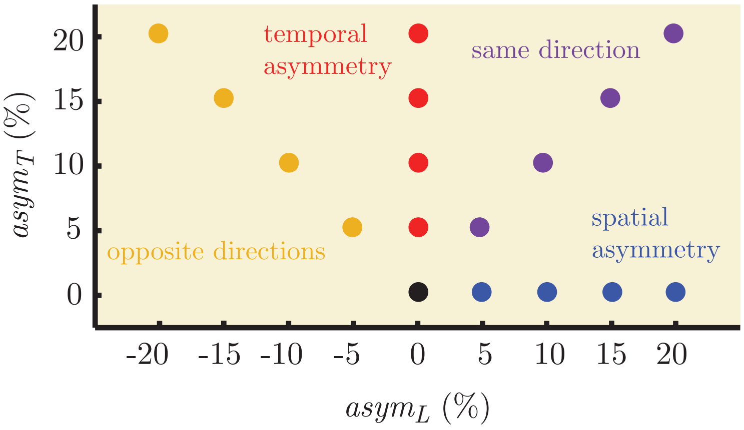

Figure 3.2: Experimental conditions for aim 1. There are 4 experimental conditions where asymmetry will be enforced in either the spatial domain (step lengths, $asym_{\mathrm{L}}$), the temporal domain (step times, $asym_{\mathrm{T}}$) or concurrently in both domains. Each condition will consist of 4 trials with asymmetry constrained to 5%, 10%, 15% and 20%. In the conditions where asymmetry is enforced in only a single domain, asymmetry in the other domain will be constrained to 0% (symmetry) in all 4 trials. In the conditions where asymmetry is enforced concurrently in both domains, asymmetry will be constrained to the same absolute value for both spatial and temporal domains simultaneously, however, since asymmetry is directional, one condition will constrain the domains in the same direction, whereas the other condition will constrain the domain in opposite directions. Additionally, subjects will walk in a symmetrical control condition in which both domains are constrained to 0%.

conditions where asymmetry is enforced in only a single domain, asymmetry in the other domain will be constrained to 0% (symmetry) in all 4 trials. In the conditions where asymmetry is enforced concurrently in both domains, asymmetry will be constrained to the same absolute value for both spatial and temporal domains simultaneously, however, since asymmetry is directional, one condition will constrain the domains in the same direction, whereas the other condition will constrain the domains in opposite directions. Additionally, subjects will walk in a symmetrical control condition in which both domains are constrained to 0%. The order of the 17 trials will be randomized between subjects. Each trial will last 5 minutes. Between trials, subjects will rest for 2 minutes, or longer as necessary, to minimize fatigue.

Experiment 2: Initially, subjects will adapt their locomotor pattern while walking on the split-belt treadmill with a speed-difference between the belts. Even though stride time is constrained, subjects are free to self-select step time asymmetry during the adaptation period. After the adaptation period, subjects will walk in 2 experimental conditions in

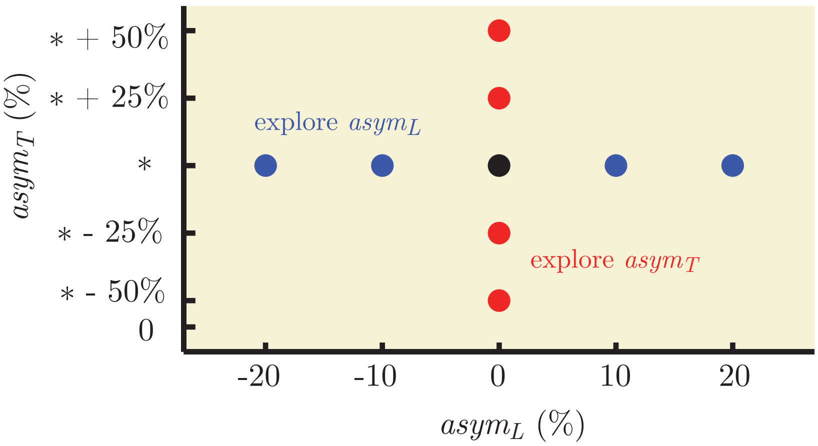

Figure 3.3: Experimental conditions for aim 2. For each speed-difference condition, subjects will walk in 2 experimental conditions in which asymmetry will be enforced in either step lengths ($asym_{\mathrm{L}}$) or times ($asym_{\mathrm{T}}$). In the condition where $asym_{\mathrm{T}}$ is constrained, $asym_{\mathrm{T}}$ will be constrained at the preferred ($*$), preferred ±25% and preferred ±50% (% refers here to percentage of the preferred step time asymmetry) while $asym_{\mathrm{L}}$ will be constrained to zero. In the condition where $asym_{\mathrm{L}}$ will be constrained, $asym_{\mathrm{L}}$ will be constrained to 0, ±5% and ±10% (% refers here to absolute percentage of $asym_{\mathrm{L}}$) while $asym_{\mathrm{T}}$ will be constrained at the preferred value.

which asymmetry will be enforced in either step lengths or step times (Fig. 3.3). In the condition where step time asymmetry is constrained, step time asymmetry will be constrained at preferred, preferred ±25% and preferred ±50% (% refers here to percentage of the preferred step time asymmetry) while step length asymmetry will be constrained to 0%. In the condition where step length asymmetry will be constrained, step length asymmetry will be constrained to 0, ±5% and ±10% (% refers here to absolute percentage of step length asymmetry) while step time asymmetry will be constrained at the preferred value. On separate days, subjects will perform 3 speed-difference conditions with different belt speed-differences on the split-belt treadmill: 0.5 m s^{-1}, 1.0 m s^{-1} and 1.5 m s^{-1} (right belt speed will be faster than left belt speed). All conditions will have the same averaged belt speeds at 1.25 m s^{-1}. The order of the 3 conditions (Δ0.5 m s^{-1}, Δ1.0 m s^{-1} and Δ1.5 m s^{-1}) will be randomized between subjects. Within each condition, the order of the 9 trials will be randomized between subjects. Trials will last 5 minutes, except the adaptation periods which will last 10 minutes (Reisman et al., 2005). Between trials, subjects will rest for 2 minutes, or longer as necessary, to minimize fatigue.

3.2.4 Data collection

Subjects will walk on a split-belt treadmill (Bertec, Columbia, Ohio). Ground reaction forces exerted on each belt will be measured by force plates that are imbedded underneath the belts. Breath-by-breath rates of oxygen consumption and carbon dioxide production will be measured (Parvo Medics, Sandy, Utah). Ten reflective markers will be put bilaterally on the fifth metatarsal, lateral malleolus, fibular head, greater trochanter and anterior superior iliac spine. Reflective markers will be recorded by 4 high-speed cameras (Oqus, Gothenburg, Sweden).

3.2.5 Data analysis

We define foot contact as the instant where the vertical ground reaction force (on separate belts) exceeds 10 N. Foot placements will be measured as the anterior-posterior position (in the global reference frame) of the lateral malleolus marker at the time of foot contact. Step time will be measured as the duration between successive bilateral foot contacts. Step lengths will be calculated analytically from foot placement differences (α), step times and individual belt speeds (Finley et al., 2015). The left-to-right step length will be calculated as:

$$l_{\mathrm{L}\to\mathrm{R}} = \alpha_{\mathrm{L}\to\mathrm{R}} + v_{\mathrm{L}} * t_{\mathrm{L}\to\mathrm{R}}\,, \tag{3.8}$$

while the right-to-left step length will be calculated as:

$$l_{\mathrm{R}\to\mathrm{L}} = \alpha_{\mathrm{R}\to\mathrm{L}} + v_{\mathrm{R}} * t_{\mathrm{R}\to\mathrm{L}}\,. \tag{3.9}$$

For the left-to-right step length, foot placement difference ($\alpha_{\mathrm{L}\to\mathrm{R}}$) is calculated as the right foot's anterior-posterior position at right foot contact subtracted the left foot's anterior-posterior position at the preceding left foot contact, and vice versa for the right-to-left step length's foot placement difference ($\alpha_{\mathrm{R}\to\mathrm{L}}$). Our calculation of step length is in accordance with standard definitions of step length (Zatsiorky et al., 1994), including our own definition, but is different from the modified step length calculation implemented in many studies using a split-belt treadmill (Finley et al., 2013; Reisman et al., 2005). See

Appendix B for a discussion of the implications of either method on step lengths and step length symmetry.

Gross metabolic power will be calculated from rates of oxygen consumption and carbon dioxide production (Brockway, 1987) as:

$$gross\, metabolic\, power = 16.58\frac{W * s}{ml\, O_2} * \dot{V}_{O_2} + 4.51\frac{W * s}{ml\, CO_2} * \dot{V}_{CO_2}\,, \tag{3.10}$$

where $\dot{V}_{O_2}$ and $\dot{V}_{CO_2}$ are rates of oxygen consumption and carbon dioxide production in milliliters per second and gross metabolic power is in watts. Rates of oxygen consumption and carbon dioxide production will be averaged over the last 2 minutes of each trial in which the subject must have reached steady-state metabolism. Net metabolic power will be calculated from gross metabolic power by subtracting the metabolic power during quiet standing. To account for the effect of body mass on metabolism, net metabolic power will be normalized to body mass and expressed as watts per kilogram.

CHAPTER 4

AMENDMENTS TO PROPOSED METHODS

The following chapter summarizes changes in or additions to the dissertation that were made following its proposal.

In experiment 1, the proposed methods do not include a description of how the metabolic cost of the 4 asymmetry conditions is tested. We have amended the methods by using linear fits to measure the metabolic cost of walking with step length asymmetry and step time asymmetry. From the metabolic cost of step length asymmetry and step time asymmetry, we tested if the costs were additive. To this end, we compared the actual metabolic cost of walking with concurrent asymmetry in step lengths and step times to 3 cost models: the cost of step length asymmetry alone, the cost of step time asymmetry alone and the added cost of asymmetry in step lengths and step times.

In experiment 1, we had hypothesized that total positive mechanical work rate is proportional to metabolic cost which would suggest that total work explains the metabolic cost of asymmetrical walking. We have amended the methods by adding the complementary hypothesis that positive work performed in pendular (single support) phases may explain the metabolic cost. This hypothesis is based on previous reports on able-bodied subjects walking asymmetrically (Ellis et al., 2013) and hemiparetic and amputee walking (Adamczyk & Kuo, 2015; Farris et al., 2015) that show an increase in pendular work. The metabolic cost derived from pendular positive work may be regarded as distinct from total positive work over the entire stride since it is possible that asymmetry redistributes work without a concomitant increase in the total amount, and vice versa.

In experiment 1, the proposed methods did not include making a comparison between the mechanical adaptations that our able-bodied subjects undertook to walk asymmetrically and the mechanics of hemiparetic and amputee walking which is often asymmetrical as a result of neurological damage or biomechanical impairment. This comparison may indicate how our results generalize to other types of asymmetry. We quantified how asymmetry influenced production of positive work at the leg-level: how was positive work distributed across the legs and how was the work temporally redistributed across the stride? In order to compare the joint-level mechanical adaptations, we performed a 2D inverse dynamics analysis to obtain mechanical power at the ankle, knee and hip in the sagittal plane. We used the joint power curves to find out if our subjects used a joint-level strategy to increase work that was different to hemiparetic or amputee walking.

In experiment 2, we had proposed to change step time asymmetry to ±50% and ±25% around each subject's preferred value. However, in pilot tests conducted after the submission of the proposal we found that this approach yielded a range of values that was too narrow to provide a meaningful cost landscape in the $\Delta 0.5$ m s^{-1} condition and that the range of values was too wide for subjects to perform in the $\Delta 1.5$ m s^{-1} condition. Instead, we choose to enforce step time asymmetry to ±10% and ±5% (percentage points) around each subject's preferred value which yielded a range that was equal between speed-difference conditions, large enough to outline a meaningful cost landscape and remained narrow enough so that our subjects could walk according to the feedback that we presented.

In experiment 2, we had not planned to report the values of foot placement difference as part of the manuscript for the study. We enforced foot placement difference and step time asymmetry in order to indirectly constrain step length asymmetry; since the relationship between the 3 variables is redundant, it is not necessary to report foot placement difference when characterizing the gait parameters. However, we have chosen to report foot placement differences which is partly motivated from recent literature on split-belt treadmill walking in which the effect of foot placement difference on metabolic cost is tested (Sánchez et al., 2019). Furthermore, other recent studies have sought to influence metabolic cost by changing foot placement difference (Roemmich et al., 2019;

Sánchez & Finley, 2018) which makes it meaningful to explicitly present the metabolic data according to foot placement difference.

CHAPTER 5

METABOLIC COST AND MECHANICS OF ASYMMETRICAL STEP LENGTHS AND STEP TIMES IN WALKING

5.1 Introduction

Hemiparetic and unilateral amputee walking is often asymmetrical so that gait parameters pertaining to the 2 steps of the stride cycle—such as step lengths and step times—are unequal (Isakov et al., 2000; Patterson et al., 2008; Roerdink et al., 2007; Sanderson & Martin, 1997). These kinematic asymmetries derive from neurological damage or biomechanical impairment: people that have suffered a stroke often have an unaffected leg and a weaker paretic leg, whereas unilateral amputees have an intact leg and a leg fitted with a prosthesis. Hemiparetic and amputee gait is also metabolically costlier than able-bodied gait (Waters & Mulroy, 1999), and, consequently, asymmetry is often attributed to account for the greater energy expenditure. Despite this contention, the energetic cost associated with having asymmetrical gait parameters is not well understood.

Asymmetry in step lengths and step times have been linked to increases in metabolic energy expenditure of walking. Step length asymmetry has been hypothesized to incur an added metabolic cost based on analysis of simple bipedal walking models (Srinivasan, 2011); yet no experimental evidence has directly shown that asymmetrical step lengths incur an added metabolic cost. A single experiment of able-bodied people walking with step time asymmetry showed an added cost compared to walking symmetrically (Ellis et al., 2013). However, step lengths were free to vary in this study which makes it difficult to ascribe the added cost of asymmetry to the separate effects of either the cost of asymmetry in step lengths or step times or, alternatively, their additive cost.

What is the biomechanical origin that makes muscles consume more metabolic energy in asymmetrical walking? Analysis of an inverted pendulum walking model suggests that collisional losses of center of mass energy—incurred during double support periods when the leading leg performs negative work on the center of mass—may increase with gait asymmetry (Adamczyk & Kuo, 2009, 2015; Srinivasan, 2011). Collisional losses may be predicted from step length and the center of mass velocity at heel-strike (Adamczyk & Kuo, 2009). Asymmetry in step lengths and step times may thus influence collisional losses from their combined effect on step lengths and center of mass velocity. Collisional losses are regarded as the dominant loss of center of mass energy over the stride cycle and net mechanical work performed on the center of mass must equal zero over the stride cycle to maintain a fixed walking speed; therefore, increases in collisional losses may increase total positive work performed on the center of mass over the stride, which, in turn, should exact a metabolic cost (Donelan et al., 2002a). Indeed, studies on amputee (Adamczyk & Kuo, 2015; Houdijk et al., 2009) and hemiparetic walking (Farris et al., 2015), and asymmetrical walking in able-bodied subjects (Ellis et al., 2013), have noted increases in collisional losses and positive work which suggest that the increased demand of total mechanical work may explain the metabolic cost of asymmetry.

A complementary explanation of why asymmetrical walking increases metabolic cost derives from a temporal shift in the generation of positive mechanical work during the stride cycle. In symmetrical, able-bodied walking, the stance leg performs positive work on the center of mass during 2 periods of stance: about a third of the total positive work is supplied during the beginning half of the pendular phase (the single support period) and about two-thirds are supplied as push-off (by the trailing leg during double support, Kuo et al. (2005)). Both amputee and hemiparetic walking are often characterized by the inability to supply ample push-off work by the prosthetic or paretic leg (Adamczyk & Kuo, 2015; Farris et al., 2015; Houdijk et al., 2009). Consequently, positive work must be generated elsewhere in the stride cycle. A temporal shift of positive work—from push-off to pendular work—has been noted in amputee (Adamczyk & Kuo, 2015; Houdijk et al., 2009) and hemiparetic walking (Farris et al., 2015), and asymmetrical walking in able-bodied subjects (Ellis et al., 2013). The metabolic cost derived from pendular positive work may be regarded as distinct from total positive work over the entire stride: it is possible that asymmetry redistributes work without a concomitant increase in the total amount, and vice versa.

Analyzing the mechanical work by each leg and their joints may provide insights into the adaptations that a person's gait undertakes when walking asymmetrically. The added positive work (over either the stride or in pendular phases) in amputee and hemiparetic walking primarily derives from greater work performed by the intact or unaffected leg (Adamczyk & Kuo, 2015; Farris et al., 2015). Likewise, in asymmetrical walking by able-bodied subjects (Ellis et al., 2013), postive work increased on the leg that had a long stance time which is equivalent to the intact and unaffected legs in amputee and hemiparetic walking. At the joint level, positive work is predominantly (but not exclusively) generated at the knee in the pendular phases and by the ankle in push-off during symmetrical, able-bodied walking (Kuo et al., 2005). In both amputee (Beyaert et al., 2008) and hemiparetic walking (Farris et al., 2015), the knee on the intact or unaffected leg performs additional positive work compared to the affected leg or to the leg of able-bodied control subjects. It is unknown whether the previously reported leg- and joint-level mechanics reflect inevitable mechanics of asymmetrical walking or specific adaptations undertaken in amputee or hemiparetic walking (Adamczyk & Kuo, 2009; Houdijk et al., 2009; Farris et al., 2015), or when able-bodied subjects are instructed to walk asymmetrically (Ellis et al., 2013).

Here, we first asked if the metabolic cost of asymmetry in step lengths and step times are additive: when people walk with concurrent asymmetry in both step lengths and step times is the metabolic cost explained by the cost of step length asymmetry, step time asymmetry or the additive cost? We devised an experimental setup which allowed us to enforce asymmetrical step lengths and step times during treadmill walking and we had able-bodied subjects complete our experimental protocol. Second, we tested the hypotheses that asymmetry would increase both collisional losses of center of mass energy and total positive work performed on the center of mass, and that asymmetry would redistribute positive work to pendular phases. To explain the mechanical origin of the metabolic cost of asymmetry, we hypothesized that the increases in positive work would explain the metabolic cost with increased asymmetry. Last, we characterized how our able-bodied subjects redistributed the positive work across the legs and which joints accounted for this redistribution in order to describe how our results, of able-bodied subjects instructed to walk asymmetrically, may generalize to other cases of gait asymmetry.

5.2 Methods

5.2.1 Subjects

Ten healthy young subjects (5 males and 5 females; age 24±3 years (mean±SD); body mass 71.7±13.7 kg; leg length 0.85±0.04 m) without orthopedic or neurological disorders completed the study. We measured the length of subjects' legs as the distance between the greater trochanter and the lateral malleolus in the supine position before enrollment in the study. Our inclusion criteria included that subjects' leg length difference was less than 2 cm which we estimate to have a negligible effect on energy consumption during walking (Gurney, 2002). All subjects gave informed written consent before the study in accordance with the protocol approved by the local Institutional Review Board (protocol 2018-4813).

5.2.2 Experimental design

Our goal was to enforce a range of different combinations of asymmetry in step lengths and step times during normal treadmill walking. In order to do so we devised an experimental setup in which we directly enforced stride time, step time asymmetry and foot placement difference and indirectly enforced step length asymmetry (Fig. 5.1A). We introduce our measures of asymmetry and foot placement difference here. We defined step time asymmetry ($asym_{\mathrm{T}}$) as:

$$asym_{\mathrm{T}} = \frac{t_{\mathrm{L}\to\mathrm{R}} - t_{\mathrm{R}\to\mathrm{L}}}{t_{\mathrm{L}\to\mathrm{R}} + t_{\mathrm{R}\to\mathrm{L}}} * 100\%\,, \tag{5.1}$$

and step length asymmetry ($asym_{\mathrm{L}}$) as:

$$asym_{\mathrm{L}} = \frac{l_{\mathrm{L}\rightarrow\mathrm{R}} - l_{\mathrm{R}\rightarrow\mathrm{L}}}{l_{\mathrm{L}\rightarrow\mathrm{R}} + l_{\mathrm{R}\rightarrow\mathrm{L}}} * 100\%\,, \tag{5.2}$$

where t is step time, l is step length and the subscript $\mathrm{L}\rightarrow\mathrm{R}$ refers to the step from the left leg's heel-strike to right leg's heel-strike and $\mathrm{R}\rightarrow\mathrm{L}$ refer to the step from the right leg's heel-strike to the left leg's heel-strike. An asymmetry of zero means equal step times or lengths. Our asymmetry measure is directional: positive asymmetry is step times or lengths that are greater from left-to-right heel-strikes than right-to-left heel-strikes, and vice versa for negative asymmetry. Foot placement difference (α) is the anterior-posterior distance between the position of an anatomical landmark on either foot at successive bilateral heel-strikes. Foot placement differences are defined for both steps; during steady-state walking, foot placement differences are equal but opposite between the 2 steps (see Fig. 5.1B for graphical overview of gait parameters). We indirectly enforced a specific step length asymmetry by setting the foot placement difference according to (see Appendix C for derivation):

$$\alpha = \frac{1}{2} * t_{stride} * v * (asym_{\mathrm{L}} - asym_{\mathrm{T}})\,, \tag{5.3}$$

where t_{stride} is stride time and v is treadmill belt speed.

5.2.3 Experimental protocol

In order for subjects to perform our experiment they had to be able to control stride time, step time asymmetry and foot placement difference. We devised an experimental setup in which stride time was enforced by the beat of a metronome while step time asymmetry and foot placement difference were enforced by real-time visual feedback projected onto a screen in front of the treadmill (Bertec, Columbus, OH, USA). Visual feedback of step time asymmetry was indicated by the height of a bar graph that continually changed depending on the subject's performance (Labview, National Instruments, Austin, TX, USA). We instructed subjects to keep the height of the bar graph near a horizontal line

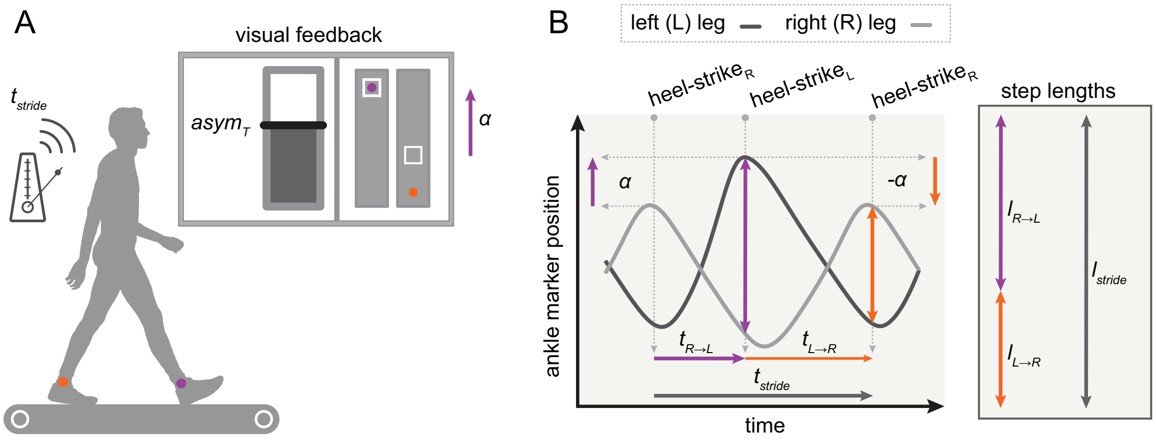

Figure 5.1: Overview of gait parameters and experimental setup. (A) Experimental setup: stride time was enforced by the beat of a metronome while step time asymmetry ($asym_{\mathrm{T}}$) and foot placement difference (α) were enforced by real-time visual feedback projected onto a screen in front of the treadmill. We indirectly enforced step length asymmetry by calculating foot placement difference according to Eq. 5.3. (B) Overview of and relationship between gait parameters: step time (t), stride time (t_{stride}), step length (l), stride length (l_{stride}), left-to-right step ($\mathrm{L} \rightarrow \mathrm{R}$), right-to-left step ($\mathrm{R} \rightarrow \mathrm{L}$) and foot placement difference (α).

that represented the target value. Once the bar graph was within ±2% of the target value the color of the bar changed from blue to green to indicate satisfactory performance. Visual feedback of foot placement difference consisted of 2 stationary boxes that each represented target positions for left and right feet at heel-strikes (Microsoft Visual Studio, Redmond, VA, USA). We indirectly controlled subjects' step length asymmetry from stride time, step time asymmetry and foot placement difference by calculating the anterior-posterior distance between the boxes using Eq. 5.3. To guide foot placements to the target boxes, real-time feedback of the anterior-posterior position of reflective markers put on each ankle were represented by blue dots. At either foot's heel-strike, the dot remained fixed at the contact position until the other foot's heel-strike. To enforce foot placements, the dot changed color to green within ±1 cm of the target box's center or changed to gray outside the interval.

It was challenging for subjects to simultaneously control stride time, step time asymmetry and foot placement difference. Therefore, on a prior day to data collection, subjects came in for a training visit to learn how to control stride time, step time asymmetry and foot placement difference according to the feedback that we presented to them. The training visit lasted about 1.5 hour and subjects only continued with the study if they were able to successfully walk according to the feedback presented to them.

Subjects fasted and refrained from coffee or energy drinks 4 hours before the data collection visit. At the beginning of the data collection visit, subjects sat for 10 minutes after which they stood for 5 minutes while we measured their standing metabolism. Next, subjects walked on the treadmill for 10 minutes at 1.25 m s^{-1} to warm up. We presented no feedback to the subjects during the warm-up period. After minute 7 of the warm-up period we timed the duration to complete 50 strides, and repeated this twice, in order to obtain each subject's preferred stride time. In all subsequent trials, subjects' stride time was enforced to their preferred value by the beat of a metronome. We chose to keep stride time constant since it is well-documented that there is a U-shaped relationship between stride time and metabolic cost when walking at a fixed speed (Umberger & Martin, 2007); by keeping stride time constant we avoided the confounding effect of stride time on energy cost.

Following the warm-up period, subjects completed 17 experimental trials, each lasting 5 minutes, in which different combinations of step time asymmetry and step length asymmetry were enforced while subjects walked on the treadmill at 1.25 m s^{-1}. The 17 trials comprised 4 asymmetry conditions of each 4 trials and one symmetrical condition in which step lengths and step times were enforced to symmetry (see Table 5.1 for overview of gait parameters in asymmetry conditions). The 4 asymmetry conditions were made up of one condition with only step length asymmetry while step times were equal ($\boldsymbol{asym}_{\mathbf{l}}$), one condition with only step time asymmetry while step lengths were equal ($\boldsymbol{asym}_{\mathbf{t}}$) and 2 conditions with concurrent asymmetry in which step lengths and step times were enforced to either equal values of asymmetry in the same direction (***same dir.***), or to equal values of asymmetry in opposite directions (**opp.dir**.). In the condition with concurrent asymmetry in the same direction, one step (left-to-right) had a long length and a long time while the other step (right-to-left) had a short length and a brief time. In the condition with concurrent asymmetry in opposite directions, one step (left-to-right) had a short length and a long time while the other step (right-to-left) had a long length and a brief time. For all asymmetry conditions, the target asymmetry values

Table 5.1: Overview of asymmetry conditions' gait parameters. The symbols +, − and 0 denote positive, negative and zero asymmetry.

Condition	Step	l	t	$asym_{\mathrm{L}}$	$asym_{\mathrm{T}}$
$\boldsymbol{asym_{\mathrm{l}}}$	L → R	long	sym.	+	0
	R → L	short	sym.		
$\boldsymbol{asym_{\mathrm{t}}}$	L → R	sym.	long	0	+
	R → L	sym.	brief		
same dir.	L → R	long	long	+	+
	R → L	short	brief		
opp. dir.	L → R	short	long	−	+
	R → L	long	brief		

in either step lengths or step times were set at 5%, 10%, 15% and 20%. In the symmetrical condition (***sym.***), asymmetry in both step lengths and step times were set at 0%. Subjects rested 2 minutes, or longer if necessary, between trials. The order of the 17 experimental trials were randomized between subjects.

5.2.4 Data collection

Four high-speed cameras (Qualisys Oqus, Gothenburg, Sweden) recorded 8 reflective markers at 100 Hz that we put bilaterally on the fifth metatarsal, lateral malleoli, fibular head and greater trochanter. Force plates embedded in each treadmill belt recorded ground reaction forces at 1000 Hz. We recorded breath-by-breath rates of oxygen consumption and carbon dioxide production (Parvo Medics Trueone 2400, Sandy, UT, USA).

5.2.5 Data processing

We low-pass filtered kinematic data at 7 Hz and kinetic data at 10 Hz. After filtering ground reaction forces, we removed offset and drift. We defined heel-strikes and toe-offs as the instant that the vertical ground reaction force crossed 10 N. We visually inspected vertical ground reaction forces and corrected any spurious heel-strikes or toe-offs. Step times were calculated as the period between consecutive bilateral heel-strikes. We calculated foot placement differences for left-to-right and right-to-left steps as the anterior-posterior difference between the ankle markers' position at subsequent bilateral heel-strikes. Step lengths were calculated from foot placement difference and the product of step time and belt speed. In order to express the value of asymmetry according to a single dimension, we converted asymmetry in step lengths and times into an aggregate asymmetry ($asym_{agg.}$) which was calculated differently between conditions: for the conditions with only step length asymmetry (***asym*_l**) and only step time asymmetry (***asym*_t**), aggregate asymmetry was set at the value of either step length asymmetry or step time asymmetry, respectively; for the symmetrical condition (***sym.***) and the conditions with concurrent asymmetry in the same direction (***same dir.***) and opposite directions (***opp. dir.***), aggregate asymmetry was calculated as the average of the absolute values of step length asymmetry and step time asymmetry. We clustered data according to the actual asymmetry values that our subjects performed in order to graphically present data. We clustered data post-hoc and determined ranges based on cut-off points that yielded an approximately equal number of data points within each cluster (4 clusters with each 7, 8, 9 and 12 data points, 9 clusters with 10 data points and 4 clusters with 11 data points). For the symmetrical condition, aggregate asymmetry varied between 0% and 2%; for all asymmetrical conditions, data were clustered based on aggregate asymmetry values of 2–7%, 7–10%, 10–15% and 15–25%.

We obtained center of mass velocity by integrating the net ground reaction forces of both legs and adding the treadmill belt speed to the anterior-posterior direction (Adamczyk & Kuo, 2009). We used the nomenclature proposed by Adamczyk & Kuo (2009) in which phases of the stride cycle refer to pendular motion of the center of mass or transitions between pendular periods; as such, we labeled double support periods as transition periods and single support periods as pendular periods. We calculated pre-transition center of mass velocity as the instantaneous center of mass velocity at the heel-strike of each leg. Predicted collisional losses of center of mass energy were calculated as the product of squared step length (l) and pre-transition center of mass velocity (v_{pre}): $l^2 * v_{pre}^2$ (Adamczyk & Kuo, 2009). We calculated the instantaneous power that each leg produced on the center of mass from the dot product of center of mass velocity and each legs' ground reaction forces (Donelan et al., 2002a). By integrating either the positive or negative portions of each legs' instantaneous power curve over intervals of the stride, we calculated the following terms: collisional losses of center of mass energy from negative power production in double support by the leading leg; and pendular, push-off and total positive work from positive power production during single support, double support by the trailing leg and across the entire stride (note that the mechanical work that the leg performs on the center of mass during swing is zero when using this method). We used 2D inverse dynamics to obtain ankle, knee and hip instantaneous power in the sagittal plane across the stride cycle (Winter, 1990). For both measures of instantaneous mechanical power (on the center of mass or at joints), we discarded the stance phases in which we detected that the stance leg produced vertical force on the opposite force plate. We divided mechanical work by stride time to get average rate of mechanical work. We calculated gross metabolic power from the rates of oxygen consumption and carbon dioxide production (Brockway, 1987) and subtracted standing metabolism to obtain net metabolic power which we refer to as metabolic cost.

We used the average of the last 2 minutes of each trial to obtain the values of all our parameters. Mechanical and kinematic data are always presented as the sum across both legs or steps; and, for joint work, as the sum across legs and joints, unless otherwise noted. In order to normalize data between subjects, we used dimensionless data using as base units body mass (M), gravitational acceleration (g) and leg length (L). Mean non-dimensionalization factors were: 0.85 for step length (L), 2.89 for center of mass velocity ($(gL)^{0.5}$), 600.80 for work (MgL) and 2035.57 for power ($Mg^{1.5}L^{0.5}$). When variables are presented at increasing levels of asymmetry, we express the effect of asymmetry by expressing the variable as its percentage relative to the symmetrical condition.

5.2.6 Statistics

To test if the metabolic cost of step length asymmetry and step time asymmetry were additive, we, first, created 3 alternative cost models based on the cost of step length asymmetry alone, the cost of step time asymmetry alone or the added cost of step length asymmetry and step time asymmetry, and, second, tested which cost model best explained the metabolic cost of concurrent asymmetry. For each individual subject, we used linear regressions to fit the metabolic cost of the $\boldsymbol{asym}_{\mathbf{l}}$ condition and the $\boldsymbol{asym}_{\mathbf{t}}$ condition versus $asym_{agg.}$. From each subject's 2 regressions, we used the slope and intercept of the $\boldsymbol{asym}_{\mathbf{l}}$ condition's data for the cost model of step length asymmetry, the slope and intercept of the $\boldsymbol{asym}_{\mathbf{t}}$ condition's data for the cost model of step time asymmetry, and the sum of slopes and the averaged intercept for the cost model of the additive cost of asymmetry in step lengths and times. For each subject's metabolic cost of concurrent asymmetry (***same dir.*** and ***opp. dir.***), we calculated the residuals between the 3 models' predicted cost and the actual metabolic cost of concurrent asymmetry. We evaluated which model best explained the metabolic cost of concurrent asymmetry as the model that yielded the minimum sum of the absolute value of residuals. We used one-sample t-tests of each models' residuals to test if the models tended to under- or over-estimate the cost of concurrent asymmetry. To test if the models predicted the actual metabolic cost differently between ***same dir.*** and ***opp. dir.*** conditions, we compared their residuals using two-sample t-tests.

We performed linear regressions to evaluate directional trends and strength of relationships between asymmetry, mechanical and metabolic data. Information on linear fits (slope, intercept, r^2 and P) are presented in Appendix D. All linear regressions were performed using all individual data points, not clustered data points. We set the level of significance at 0.05. All statistical tests were performed in Matlab (Mathworks, Natick, MA, USA).

5.3 Results

Subjects successfully walked on the treadmill according to the feedback so that asymmetrical step lengths and step times were enforced according to the different conditions (Fig. 5.2A). In the condition with asymmetrical step lengths and equal step times ($\boldsymbol{asym}_{\mathbf{l}}$), step time asymmetry was kept constant around zero (ensemble mean 0.4%); and in the condition with asymmetrical step times and equal step lengths ($\boldsymbol{asym}_{\mathbf{t}}$), step length asymmetry was kept constant around zero (ensemble mean 0.0%).

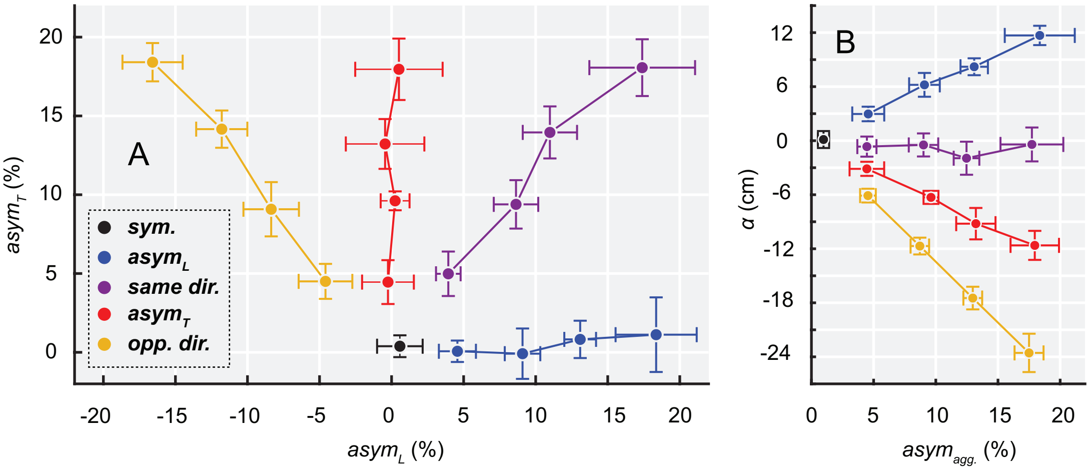

Figure 5.2: Asymmetrical gait parameters. (A) Subjects successfully walked with step length asymmetry ($asym_{\mathrm{L}}$) and step time asymmetry ($asym_{\mathrm{T}}$) according to the conditions that we enforced through visual real-time feedback. (B) Step length asymmetry was enforced by systematically changing foot placement difference (α). Dots are clustered data and error bars are standard deviations.

We did, however, note that conditions with concurrent asymmetry (***same dir.*** and ***opp. dir.***) were, on average, slightly biased toward greater asymmetry in step times than in step lengths: step time asymmetry was on average 1.4% and 1.2% greater than step length asymmetry for ***same dir.*** and ***opp. dir.***, respectively. Desired step length asymmetry was indirectly enforced by foot placement differences (Fig. 5.2B): at an asymmetry of 10%, foot placement difference increased (right leg steps anteriorly to the left leg's step) by about 7.0 cm for $\boldsymbol{asym}_{\mathbf{l}}$, and decreased (left leg steps anteriorly to the right leg's step) by about 7.0 cm and 14.0 cm for $\boldsymbol{asym}_{\mathbf{t}}$ and ***opp. dir.***, respectively; while for ***same dir.***, foot placement difference remained constant around 0 cm. For all trials, stride time was enforced to subjects' preferred value (ensemble mean±SD 1.08±0.06 s) and was kept constant throughout the experiment (coefficient of variation 0.4%).

5.3.1 The metabolic cost of step time asymmetry best explains the cost of concurrent asymmetry

Walking with either step length asymmetry and equal step times ($\boldsymbol{asym}_{\mathbf{l}}$) or step time asymmetry and equal step lengths ($\boldsymbol{asym}_{\mathbf{t}}$) incurred a metabolic cost (Fig. 5.3A). However, the cost of $\boldsymbol{asym}_{\mathbf{t}}$ (slope=3.65) was more than twice the cost of $\boldsymbol{asym}_{\mathbf{l}}$

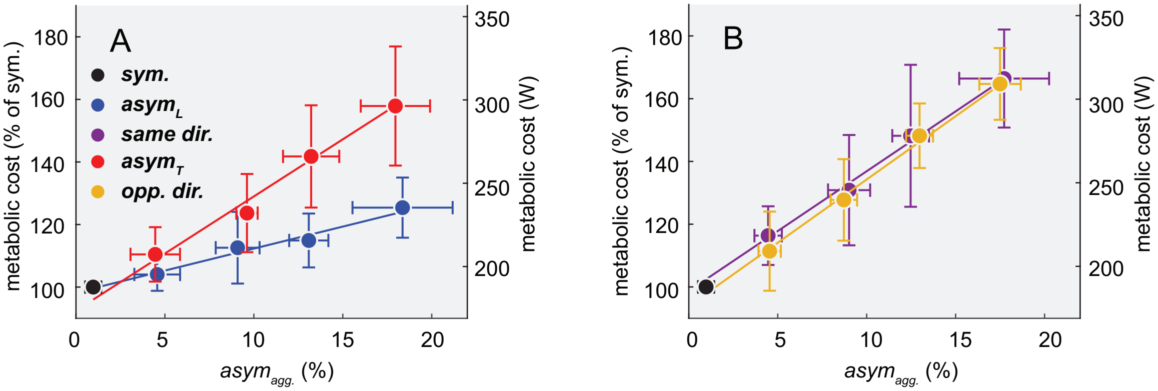

Figure 5.3: Metabolic cost of asymmetry. Cost in (A) only step lengths ($\boldsymbol{asym}_{\mathbf{l}}$) and only step times ($\boldsymbol{asym}_{\mathbf{t}}$) and (B) concurrent asymmtry in the same direction (***same dir.***) or opposite directions (***opp. dir.***). Dots are clustered data and error bars are standard deviations. See Table D.1 on page 116 for information on linear fits.

(slope=1.41). Walking with concurrent asymmetry in step lengths and step times also incurred a metabolic cost (Fig. 5.3B; ***same dir.***: slope=3.81; ***opp. dir.***: slope=4.03). Walking with an asymmetry of 10% incurred an added metabolic cost of about 12% when walking with step length asymmetry and equal step times ($\boldsymbol{asym}_{\mathbf{l}}$); when walking with step time asymmetry ($\boldsymbol{asym}_{\mathbf{t}}$, ***same dir.*** and ***opp. dir.***), the added cost covered the range of 29–37% and agreed well with previously reported data on the metabolic cost of step time asymmetry (Ellis et al., 2013).

The cost model of the separate metabolic cost of step time asymmetry alone ($\boldsymbol{asym}_{\mathbf{t}}$; slope 3.52±0.79 (ensemble mean±SD) and intercept 94.6±4.4) best explained the cost of concurrent asymmetry (Fig. 5.4C,D; sum of absolute value of residuals=817). The cost model of step time asymmetry did, however, slightly underestimate the cost of concurrent asymmetry (average residual=−6.3; $P<0.001$), but the underestimation was not affected by magnitude of asymmetry (Fig. 5.4D; slope=−0.50, $P=0.070$). Furthermore, residuals were not statistically different between the conditions with concurrent asymmetry ($P=0.380$). This suggests that the metabolic cost of step time asymmetry predicts the cost of walking with concurrent asymmetry well, regardless of the asymmetries' direction.

The cost model of the separate cost of step length asymmetry alone and of the additive cost yielded opposing trends. The model of the separate cost of step length asymmetry (Fig. 5.4A,B; $\boldsymbol{asym}_{\mathbf{l}}$; slope 1.45±0.55 (ensemble mean±SD) and intercept

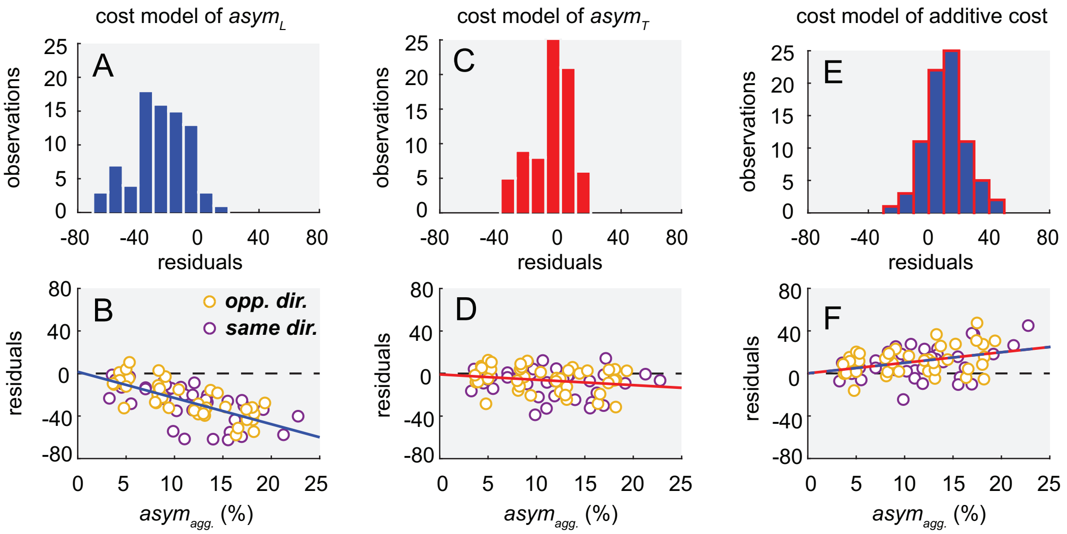

Figure 5.4: Residuals between actual metabolic cost of concurrent asymmetry and predicted cost from 3 cost models. Histograms of residuals for cost model of step length asymmetry (A), step time asymmetry (C) and additive cost (E). Residuals shown versus magnitude of asymmetry ($asym_{agg.}$) for cost model of step length asymmetry (B), step time asymmetry (D) and additive cost (F). See Table D.1 on page 116 for information on linear fits.

98.1±4.2; sum of absolute residuals=2073) underestimated the cost of concurrent asymmetry (average residual $=-25.5$; $P<0.001$) and the underestimation increased with greater magnitude of asymmetry (Fig. 5.4B; slope$=-2.40$, $P<0.001$). On the other hand, the cost model of the additive cost of asymmetry in step lengths and step times (Fig. 5.4E,F; slope 4.97±1.26 (ensemble mean±SD) and intercept 96.3±3.8; sum of absolute residuals=1121) overestimated the cost of concurrent asymmetry (average residual=11.3; $P<0.001$) and the overestimation increased with greater asymmetry (Fig. 5.4F; slope=0.99, $P=0.001$).

Overall, our metabolic data show that the metabolic cost of step time asymmetry is more than twice the cost of step length asymmetry, that the cost of asymmetrical step lengths and step times are not additive and that the cost of walking with concurrent asymmetry is best explained by the cost of step time asymmetry alone.

5.3.2 Asymmetry increases collisional losses and positive work, and redistributes work to pendular phases

The combination of asymmetrical step lengths and step times yielded differences in the 2 steps' pre-transition center of mass velocity and the effect was different between the asymmetry conditions (see Fig. D.1A–E on page 113 in Appendix D). The pre-transition velocity for the left-to-right step was greater than for the right-to-left step in the $\boldsymbol{asym}_{\mathbf{l}}$ condition. When walking with step time asymmetry, the pre-transition velocity went from being about equal (***same dir.***) to being greater ($\boldsymbol{asym}_{\mathbf{t}}$) and much greater (***opp. dir.***) for the right-to-left than the left-to-right step. Overall, asymmetry influenced step lengths and pre-transition velocities such that the predicted collisional losses of center of mass energy increased with asymmetry (Fig. 5.5A, slopes between 0.57 and 1.50). Actual collisional losses were well-correlated with predicted collisional losses (Fig. 5.5B, r^2=0.57) which suggests that simple gait parameters can predict collisional losses during walking as proposed by Adamczyk & Kuo (2009).

Next, we tested correlations between collisional losses and positive mechanical work performed on the center of mass over the entire stride or only during the pendular phases. Positive work increased with collisional losses: a 10 J increase in collisional losses increased total positive work by about 8.0 J (Fig. 5.5C, r^2=0.77) while pendular work increased by about 10.2 J (Fig. 5.5D, r^2=0.85). These correlations reflect strong relationships between collisional losses and positive mechanical work that is consistent with the assumptions of collisional walking models (Donelan et al., 2002a); however, they do not necessarily reflect an effect of asymmetry.

To express the effect of asymmetry on the magnitude of mechanical work, we compared collisional losses and positive work with asymmetry. Collisional losses (Fig. 5.6A; slopes between 1.85 and 3.89) and total positive work (Fig. 5.6B; slopes between 0.71 and 0.98) increased with asymmetry which is consistent with our predictions. Total positive work increased modestly compared to collisional losses: an asymmetry of 10% increased losses within the range of 4.7–9.8 J (from 25.3 J during symmetrical walking), and total positive work within the range of 3.2–4.4 J (from 45.4 J

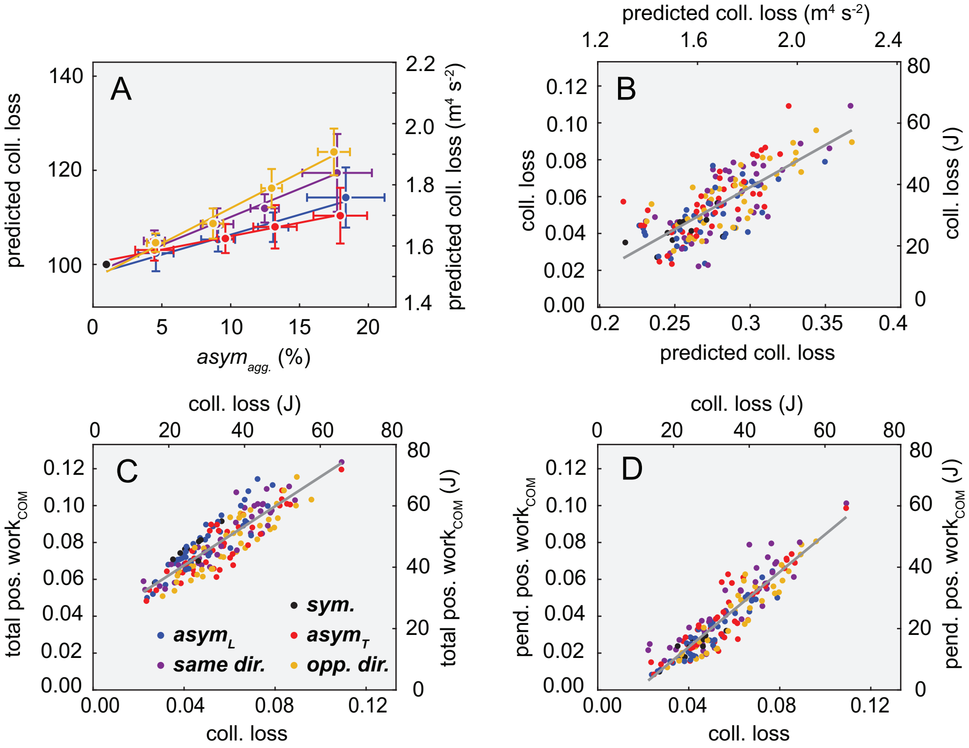

Figure 5.5: Relationships between measures of center of mass mechanics. (A) The effect of asymmetry ($asym_{agg.}$) on predicted collisional losses of center of mass energy (calculated as $l^2 * v_{pre}^2$). Dots are clustered data and error bars are standard deviations. (B) Relationship between predicted and actual collisional losses. (C) Relationship between collisional losses and total positive work performed on the center of mass over the entire stride. (D) Relationship between collisional losses and pendular positive work. Top x-axes and right-hand y-axes display dimensionalized predicted collisional losses in m^4 s^{-2} (A,B) and work in J (B–D). See Table D.2 on page 116 for information on linear fits.

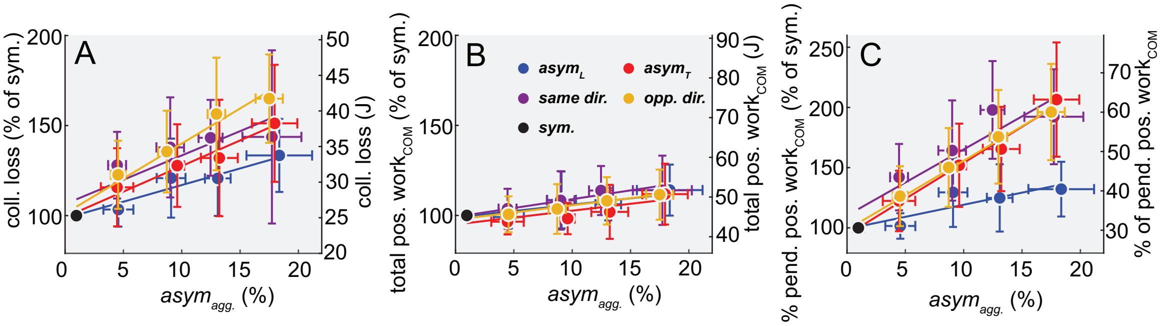

Figure 5.6: Relationships between asymmetry and mechanical work performed on the center of mass. (A) Relationship between asymmetry ($asym_{agg.}$) and collisional losses of center of mass energy. (B) Relationship between asymmetry and total positive work performed on the center of mass over the entire stride. (C) Relationship between asymmetry and the percentage of pendular positive work relative to total positive work. Dots are clustered data and error bars are standard deviations. Right hand Y-axes display work quantities dimensionalized to J (A,B) or in percentage of total positive work (C). See Table D.2 on page 116 for information on linear fits.

during symmetrical walking). We note that even though asymmetry increases collisional losses, asymmetry also decreases negative work in the last half of single support (see Fig. D.1F-J on page 113 in Appendix D) and, therefore, total negative (and thereby positive) work increase at a lower rate than collisional losses. We also note that the effect of asymmetry on collisional losses (r^2 between 0.27 and 0.54) and total positive work (r^2 between 0.15 and 0.17) yielded rather weak relationships which partly reflect a large inter-subject variability of the effect of asymmetry.

As asymmetry increased, there was a temporal redistribution in positive work (Fig. 5.6C): while 30.6% of the positive work was performed during the pendular phase in symmetrical walking, an asymmetry of 10% increased the proportion to about 36.5% when walking with asymmetrical step lengths and equal step times (**$asym_{\mathrm{l}}$**), and when walking with asymmetrical step times the proportion increased to 47.1%, 50.6% and 47.6% for **$asym_{\mathrm{t}}$**, ***same dir.*** and ***opp. dir.***, respectively. This temporal shift in positive work is consistent with our predictions and previous studies on asymmetry in able-bodied subjects (Ellis et al., 2013), and amputee (Adamczyk & Kuo, 2015) and hemiparetic walking (Farris et al., 2015).

5.3.3 Does mechanical work explain the metabolic cost of asymmetry?

We had hypothesized that increases in positive mechanical work explained the metabolic cost associated with walking asymmetrically. Therefore, we tested the relationship between metabolic cost and rate of positive work performed over either the entire stride or only during pendular phases. The rate of total positive work across the stride poorly explained metabolic cost when expressed as the rate of work that the legs performed on the center of mass (Fig. 5.7A, r^2=0.26) or even when expressed as the summed work across joints (Fig. 5.7B, r^2=0.13). On the other hand, the relationship between rate of positive pendular work and metabolic cost yielded stronger correlations for both rate of work performed on the center of mass (Fig. 5.7C, r^2=0.51) and summed joint work (Fig. 5.7C, r^2=0.63). This suggests that the increase in pendular work with asymmetry may exact a metabolic cost that explains a significant portion of the metabolic cost of asymmetrical walking.

5.3.4 Leg- and joint-level adaptations to asymmetrical walking

The temporal shift in positive work from push-off to pendular phases with increasing asymmetry was performed differently between the conditions with step time asymmetry ($\boldsymbol{asym}_{\mathbf{t}}$, ***same dir.*** and ***opp. dir.***) and the condition with asymmetrical step lengths and equal step times ($\boldsymbol{asym}_{\mathbf{l}}$). For the conditions with step time asymmetry, push-off work tended to decrease in both legs (Fig. 5.8A,B; slopes between -0.0002 and -0.0009) and the increase in pendular work was mainly driven by the left leg (Fig. 5.8C,D; slopes for left and right legs from 0.0013 to 0.0015 and from 0.0002 to 0.0007, respectively). For the condition with asymmetrical step lengths and equal step times, push-off work increased on the left leg (Fig. 5.8A; slope=0.0004), but decreased on the right leg (Fig. 5.8A; slope=-0.0005), while pendular work tended to increase on both legs (Fig. 5.8C,D). Amputee and hemiparetic gaits often have step time asymmetry (Isakov et al., 2000; Roerdink et al., 2007) and the leg-level mechanics of our conditions with step time asymmetry (in which work performed by the left leg—which has a long stance time—increased) agree with amputee and hemiparetic gait mechanics in which more work

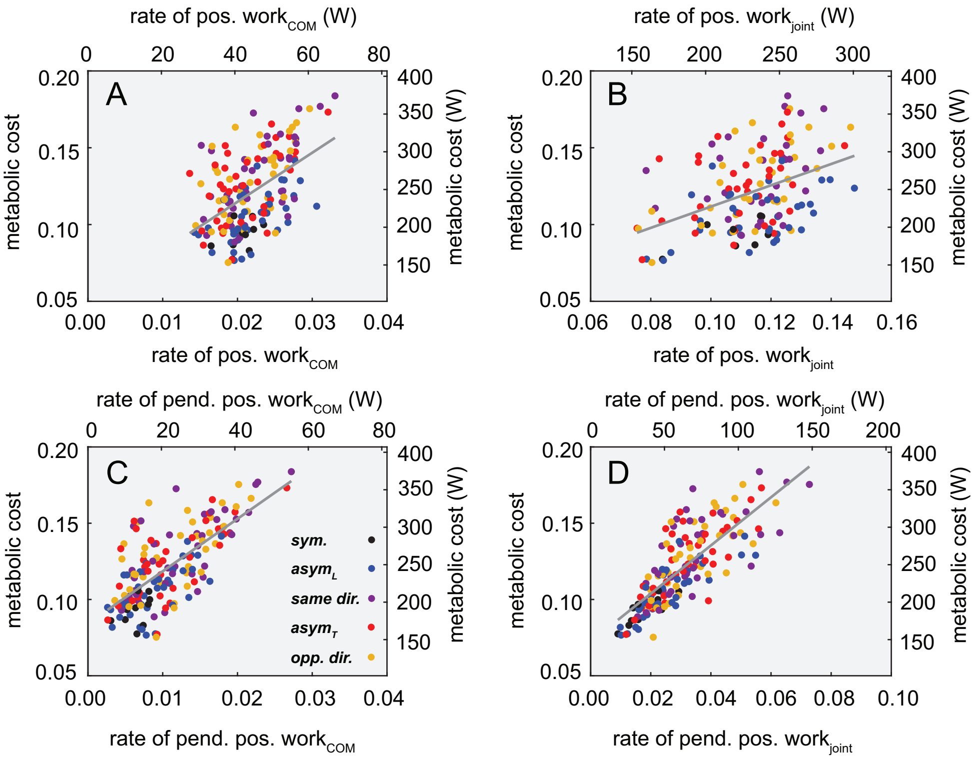

Figure 5.7: Relationships between the rate of positive mechanical work, performed over entire stride or in pendular phases, and metabolic cost. Rate of work is calculated using both work performed on the center of mass (A,C) and summed joint work (B,D); and, furthermore, over the entire stride (A,B) and in pendular phases (C,D). Top X-axes and right-hand Y-axes display work rates and metabolic cost dimensionalized to W. See Table D.3 on page 117 for information on linear fits.

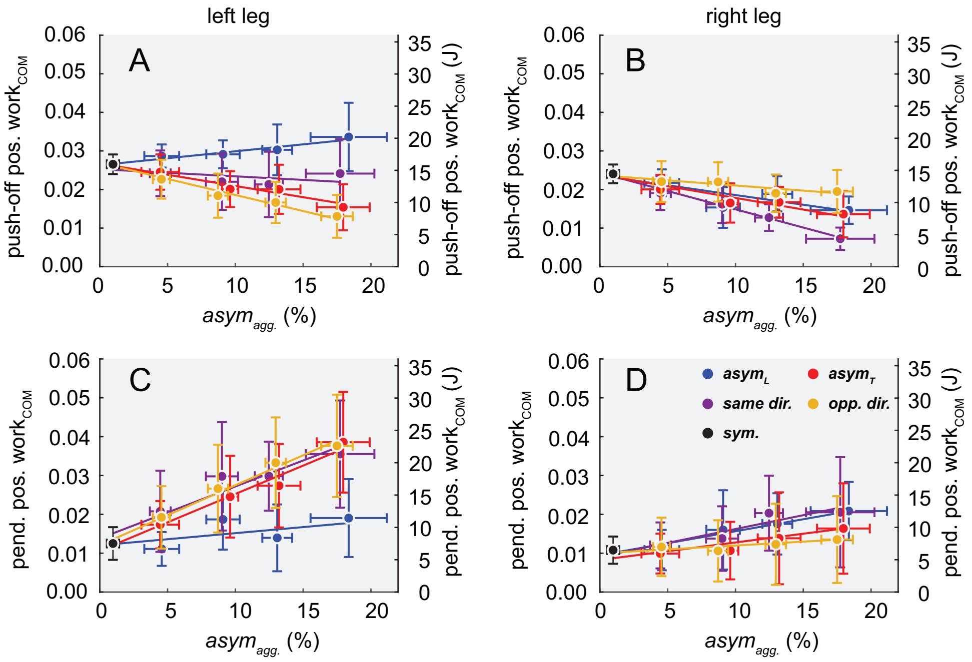

Figure 5.8: Positive work performed on the center of mass by left and right legs during push-off and pendular phases. Positive work during push-off (A,B) and pendular phases (C,D). Dots are clustered data and error bars are standard deviations. Right-hand Y-axes display work dimensionalized to J. See Table D.4 on page 117 for information on linear fits.

is performed by the intact or unaffected leg—which have a long stance duration compared to the prosthetic or affected legs—particularly in the pendular phase (Adamczyk & Kuo, 2015; Farris et al., 2015). Averaged across legs, at an asymmetry of 10%, push-off work decreased by about 0.9 J for $\boldsymbol{asym}_{\mathbf{l}}$ and within the range of 6.6–7.1 J for the conditions with step time asymmetry, relative to 30.4 J performed in the symmetrical condition. In the pendular phases, an asymmetry of 10% increased positive work by about 5.6 J for $\boldsymbol{asym}_{\mathbf{l}}$ and within the range of 10.5–12.3 J for the conditions with step time asymmetry, relative to 14.3 J in symmetrical walking.

Next, we tested if the increase in pendular positive work with asymmetry was driven by work performed around the ankle, knee or hip in order to characterize our subjects' joint-level adaptation to asymmetrical walking. We found that work at the ankle primarily drove the increase in pendular positive work across all conditions (Fig. 5.9A, r^2=0.71 for ankle work; Fig. 5.9B, r^2=0.12 for knee work; Fig. 5.9C, r^2=0.21 for hip work). An increase in pendular ankle work has, to our knowledge, not been observed in

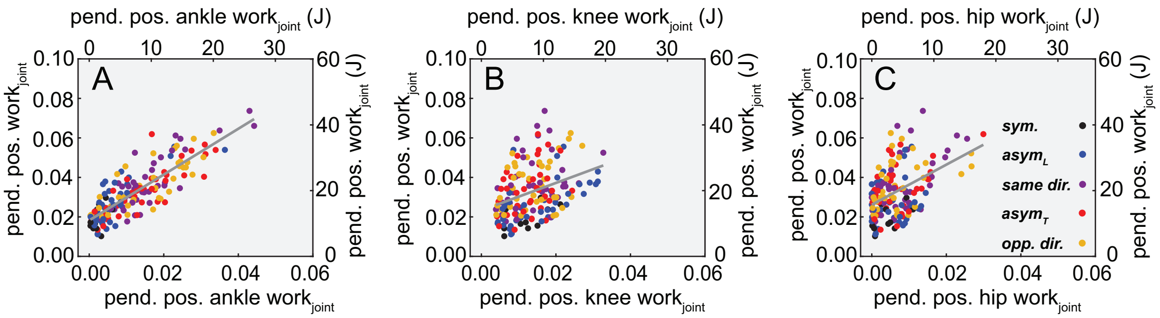

Figure 5.9: Relationships between pendular positive work summed across joints and pendular work of individual joints. Relationships are presented between summed pendular joint work and joint work at the ankle (A), knee (B) and hip (C). Top X-axes and right-hand Y-axes display work dimensionalized to J. See Table D.4 on page 117 for information on linear fits.

amputee or hemiparetic gait which suggest that our able-bodied subjects performed an adaptation to asymmetrical walking that is distinct from other types of gait asymmetry. See Appendix D (pages 113–115) for mechanical power at the ankle, knee and hip (Fig. D.1K–Z) and overview of total push-off and pendular work together with each joint's relative contribution (Figs. D.2 and D.3).

5.4 Discussion

We instructed able-bodied people to walk with a range of different combinations of asymmetry in step lengths and step times and found that metabolic cost of step time asymmetry was more than twice the cost of step length asymmetry, but that the costs were not additive. Rather, the metabolic cost of walking with concurrent asymmetry in step lengths and step times is best explained by the separate cost of step time asymmetry alone. Across all combinations of asymmetry, our data suggest that a significant portion of the metabolic cost of asymmetry derives from an increase in positive work performed during the pendular phases of walking. The leg-level mechanical similarities between our able-bodied subjects and hemiparetic or amputee walkers suggest that our findings may generalize to people who habitually walk asymmetrically. Still, joint-level mechanics suggest differences and we discuss the implications below.

Our data show that step time asymmetry better captures the metabolic cost of asymmetry than step length asymmetry or foot placement difference which we systematically enforced. Recent studies have tried to influence the metabolic cost of hemiparetic gait through changes in step length asymmetry or foot placements (Sánchez & Finley, 2018; Roemmich et al., 2019). However, both studies found that metabolic cost remained invariant to changes in these gait parameters. Our results may explain these surprising findings. Since hemiparetic gait already has asymmetrical step times (Roerdink et al., 2007), metabolic cost is largely invariant to changes in step length asymmetry or foot placement difference and is instead determined by the cost of step time asymmetry. Other studies have found correlations between metabolic cost and step length asymmetry or foot placement differences in hemiparetic walking (Awad et al., 2015; Finley & Bastian, 2017). However, this may not indicate a causal relationship and the correlations may be explained from concomitant changes to step time asymmetry (or equivalent temporal asymmetries in stance or swing time) or changes in other confounding gait parameters. We acknowledge that our data also show that step length asymmetry, when walking with equal step times, increases metabolic cost so we cannot discount that contribution completely even though the of cost step length asymmetry was less than half of the cost of step time asymmetry. Overall, we conclude that changing step time asymmetry is more effective than changing step length asymmetry or foot placement differences for inducing changes in metabolic cost.

We found that positive work increases when quantified across the entire stride or only in pendular phases which is consistent with our predictions. Positive work has been proposed to drive the increases in metabolic cost of asymmetrical walking (Srinivasan, 2011; Ellis et al., 2013). We found that rate of work across the stride poorly explained the metabolic cost—which was true even when work rate was quantified by summed joint work to address the short-comings of center of mass measures of work in estimating musculotendon work (Sasaki et al., 2009). On the other hand, rate of pendular work correlated better with metabolic cost which suggest that the increase in positive work during the pendular phases explained a significant portion of the metabolic cost of asymmetry. This finding agrees with studies of hemiparetic gait that suggest that the increased metabolic cost is mainly derived from work by the unaffected leg in pendular phases (Stoquart et al., 2012; Chen et al., 2005). We propose that this cost is not specific to hemiparetic walking, but reflects a metabolic cost of asymmetry that may generalize to asymmetrical walking in other populations.

We do not rule out other sources of the metabolic cost of asymmetry. Importantly, the swing phases may incur a metabolic cost in asymmetrical walking. This may especially be important for conditions with asymmetrical step times in which the 2 legs have either a long or a brief swing period. Based on the non-linear changes in estimated metabolic cost of leg swing, the cost of swinging one leg quickly may not offset the reduced cost of swinging the other leg slowly (Doke et al., 2005; Doke & Kuo, 2007). We do not present data on swing cost for the present study, but we note that hip power of the leg with a short swing period (left leg) in the conditions with step time asymmetry ($\boldsymbol{asym}_{\mathbf{t}}$, ***same dir.*** and ***opp. dir.***; see Fig. D.1X–Z on page 113 in Appendix D) appeared to increase around the onset of the swing phase which may exact a high metabolic cost. Mechanical power at the hip does, however, not quantify rate of force production of hip muscles which has been suggested to dominate the metabolic cost of leg swing for brief swing periods (Doke & Kuo, 2007). In addition, subjects may also have increased muscle co-contraction which will increase metabolic cost, but we did not record muscle activity and cannot quantify this contribution. Subjects did, however, come to the laboratory for a training visit which means that the co-contraction normally associated with initial motor learning was likely minimized in the present study. While we suggest that pendular work explained a significant portion of the metabolic cost of asymmetry and propose additional costs, it is important to note that the metabolic cost of asymmetry in amputee or hemiparetic walking is likely subjected to additional interacting costs that may be specific to each person's particular impairment.

In our conditions with step time asymmetry ($\boldsymbol{asym}_{\mathbf{t}}$, ***same dir.*** and ***opp. dir.***), mechanical work increased on the leg with a long stance time (left leg). This is equivalent to amputee and hemiparetic walking which has step time asymmetry and in which the intact or unaffected leg has a long stance time and performs more work than the other leg. It is difficult to compare our condition with asymmetrical step lengths and equal step times ($\boldsymbol{asym}_{\mathbf{l}}$) to asymmetry in amputee or hemiparetic gaits which show step time asymmetry (Roerdink et al., 2007; Isakov et al., 2000). Overall, our conditions with step time asymmetry show important leg-level mechanical similarities to amputee and hemiparetic walking which suggest that our results may generalize to other types of gait asymmetry. We did, however, note a major difference between joint work in our able-bodied subjects and amputee or hemiparetic walking: a large portion of the increase in pendular positive work by our subjects was accomplished by work at the ankle. Naturally, pendular ankle work is not increased on an amputated leg or a paretic leg with weak plantarflexor muscles, but ankle work may still be increased on the intact or unaffected leg. However, increased ankle work has not been observed in amputee or hemiparetic walking. Rather, an increase in positive knee work appears to drive much of the increase in pendular work (Beyaert et al., 2008; Farris et al., 2015). There are several possibilities to why our subjects increased pendular ankle work: first, work performed at the ankle may be a task-specific control strategy that our subjects chose in order to match the real-time feedback that we presented to them; second, ankle work may be metabolically cheaper than performing the same work at other joints because of ankle plantarflexors' high capacity for elastic energy storage and release (Sawicki et al., 2009). If the pendular ankle work is indeed performed at a lower metabolic cost than work at other joints, that suggest that the metabolic cost of asymmetry in amputee or hemiparetic gait may exact an even higher cost than we present here.

We found that pendular positive work (rather than total positive work as we had hypothesized) explained a significant portion of the metabolic cost of asymmetrical walking. The metabolic cost of pendular work contrasts the idea that positive work performed in step-to-step transitions is a major determinant of the metabolic cost of walking (Donelan et al., 2002a). Even though step-to-step transitions require substantial mechanical work, several studies have suggested that the work is performed at a relatively low metabolic cost (Sawicki & Ferris, 2009; Umberger, 2010). It is important to note that pendular and step-to-step transition work may be causally linked: if transition work is decreased, which we noted in our study, pendular work may be the only feasible period in which this work can be made up in order to maintain a fixed walking speed (Huang et al., 2015). Regardless, our data suggest that it is the metabolic cost of performing pendular work that is driving the metabolic cost of asymmetry. The cost of performing positive work in pendular phases agree with the cost of raising the body's center of mass in normal (Neptune et al., 2004) or hemiparetic walking (Chen et al., 2005; Stoquart et al., 2012). However, we do not necessarily contend that the function of the positive pendular work in asymmetrical walking is to raise the center of mass. We note that positive ankle power in the pendular phases (see Fig. D.1F–J on page 113 in Appendix D) is not exclusively performed in the first half of the pendular phase (single support) which is the period in which gravitational potential energy increases, but extend to the later part in which kinetic energy increases—it is therefore possible that a function of the increased pendular work is to increase the body's kinetic energy.

Step time asymmetry in both hemiparetic and amputee walking is generally consistent between people: the step time from the unaffected leg's heel-strike to the affected leg's heel-strike spans a longer duration than the other step (Isakov et al., 2000; Roerdink et al., 2007); as such, the unaffected leg has the longest stance time and the briefest swing time (Patterson et al., 2008; Sanderson & Martin, 1997). The direction of step length asymmetry, on the other hand, does not show a clear directionality between people (Roerdink & Beek, 2011; Roerdink et al., 2012). Our result may partly explain why the direction of step length asymmetry is so variable between people with amputation or stroke survivors. When walking with step time asymmetry, step length asymmetry does not change metabolic cost. It is therefore possible that step length asymmetry is not controlled based on people's propensity to walk with energetically optimal gait parameters (Selinger et al., 2015). Instead other factors such as joint loading, capacity for leg-swing propulsion or stability may influence the preferred direction of step length asymmetry. We note that the leading leg's knee absorbs energy during transition periods that is likely accompanied by a large extensor moment at the knee which may increase loading (see Fig D.1P–T on page 113 in Appendix D). Step length asymmetry systematically changed the magnitude of negative knee work in the 2 steps' transitions. The systematic differences in the legs' energy absorption at the knee may suggest that the direction of step length asymmetry could be controlled by individual strategies to distribute knee loading optimally across the legs.

Even though we have shown that asymmetrical walking exacts a metabolic cost, that does not necessarily imply that asymmetry is energetically sub-optimal in amputee or hemiparetic gait. Recent studies indicate that the preferred asymmetry in amputee gait is energetically optimal (Handford & Srinivasan, 2018; Wedge, 2019). Wedge (2019) had people with a unilateral trans-tibial amputation walk on a treadmill while stance time asymmetry was enforced to a range of values around each person's preferred value and found that amputee walkers preferred asymmetry in stance times and that the preferred asymmetry was energetically optimal. It is unknown how this may generalize to other types of asymmetry or hemiparetic gait. Furthermore, there have been recent attempts to use gait training of hemiparetic walking to test how people's propensity to use energetically optimal gait parameters may be leveraged in order to enforce more symmetrical gait patterns (Roemmich et al., 2019; Sánchez & Finley, 2018). So far, conclusive evidence for the efficacy of this approach is lacking which may be explained from our finding that metabolic cost remains invariant to changes in step length asymmetry and foot placement differences when walking with concurrent step time asymmetry. Understanding how gait asymmetry can be manipulated in order to create more economical gait remains an important question with implications for rehabilitation. But further studies are required to understand the costs associated with and the control of asymmetry in step lengths and step times in clinical populations.

CHAPTER 6

HUMANS EXPLOIT GAIT ASYMMETRY TO MINIMIZE ENERGY COST OF WALKING: ENERGETIC OPTIMIZATION DURING SPLIT-BELT TREADMILL WALKING IS DEPENDENT ON STEP TIME ASYMMETRY

6.1 Introduction

Human walking is normally symmetrical with gait parameters like step times and step lengths being about equal across left and right legs (Ankaralı et al., 2015; Kodesh et al., 2012). It is possible that symmetrical walking is preferred because symmetry is energetically optimal (Ellis et al., 2013; Srinivasan, 2011). Even though symmetry is preferred in healthy human walking, people that have suffered a stroke or amputees that use a prosthetic leg often walk asymmetrically as a result of neurological damage or biomechanical impairment. Furthermore, they often expend more energy to walk than healthy humans do (Waters & Mulroy, 1999), and, consequently, their asymmetry has been proposed to account for the added energy cost. An alternative explanation is that—even though symmetry is energetically optimal under normal circumstances—asymmetrical gait parameters may be adopted because *asymmetry* is energetically optimal under the imposed constraints, whether neurological or biomechanical.

Symmetry may be one among other gait parameters, such as walking speed and the combination of stride time and stride length, that may be selected because they are energetically optimal (Bertram, 2005; Sparrow & Newell, 1998). The idea that preferred gait parameters are selected from optimization of energy cost is illustrated from *cost landscapes* that outline how different values of given gait parameters affect energy use

(Croft et al., 2019). For example, if people walk on a normal treadmill which constrains the combination of stride time and stride length to match the treadmill's speed, the range of combinations of stride time and stride length that satisfies the treadmill's constraint outlines a U-shaped cost landscape from which people prefer to use the energetically optimal combination of stride time and stride length (Umberger & Martin, 2007).

Adaptability of walking symmetry has been demonstrated using a split-belt treadmill in which the treadmill's 2 belts run at different speeds (Reisman et al., 2005). We and others have shown that step lengths are initially asymmetrical during split-belt treadmill walking, but return to symmetry following a short adaptation period on the treadmill of about 10 minutes (Choi et al., 2009; Reisman et al., 2005). Distinct temporal and spatial motor outputs (identified as step time asymmetry and foot placement difference) contribute to the adaptation of symmetry in step lengths during split-belt treadmill walking (Malone et al., 2012). Neurophysiological studies have suggested that different neural structures control temporal and spatial motor outputs (McCrea & Rybak, 2008; Darmohray et al., 2019) which may also imply that temporal and spatial outputs are controlled separately.

While symmetry is preferred during normal conditions, it is not obvious that symmetry is preferred during split-belt treadmill walking. Indeed, symmetry in some gait parameters, such as step lengths, can only be achieved from asymmetry in other gait parameters, such as step time asymmetry or foot placement difference. During split-belt treadmill walking, healthy humans adopt a combination of steady-state gait parameters with asymmetrical step times and different foot placements (such that the leg on the fast belt steps anteriorly to the leg on the slow belt), while step lengths are about symmetrical (Finley et al., 2015). Error-based learning prescribes that symmetrical gait parameters are desirable during split-belt treadmill walking (Roemmich & Bastian, 2018), but the underlying reason why people adopt their combination of preferred, steady-state gait parameters, some of which are symmetrical while others are asymmetrical, remains unclear.

A complementary idea to error-based learning is that split-belt treadmill adaptation may be driven by energy optimization (Finley et al., 2013). But since the energetic cost landscape during split-belt treadmill walking is poorly understood, the idea that energy optimization controls split-belt treadmill adaptation remains unresolved. Adaptation of step lengths towards symmetry has been proposed to drive reductions in energy cost during the adaptation period (Finley et al., 2013). However, experimental data that map the cost landscape by changing foot placement differences in order to change step length asymmetry have not shown conclusive trends: one study did not report a clear relationship (Sánchez et al., 2017) while another study (Sánchez et al., 2019) suggested that energy cost decreased, plateaued and thereafter increased moderately as foot placement differences increased in order to enforce step length asymmetry within a range of values from asymmetry, in which the step length from fast-to-slow belts was longest, over symmetry and, finally, to asymmetry, in which the step length from slow-to-fast belts was longest. Both studies reported that symmetrical step lengths did not optimize energy cost and estimated that a value of step length asymmetry, where the step length from slow-to-fast belts was longest, was energetically optimal. A major drawback of the reported cost landscapes of split-belt treadmill walking is that they do not capture a range of combinations of step time asymmetry, foot placement difference and step length asymmetry to thoroughly describe the cost landscapes. Furthermore, stride time was allowed to vary which may have affected energy cost (Stenum & Choi, 2017). Moreover, it is unknown how the magnitude of speed-differences between the treadmill's 2 belts influence the cost landscapes.

Here, we tested if adapted, steady-state step time asymmetry, foot placement difference and step length asymmetry are energetically optimal across 3 different split-belt treadmill conditions in which speed-differences between the treadmill's belts were set at 0.5 m s^{-1}, 1.0 m s^{-1} and 1.5 m s^{-1} around an average belt speed of 1.25 m s^{-1}. Our results show that people choose step time asymmetry to optimize cost, but that foot placement differences and step length asymmetry are not energetically optimal. From analyzing a simple cost model of walking, we show that the existence of an energetically optimal step time asymmetry may arise from the split-belt treadmill's constraint on stride length and stride time. Overall, our results suggest that asymmetrical gait parameters may be selected to optimize energy cost when human gait adapts to an asymmetrical constraint.

6.2 Methods

6.2.1 Definitions

Because the definition of gait parameters can be equivocal on a split-belt treadmill (Hoogkamer et al., 2014), we start by defining our gait parameters of interest. During split-belt treadmill walking, the experimenter can set one treadmill belt to run at a slow speed (v_{S}) and the other treadmill belt to run at a fast speed (v_{F}). The treadmill's environment can be described using the average belt speed ($\overline{v} = \frac{1}{2}(v_{\mathrm{F}} + v_{\mathrm{S}})$) and belt speed-difference ($\Delta v = v_{\mathrm{F}} - v_{\mathrm{S}}$). One leg, therefore, contacts the slow treadmill belt while the other leg contacts the fast treadmill belt. The stride cycle consists of 2 steps: a step from the slow leg's heel-strike to the fast leg's heel-strike ($\mathrm{S}\to\mathrm{F}$) and a step from the fast leg's heel-strike to the slow leg's heel-strike ($\mathrm{F}\to\mathrm{S}$). We define step time (t) as the duration between successive bilateral heel-strikes and stride time (t_{stride}) as the sum of a pair of successive step times. We define step length (l) as the anterior-posterior distance between the same anatomical landmark on either foot between successive bilateral foot contacts and stride length (l_{stride}) as the sum of a pair of successive step lengths (Hoogkamer et al., 2014; Zatsiorky et al., 1994). We use a standard method to define asymmetry and calculate step time asymmetry ($asym_{\mathrm{T}}$) as:

$$asym_{\mathrm{T}} = \frac{t_{\mathrm{S}\to\mathrm{F}} - t_{\mathrm{F}\to\mathrm{S}}}{t_{\mathrm{S}\to\mathrm{F}} + t_{\mathrm{F}\to\mathrm{S}}} * 100\%\,, \tag{6.1}$$

and step length asymmetry ($asym_{\mathrm{L}}$) as:

$$asym_{\mathrm{L}} = \frac{l_{\mathrm{S}\to\mathrm{F}} - l_{\mathrm{F}\to\mathrm{S}}}{l_{\mathrm{S}\to\mathrm{F}} + l_{\mathrm{F}\to\mathrm{S}}} * 100\%\,. \tag{6.2}$$

An asymmetry of zero means equal step times or lengths. Our asymmetry measure is directional: positive asymmetry is step times or lengths that are greater from slow-to-fast heel-strikes than fast-to-slow heel-strikes, and vice versa for negative asymmetry.

Foot placement difference (α) is the anterior-posterior distance between the position of an anatomical landmark on either foot at successive bilateral heel-strikes. Foot placement differences are defined from heel-strikes on slow-to-fast belts and from fast-to-slow belts; however, with steady-state gait parameters, foot placement differences are equal but opposite between the 2 steps. In our analysis of split-belt treadmill walking, we assume steady-state gait parameters in which foot placement difference indicates the slow-to-fast parameter. A positive foot placement difference indicates that the leg on the fast belt steps anteriorly to the leg on the slow belt (see Fig. 6.1A for overview of gait parameters).

During split-belt treadmill walking with steady-state gait parameters, step time asymmetry, step length asymmetry and foot placement difference are related according to (see derivation in Appendix C):

$$\alpha = \frac{1}{2} * t_{stride} * \left(\overline{v} * (asym_{\mathrm{L}} - asym_{\mathrm{T}}) + \frac{\Delta v}{2} * (1 - asym_{\mathrm{L}} * asym_{\mathrm{T}})\right). \tag{6.3}$$

This means that steady-state gait parameters are produced by a unique combination of step time asymmetry, foot placement difference and step length asymmetry. For example, one, and only one, foot placement difference satisfies a given combination of step time asymmetry and step length asymmetry. If step time asymmetry is constant, foot placement difference and step length asymmetry vary proportionally. Likewise, foot placement difference and step time asymmetry vary proportionally if step length asymmetry is constant.

6.2.2 Split-belt treadmill's constraint on the combination of stride length and stride time

In normal walking the combination of stride time and stride length yields a walking speed (v) according to:

$$l_{stride} * t_{stride}^{-1} = v\,. \tag{6.4}$$

When walking on a normal treadmill, the belt's speed constrains the combination of stride time and stride length so that they must match the treadmill's speed. How does the split-belt treadmill's 2 different speeds constrain the combination of stride time and stride length? We show (see derivation in Appendix A) that the combination of stride time and stride length is constrained by the average belt speed, the belt speed-difference and people's self-selected step time asymmetry:

$$l_{stride} * t_{stride}^{-1} = \overline{v} - \frac{\Delta v}{2} * asym_{\mathrm{T}}\,. \tag{6.5}$$

During split-belt treadmill walking, stride time and stride length remain proportional like on a normal treadmill, but on a split-belt treadmill they are proportional to average belt speed, belt speed-differences and step time asymmetry. Average belt speed and belt speed-difference is set by the experimenter and cannot be changed by the person walking on the treadmill. Step time asymmetry, on the other hand, can be changed volitionally by the person on the treadmill. Step time asymmetry interacts linearly with the belt speed-difference to change the proportionality of stride time and stride length. At constant stride time, step time asymmetry linearly decreases stride length and the rate depends on belt speed-difference.

6.2.3 Cost model and prediction of optimal step time asymmetry

We use a cost model of walking that includes a stance cost and a swing cost (Kuo, 2001). The cost of stance is based on the positive muscle work that must be performed to make up for collisional losses of center of mass energy incurred by the leading leg during step-to-step transitions (Donelan et al., 2002b). Collisional losses of center of mass energy can be derived from the step-to-step transition's step length (l) and the instantaneous center of mass velocity at the onset of the transition (v_{pre}) such that collisional energy losses are proportional to the product of squared step length and center of mass velocity (Adamczyk & Kuo, 2009). Therefore, stance cost is proportional to:

$$stance\,cost \propto \Sigma l^2 * v_{pre}^2\,, \tag{6.6}$$

where Σ denotes the sum of the 2 steps of the stride cycle. Our swing cost is based on hip muscles' rate of force production during the swing phase (Doke & Kuo, 2007). Swing cost can be derived from step time (t), which we assume to be proportional to swing time, such that swing cost is proportional to the inverse of step time raised to the third power (Doke & Kuo, 2007; Kuo, 2001):

$$swing\,cost \propto \Sigma t^{-3}\,, \tag{6.7}$$

where Σ denotes the sum of the 2 steps of the stride cycle. To convert our mechanical stance and swing costs to metabolic cost, we weigh the stance cost to account for 74% of the cost of the stride cycle and the swing cost to account for the remaining 26% when walking on a normal treadmill at 1.25 m s^{-1} (Doke et al., 2005; Gottschall & Kram, 2005; Marsh et al., 2004; Umberger, 2010). Our cost model therefore expresses metabolic cost as the percentage of the cost of normal, symmetrical walking at 1.25 m s^{-1}.

We use the split-belt treadmill's constraint on stride time and stride length (Eq. 6.5) together with our cost model (Eqs. 6.6 and 6.7) to predict how step time asymmetry changes metabolic cost of split-belt treadmill walking. We do this for 3 speed-difference conditions in which the average speed of the treadmill's belts is always at 1.25 m s^{-1} and the speed-differences are set at 0.5 m s^{-1}, 1.0 m s^{-1} and 1.5 m s^{-1}. We denote the conditions Δ0.5 m s^{-1}, Δ1.0 m s^{-1} and Δ1.5 m s^{-1}. The belt speeds are set at 1.00 m s^{-1} and 1.50 m s^{-1} for the Δ0.5 m s^{-1} condition, at 0.75 m s^{-1} and 1.75 m s^{-1} for the Δ1.0 m s^{-1} condition and 0.50 m s^{-1} and 2.00 m s^{-1} for the Δ1.5 m s^{-1} condition. In all scenarios, we keep stride time constant and constrain step lengths to be symmetrical while step time asymmetry changes. As step time asymmetry changes, it interacts with the belt speed-difference to shorten stride length (Eq. 6.5) which, in turn, decreases stance cost (Eq. 6.6). The belt speeds of each speed-difference condition also influence stance cost through the pre-transition center of mass velocity term (Eq. 6.6); we set pre-transition center of mass velocity to the belt speed that the leading leg steps onto at each step (Adamczyk & Kuo, 2009). As belt speed-differences increase, stance cost also increases. Step time asymmetry influences swing cost because one leg has a brief step time while the other leg has a long step time; this, in turn, increases swing cost (Eq. 6.7).

6.2.4 Subjects

Ten healthy young subjects (5 males and 5 females; age 20±1 years (mean±SD); body mass 66.1±12.7 kg; leg length 0.82±0.06 m) without orthopedic or neurological disorders completed the study. Another 6 subjects only performed a training visit and did not perform the data collection visits either because they did not learn to use our real-time visual feedback to guide walking or because they did not wish to participate in the study. All subjects gave informed written consent before the study in accordance with the protocol approved by the local Institutional Review Board (protocol 2018-4813).

6.2.5 Experimental design

Our experiment consisted of 2 parts. First, we assessed the preferred, steady-state step time asymmetry, foot placement difference and step length asymmetry that people adopt in split-belt treadmill walking. Second, we tested if the preferred gait parameters are energetically optimal in a series of cost mapping trials.

During 3 laboratory visits on separate days, subjects walked on a split-belt treadmill (Bertec, Columbus, OH, USA) in 3 different conditions in which the average belt speed was always 1.25 m s^{-1} and the speed-difference between the belts was 0.5 m s^{-1}, 1.0 m s^{-1} and 1.5 m s^{-1} (Fig. 6.1B). The left belt was always set at the slow belt speed in all conditions. The order of the 3 speed-difference conditions was randomized between subjects.

During each visit, subjects performed an adaptation period to split-belt treadmill walking to assess the preferred, steady-state step time asymmetry, foot placement difference and step length asymmetry that subjects adopted. Following the adaptation period, subjects performed a series of 9 cost mapping trials to assess how metabolic energy expenditure changed with step time asymmetry, foot placement difference and step length asymmetry. We partitioned the cost mapping trials into 2 sets: one set in which step time asymmetry varied around the subject's preferred value while foot placement difference varied in order to keep step lengths symmetrical (trials where step time asymmetry and foot placement difference varied); and another set in which foot placement difference varied in order to enforce different values of step length asymmetry within a range around symmetry while step time asymmetry was kept constant at the subject's preferred value (trials where step length asymmetry and foot placement difference varied). In 4 trials, that were used for cost mapping in which step time asymmetry and foot placement difference varied, step time asymmetry was enforced to −10%, −5%, +5% and +10% (percentage points) of the subject's preferred step time asymmetry while step length asymmetry was enforced to symmetry. In another 4 trials, that were used for cost mapping in which step length asymmetry and foot placement difference varied, step time asymmetry was enforced to the subject's preferred value while step length asymmetry was enforced to −10%, −5%, 5% and 10%. Subjects' also performed one trial, that was included in both cost mapping sets, in which step time asymmetry was enforced to the subject's preferred value while step lengths were enforced to symmetry. The order of the 9 cost mapping trials was randomized between subjects and between speed difference conditions.

6.2.6 Experimental setup

In order for subjects to perform our experiment they had to be able to control stride time, step time asymmetry and foot placement difference. We devised an experimental setup in which stride time was enforced by the beat of a metronome while step time asymmetry and foot placement difference were enforced by real-time visual feedback projected onto a screen in front of the treadmill (Fig. 6.1C). Visual feedback of step time asymmetry was indicated by the height of a bar graph that continually changed depending on the subject's performance (Labview, National Instruments, Austin, TX, USA). We instructed subjects to keep the height of the bar graph near a horizontal line that represented the target value. Once the bar graph was within ±2% of the target value the color of the bar changed from blue to green to indicate satisfactory performance. Visual feedback of foot placement difference consisted of 2 stationary boxes that each represented target positions for left and right feet at heel-strikes (Microsoft Visual Studio, Redmond, WA, USA). We indirectly controlled subjects' step length asymmetry from stride time, step time asymmetry and foot placement difference by calculating the anterior-posterior distance between the boxes using Eq. 6.3. To guide foot placements to the target boxes, real-time

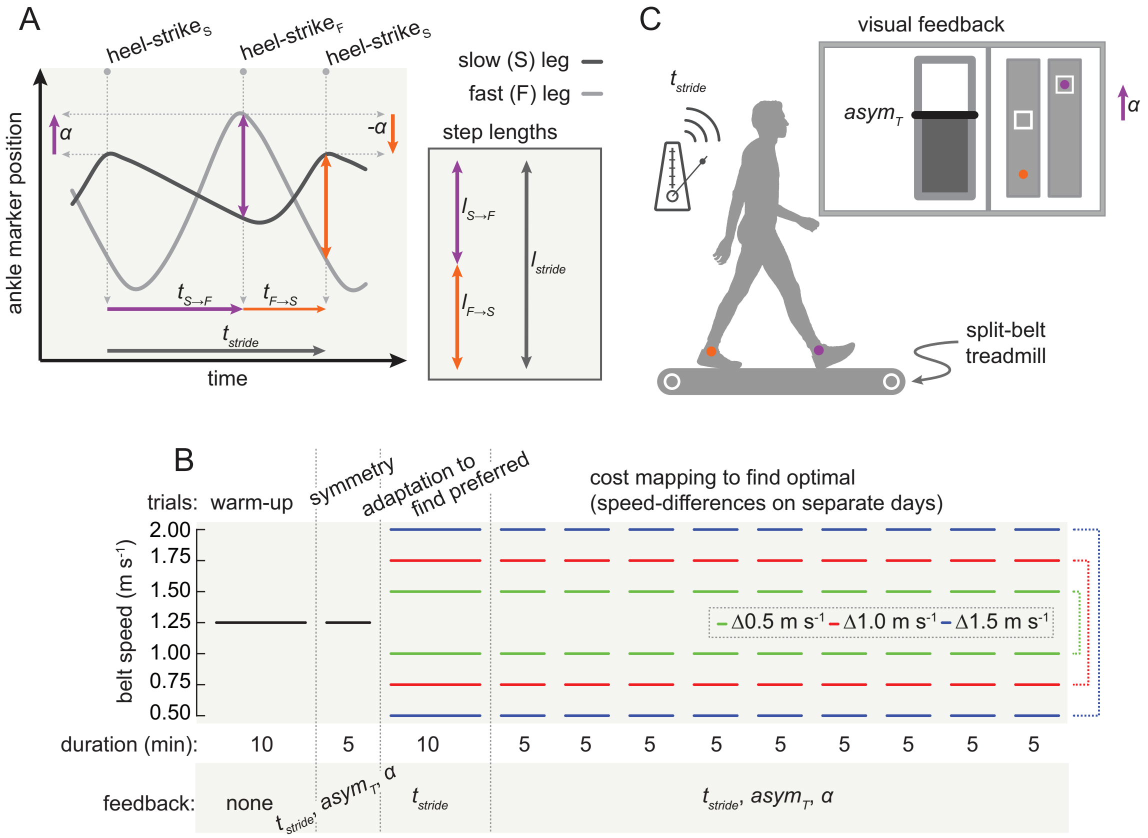

Figure 6.1: Experimental setup. (A) Overview of gait parameters: slow-to-fast step time ($t_{\mathrm{S}\to\mathrm{F}}$), fast-to-slow step time ($t_{\mathrm{F}\to\mathrm{S}}$), stride time ($t_{stride}$), slow-to-fast step length ($l_{\mathrm{S}\to\mathrm{F}}$), fast-to-slow step length ($l_{\mathrm{F}\to\mathrm{S}}$), stride length ($l_{stride}$) and foot placement difference (α). (B) Experimental protocol: on 3 separate data collection visits subjects walked on a split-belt treadmill with speed-differences at 0.5 m s^{-1}, 1.0 m s^{-1} and 1.5 m s^{-1} while the average belt speed was at 1.25 m s^{-1}. (C) Experimental setup during split-belt treadmill walking: stride time was enforced by the beat of a metronome while step time asymmetry ($asym_{\mathrm{T}}$) and foot placement difference (α) were enforced by real-time visual feedback projected onto a screen in front of the treadmill. We indirectly enforced step length asymmetry by calculating foot placement difference according to Eq. 6.3

.

feedback of the anterior-posterior position of reflective markers put on each ankle were represented by blue dots. At either foot's heel-strike, the dot remained fixed at the contact position until the other foot's heel-strike. To enforce foot placements, the dot changed color to green within ±1 cm of the target box's center or changed to gray outside the interval.

It was challenging for subjects to walk on the split-belt treadmill while simultaneously controlling their stride time, step time asymmetry and foot placement difference. Controlling step times—simultaneously matching stride time to the beat of the metronome and controlling step time asymmetry from visual feedback—was especially challenging as noted previously (Malone et al., 2012). Therefore, subjects came in for a training visit to learn how to control stride time, step time asymmetry and foot placement difference. The training visits lasted between 1.5 and 2 hours and subjects only continued with the study if they were able to successfully walk according to the feedback presented to them.

Subjects fasted and refrained from coffee or energy drinks 4 hours before each data collection visit. At the beginning of each data collection visit, subjects sat for 10 minutes after which they stood for 5 minutes while we measured their standing metabolism. Next, subjects warmed up by walking on the treadmill for 10 minutes while both belts ran at 1.25 m s^{-1}. No feedback was presented during the warm-up period. During the first data collection visit, we calculated the subjects' preferred stride time while walking with tied treadmill belts at 1.25 m s^{-1} during the warm-up period (Umberger & Martin, 2007). In all subsequent trials, subjects' preferred stride time was enforced by the beat of a metronome. We chose to keep stride time constant for several reasons. First, our preliminary data showed a U-shaped relationship between stride time and energy cost during split-belt treadmill walking (Stenum & Choi, 2017). By keeping stride time constant, we avoided the confounding effect of stride time on energy cost. Second, we analyzed previously published data (Stenum & Choi, 2016) and noted that self-selected stride time and step time asymmetry co-varied during walking across a range of belt speed combinations. We also noted this co-variation between stride time and step time asymmetry during pilot tests for this study. By enforcing subjects' stride time during the adaptation period in which subjects' preferred step time asymmetry was assessed, we avoided the confounding effect of stride time on preferred step time asymmetry. Our approach is inspired from constrained optimization studies of human gait (Bertram & Ruina, 2001) in which self-selected, unconstrained gait parameters (i.e., step time asymmetry, foot placement difference and step length asymmetry) are observed in a constrained task (i.e., walking on the split-belt treadmill with constant stride time).

Following the warm-up period, subjects walked for 5 minutes at 1.25 m s^{-1} while both step lengths and step times were enforced to symmetry. We used the metabolic cost of this trial to normalize the metabolic cost of split-belt treadmill walking from that day's data collection visit.

Then, subjects performed an adaptation period in which they walked on the split-belt treadmill with the belts set at different speeds for 10 minutes. During the adaptation period, stride time was enforced to the subjects' preferred stride time, but no feedback about step time asymmetry and foot placement was presented so that subjects were free to choose a preferred combination of step time asymmetry, foot placement difference and step length asymmetry. Before the adaptation period we instructed the subjects to walk in a way that felt comfortable or natural to them and we told them that the only requirement was to match their stride time to the beat of the metronome.

Following the adaptation period, subjects performed 9 cost mapping trials, of each 5 minutes, that were divided into one trial in which step time asymmetry was enforced to the preferred value while step length asymmetry was enforced to symmetry; 4 trials in which step time asymmetry was enforced to -10%, -5%, $+5\%$ and $+10\%$ (percentage points) of the preferred value while step length asymmetry was enforced to symmetry; and 4 trials in which step time asymmetry was enforced to the subject's preferred value while step length asymmetry was enforced to -10%, -5%, 5% and 10%. Subjects rested for 2 minutes, or longer when necessary, between trials. The order of the 9 trials was randomized between subjects.

6.2.7 Data collection

Four high-speed cameras (Qualisys Oqus, Gothenburg, Sweden) recorded 2 reflective markers at 100 Hz that we put bilaterally on the lateral malleoli. Force plates embedded in each treadmill belt recorded ground reaction forces at 1000 Hz. We recorded breath-by-breath rates of oxygen consumption and carbon dioxide production (Parvo Medics TrueOne 2400, Sandy, UT, USA).

6.2.8 Data processing

We low-pass filtered kinematic data at 7 Hz and kinetic data at 10 Hz. We defined heel-strikes as the instant that the vertical ground reaction force exceeded 10 N. Step times were calculated as the period between consecutive bilateral heel-strikes. We calculated foot placement differences for slow-to-fast and fast-to-slow steps as the anterior-posterior difference between the ankle markers' position at subsequent bilateral heel-strikes. Step lengths were calculated from foot placement difference and the product of step time and belt speed (Finley et al., 2015). All gait parameters were calculated as the average across the last 2 minutes of each trial.

We calculated gross metabolic power from the average rates of oxygen consumption and carbon dioxide production of the last 2 minutes of each trial (Brockway, 1987). We subtracted standing metabolism to obtain net metabolic power. We express metabolic cost of split-belt treadmill walking as the percentage of the net metabolic power relative to normal treadmill walking in which both belts ran at 1.25 m s^{-1} while stride time was enforced to preferred and step times and lengths were enforced to symmetry. Average net metabolic power of normal treadmill walking at 1.25 m s^{-1} was (mean±SD) 2.84±0.36 W kg^{-1} during the Δ0.5 m s^{-1} data collection visit, 2.77±0.39 W kg^{-1} during the Δ1.0 m s^{-1} data collection visit and 2.84±0.36 W kg^{-1} during the Δ1.5 m s^{-1} data collection visit.

6.2.9 Statistics

We performed one-way repeated measures ANOVA to test if speed-difference affected preferred step time asymmetry, step length asymmetry and foot placement difference. In the event of a statistical significance, we performed post-hoc comparisons with Bonferroni corrections. To test if there was an effect on energy cost during cost mapping trials, we performed one-way repeated measures ANOVA for each speed-difference condition. We obtained individual subjects' energetically optimal value of step time asymmetry, foot placement difference and step length asymmetry as the gait parameter's value of the cost mapping trial that had the minimal metabolic cost. For each gait parameter, we used the cost mapping trials in which the gait parameter was systematically changed: we tested if preferred step time asymmetries and foot placement differences were energetically optimal in the cost mapping trials in which step time asymmetry and foot placement difference varied; we tested if preferred step length asymmetries and foot placement differences were energetically optimal in the cost mapping trials in which step length asymmetry and foot placement difference varied. We used one-sample t-tests to test if the values of the preferred gait parameters were different from the optimal values. We set the level of significance at 0.05. We performed statistical tests using SPSS (IBM Corp., Armonk, NY, USA).

6.3 Results

6.3.1 Greater belt speed-differences increase preferred step time asymmetry and foot placement difference while step lengths remain nearly symmetrical

With greater speed-differences between the treadmill belts at 0.5 m s^{-1}, 1.0 m s^{-1} and 1.5 m s^{-1}, subjects preferred greater step time asymmetry at 8.0%, 17.8% and 28.2% (Fig. 6.2A; $F_{2,18}$=288.1, P<0.001; post-hoc tests P<0.001) and greater foot placement differences at 6.4 cm, 12.8 cm and 18.8 cm (Fig. 6.2B; $F_{2,18}$=381.3, P<0.001; post-hoc tests P<0.001), while their preferred step length asymmetry remained constant, and

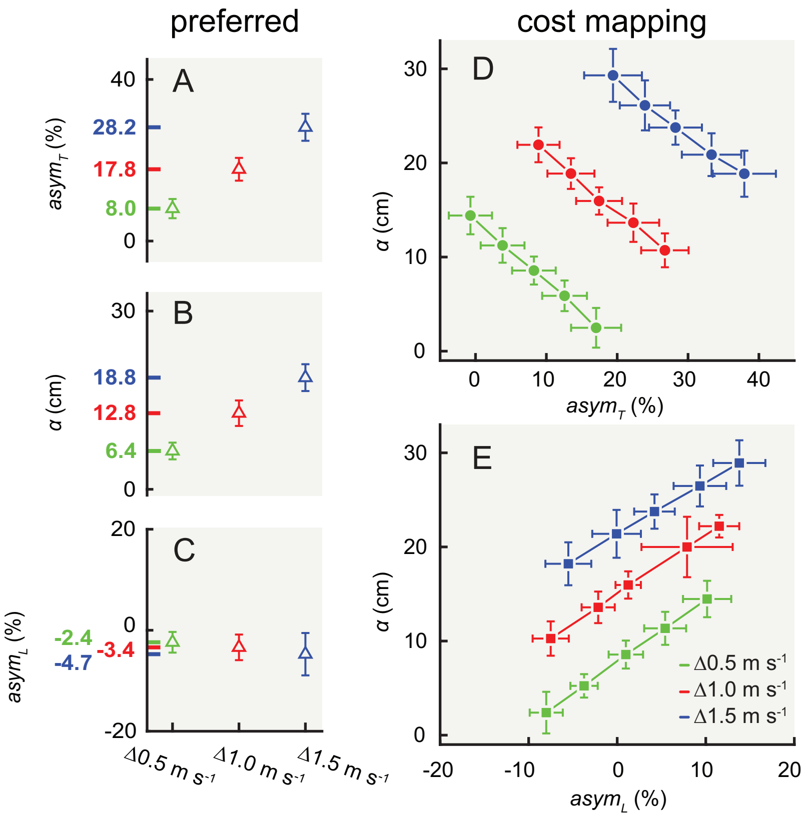

Figure 6.2: Gait parameters during preferred and cost mapping trials. (A–C) Preferred step time asymmetry ($asym_\mathrm{T}$), foot placement difference (α) and step length asymmetry ($asym_\mathrm{L}$) for speed-differences of 0.5 m s^{-1}, 1.0 m s^{-1} and 1.5 m s^{-1}. Colored tick marks show ensemble means. Error bars are standard deviations. (D,E) Cost mapping trials where step time asymmetry and foot placement difference varied (D) and trials where step length asymmetry and foot placement difference varied (E). Vertical and horizontal error bars are standard deviations.

nearly symmetrical, at -2.4%, -3.4% and -4.7% (Fig. 6.2C; $F_{2,18}$=4.0, P=0.037; post-hoc tests $P \geq 0.168$). To test if subjects' preferred gait parameters coincided with their energetically optimal gait parameters, we conducted a series of cost mapping trials to describe the cost landscape across different values of the gait parameters.

6.3.2 Cost mapping: effects of step time asymmetry, foot placement difference and step length asymmetry

Subjects successfully walked according to our cost mapping trials which consisted of one set of trials in which step time asymmetry varied around the preferred values while foot placement difference varied in order to keep step lengths symmetrical (Fig. 6.2D), and another set of trials in which foot placement differences varied in order to enforce step length asymmetry to different values within a range around symmetry while step time asymmetry remained constant at the preferred value (Fig. 6.2E). Foot placement difference changed systematically in both sets of cost mapping trials: foot placement difference shortened to keep step lengths symmetrical in cost mapping trials where step time asymmetry increased (Fig. 6.2D), while foot placement difference increased to reach the desired step length asymmetry in cost mapping trials where step length asymmetry went from negative to positive values (Fig. 6.2E). Subjects' stride time was enforced to their preferred stride time in normal treadmill walking at 1.25 m s^{-1} which was 1.08±0.06 s (ensemble mean±SD). Subjects kept their stride time constant throughout all split-belt treadmill adaptation and cost mapping trials: the ensemble average coefficient of variation was 0.3%.

Next we describe qualitative features of the energetic cost landscapes that the cost mapping trials produced. For the trials in which step time asymmetry and foot placement difference varied (Fig. 6.3A,B), there was a significant effect on energy cost (Δ0.5 m s^{-1}, $F_{4,36}$=12.8, P<0.001; Δ1.0 m s^{-1}, $F_{4,36}$=11.0, P<0.001; Δ1.5 m s^{-1}, $F_{4,36}$=15.3, P<0.001). The outlines of the cost landscapes were qualitatively similar between speed-difference conditions: all the curves exhibited J-shaped curves in which optima were evident (Fig. 6.3A,B). The cost curves' slopes were, however, steepest in the portion with decreasing step time asymmetry (Fig. 6.3A) and increasing foot placement differences (Fig. 6.3B). For the trials in which step length asymmetry and foot placement difference varied (Fig. 6.3C,D), there was a significant effect on metabolic cost (Δ0.5 m s^{-1}, $F_{4,36}$=4.0, P=0.009; Δ1.0 m s^{-1}, $F_{4,36}$=10.0, P<0.001; Δ1.5 m s^{-1}, $F_{4,36}$=9.7, P<0.001). The outlines of the cost landscapes were qualitatively similar in the portion of the curves with negative step length asymmetry (Fig. 6.3C) and short foot placement differences (Fig. 6.3D): energy cost decreased in this portion. However, the portion of the cost curves with positive step length asymmetry (Fig. 6.3C) and greater foot placement differences (Fig. 6.3D) differed between speed-difference conditions: cost increased to form a U-shaped curve for Δ0.5 m s^{-1}, cost increased moderately for Δ1.0 m s^{-1}, and cost plateaued for Δ1.5 m s^{-1}.

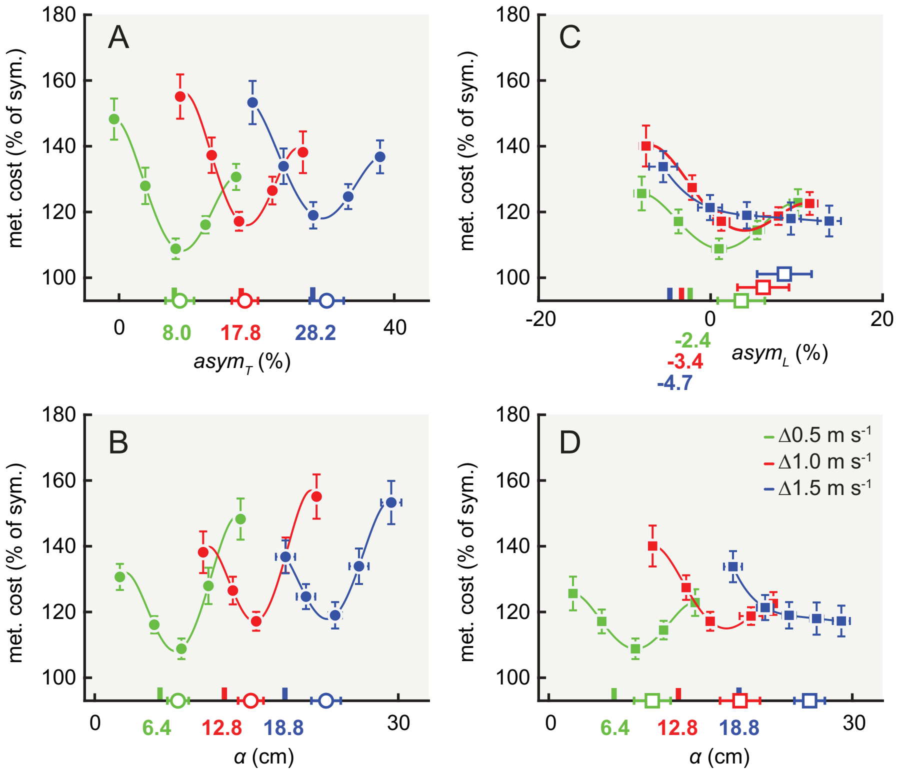

Figure 6.3: Cost landscapes during split-belt treadmill walking. (A,B) Cost landscapes in cost mapping trials where step time asymmetry ($asym_{\mathrm{T}}$) and foot placement difference (α) varied. (C,D) Cost landscapes in cost mapping trials where step length asymmetry ($asym_{\mathrm{L}}$) and foot placement difference varied. Cost landscapes are outlined by 4th order polynomial fits. Vertical and horizontal error bars in cost landscape data are standard error of the mean. Colored tick marks show the ensemble mean of preferred gait parameters. Open circles (A,B) and squares (C,D) show the energetically optimal gait parameters. Horizontal error bars around optima are 95% confidence intervals. For all gait parameters (cost landscapes, ensemble mean of preferred gait parameters and optimal gait parameters), data are aligned along the x-axis by, first, subtracting each subject's preferred value and, second, adding the ensemble mean preferred value of each gait parameter. Metabolic cost is expressed as the percentage of net metabolic power relative to normal, symmetrical treadmill walking at 1.25 m s^{-1}.

6.3.3 People adopt asymmetrical step times to optimize energy cost

In the trials where step time asymmetry and foot placement difference varied, subjects selected a preferred step time asymmetry that was energetically optimal across all speed-difference conditions: preferred step time asymmetries were 8.0%, 17.8% and 28.2% and optimal step time asymmetries were 8.8%, 18.3% and 30.2% for $\Delta 0.5$ m s^{-1}, $\Delta 1.0$ m s^{-1} and $\Delta 1.5$ m s^{-1}, respectively (Fig. 6.3A, compare colored tick marks to open circles: $\Delta 0.5$ m s^{-1}, P=0.407; $\Delta 1.0$ m s^{-1}, P=0.545; $\Delta 1.5$ m s^{-1}, P=0.096).

6.3.4 Neither foot placement difference nor step length asymmetry optimize energy cost

In the trials where step time asymmetry and foot placement difference varied, foot placement differences changed systematically in order to keep step lengths symmetrical; however, the preferred foot placement differences were not energetically optimal: preferred foot placement differences were 6.4 cm, 12.8 cm and 18.8 cm while optimal foot placement differences were 8.2 cm, 15.4 cm and 22.9 cm (Fig. 6.3B, compare colored tick marks to open circles: $\Delta 0.5$ m s^{-1}, P=0.004; $\Delta 1.0$ m s^{-1}, P<0.001; $\Delta 1.5$ m s^{-1}, P<0.000). By adopting optimal foot placement differences, subjects would have experienced cost savings of 4%, 14% and 14% of the metabolic cost of the preferred foot placement differences (estimated from ensemble data curve fits).

In the trials where step length asymmetry and foot placement difference varied, neither preferred step length asymmetry (Fig. 6.3C, compare colored tick marks to open squares: $\Delta 0.5$ m s^{-1}, P=0.001; $\Delta 1.0$ m s^{-1}, P<0.000; $\Delta 1.5$ m s^{-1}, P<0.000) nor foot placement differences were energetically optimal (Fig. 6.3D, compare colored tick marks to open squares: $\Delta 0.5$ m s^{-1}, P=0.001; $\Delta 1.0$ m s^{-1}, P<0.000; $\Delta 1.5$ m s^{-1}, P<0.000). The preferred step length asymmetries were −2.4%, −3.4% and −4.7% while the optimal step length asymmetries were 3.6%, 6.1% and 8.6% (Fig. 6.3C, open squares). The preferred foot placement differences were 6.4 cm, 12.8 cm and 18.8 cm while the optimal foot placement differences were 10.2 cm, 18.9 cm and 25.8 cm (Fig. 6.3D, open squares). By adopting optimal step length asymmetries and foot placement differences, subjects would

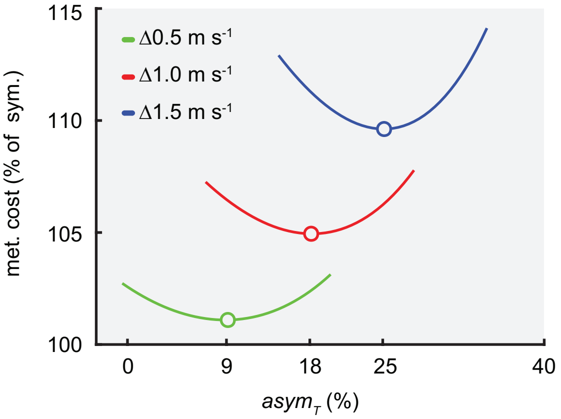

Figure 6.4: Cost model predictions with varying step time asymmetry in split-belt treadmill walking. We used a cost model of the stride cycle (Eqs. 6.6 and 6.7) and the split-belt treadmill's constraint on the combination of stride length and stride time (Eq. 6.5) to predict the metabolic cost of split-belt treadmill walking with a range of step time asymmetries ($asym_{\mathrm{T}}$) for speed-differences at 0.5 m s^{-1}, 1.0 m s^{-1} and 1.5 m s^{-1}. Average speed was 1.25 m s^{-1}. Stride time was constant and step length asymmetry was set to symmetry. Our cost model predicts the existence of an energetically optimal step time asymmetry. The optimal step time asymmetry increases with speed-difference. Open circles show optima. Metabolic cost is expressed relative to normal, symmetrical walking at 1.25 m s^{-1}.

have experienced cost savings of 3%, 12% and 10% of the metabolic cost of the preferred gait parameters (estimated from ensemble data curve fits).

6.3.5 Optimal step time asymmetry is predicted from split-belt treadmill's constraint on locomotor pattern

Our cost model predicts the existence of an energetically optimal step time asymmetry in split-belt treadmill walking (Fig. 6.4). The optimum arises from the split-belt treadmill's constraint on the combination of stride length and stride time which creates a trade-off in mechanical stance and swing costs: stance cost decreases and swing cost increases with greater step time asymmetry (not shown). The speed-difference between the treadmill's belts increases the value of the energetically optimal step time asymmetry (9% for Δ0.5 m s^{-1}; 18% for Δ1.0 m s^{-1}; 25% for Δ1.5 m s^{-1}) which predicts the trend of our experimental data (8.0%, 17.8% and 28.2%).

6.4 Discussion

We tested if people's preferred, steady-state gait parameters during split-belt treadmill walking were energetically optimal. Our experimental results showed that only preferred step time asymmetry was energetically optimal and that neither foot placement difference nor step length asymmetry were selected to optimize energy cost. Our results support the idea that people may select asymmetrical gait parameters to optimize energetic cost.

In order to test if people adopted preferred gait parameters to optimize metabolic cost, we mapped the energetic cost landscape of split-belt treadmill walking. We chose to map 2 cost landscapes. We mapped a cost landscape in which step time asymmetry varied around the preferred value and a cost landscape in which step length asymmetry varied around symmetry. In both cost landscapes, foot placement difference varied systematically which allowed us to test if the preferred foot placement differences were energetically optimal. The cost landscapes in which step time asymmetry and foot placement difference varied were J-shaped with evident optima for all speed-difference conditions. The cost landscapes in which step length asymmetry and foot placement difference varied were similar between speed-difference conditions in the portions with negative step length asymmetry (the step length from slow-to-fast belts is shortest): energy cost decreased as step lengths went from negative asymmetry toward symmetry. However, the cost landscapes differed between the 3 speed-difference conditions in the portions with positive step length asymmetry (the step length from slow-to-fast belts is longest): cost increased for $\Delta0.5$ m s^{-1}, cost increased moderately for $\Delta1.0$ m s^{-1} and cost plateaued for $\Delta1.5$ m s^{-1}. While our cost landscapes that show the effects of step time asymmetry are novel and cannot be compared to existing data, two previous studies have reported cost landscapes in which step length asymmetry and foot placement difference varied (Sánchez et al., 2017, 2019). Importantly, the outlines of the previously reported cost landscapes may not generalize across studies because they used different speed combinations to ours and they allowed stride time and step time asymmetry to vary while we constrained these gait parameters. Despite these differences, both studies estimated that step length asymmetry is energetically optimal at a positive asymmetry (step lengths from slow-to-fast belts are longest) which is consistent with our estimate of optimal step length asymmetry. It is important to note that we only mapped a portion of the cost landscape within each speed-difference condition and that many other combinations of step time asymmetry, foot placement difference and step length asymmetry are possible. Therefore, we do not know how the cost landscapes change across the entire range of combinations of gait parameters. Consequently, even though we report optimal values of step time asymmetry, foot placement difference and step length asymmetry, they may not be global optima. Rather, we interpret the optimal values of our gait parameters as local minima within a constrained parameter space. With this caveat in mind, we did, however, carefully choose appropriate combinations of gait parameters for our cost mapping trials that allowed us to test whether people's preferred gait parameters were energetically optimal. Taken together, our cost landscapes present novel insight into the energetics of split-belt treadmill walking that allow us to determine whether people adopt steady-state gait parameters in order to optimize metabolic energy cost.

We found that people adopted a preferred combination of steady-state gait parameters with asymmetrical step times, different foot placements and nearly symmetrical step lengths; and, furthermore, that greater speed-differences between the treadmill's belts increased preferred step time asymmetry and foot placement differences, but that step length asymmetry remained constant. Error-based learning prescribes that gait parameters are driven to symmetry (Roemmich & Bastian, 2018). However, symmetry in some gait parameters, such as step lengths, can only be accomplished by asymmetry in other gait parameters, such as step times or foot placements. Therefore, it is not clear why some gait parameters are adapted to symmetry while others are adapted to asymmetry. We found that preferred step time asymmetry were energetically optimal across all speed-difference conditions and, so, we contend that part of the adaptation to split-belt treadmill walking is driven towards asymmetrical gait parameters because asymmetry is energetically optimal.

We found that foot placement difference and step length asymmetry were not energetically optimal. Preferred gait parameters are typically assessed after a short adaptation period of about 10 minutes. Recent work has suggested that people adopt an energetically optimal step length asymmetry when preferred gait parameters are assessed after an extended period of split-belt treadmill walking that allows people to explore the energetic cost landscape (Sánchez et al., 2019). Our results do not support the idea that preferred step length asymmetry is energetically optimal with extended split-belt treadmill walking: at the start of the first, second and third data collection visits our subjects had accumulated about 1, 2 and 3 hours of split-belt treadmill walking, respectively. Furthermore, the energetic cost our subjects could have saved by adopting the optimal values of step length asymmetry or foot placement difference was up to 14% which is greater than previously reported energetic savings for which people have been shown to adopt optimal gait parameters (Selinger et al., 2015). This suggests that our subjects had the sensitivity to detect the energetic savings that the optimal gait parameters offered, but that they, nonetheless, did not choose optimal values of foot placement difference and step length asymmetry. We, therefore, conclude that our participants used neither foot placement difference nor step length asymmetry to optimize cost. Even though our results do not support that foot placement difference or step length asymmetry are tuned to energetic *optima*, we cannot rule out that these gait parameters may be changed during the adaptation period to reduce cost: foot placement difference increases and step length asymmetry changes from negative values to nearly symmetrical over the course of adaptation, thereby descending an energetic gradient during the adaptation period. It would be interesting to test other explanations than energy optimization to predict people's preferred values of foot placement difference and step length asymmetry; for example, stability has been suggested to be directly influenced by foot placements (Park & Finley, 2017).

Temporal—identified as step time asymmetry—and spatial—captured by foot placement difference—motor outputs have been suggested to control split-belt treadmill adaptation (Malone et al., 2012). Step length asymmetry depends on the combination of step time asymmetry and foot placement difference (Finley et al., 2015), and, therefore, we interpret step length asymmetry as a spatiotemporal gait parameter that may not be directly controlled by the nervous system. Temporal and spatial gait parameters have been suggested to be independently controlled by different neural structures (Darmohray et al., 2019; Malone et al., 2012; McCrea & Rybak, 2008). We find that step time asymmetry, a temporal gait parameter, is energetically optimal while the spatial and spatiotemporal gait parameters (foot placement difference and step length asymmetry) are not energetically optimal. It is possible that energy optimization may reflect a functional distinction between temporal and spatial adaptable control of locomotion. Furthermore, temporal gait parameters have been suggested to be controlled more tightly than spatial gait parameters which may reflect that temporal control is tuned to energy optima while spatial control is not (Malone et al., 2012). The idea that temporal control is tuned to energy optima while spatial control is not may also partly explain recent work showing that constraining foot placement difference during adaptation does not influence step time asymmetry, while constraining step time asymmetry influences foot placement difference (Gonzalez-Rubio et al., 2019). Alternatively, it is also possible that our finding that step time asymmetry is tuned to energetic optima may not reflect a distinct role of temporal control. Our own recent work shows that the metabolic cost of asymmetrical gait parameters during normal treadmill walking is best explained by the cost of step time asymmetry alone (see chapter 5). Similarly, step time asymmetry may influence the timing of ankle work in stance which has been proposed as an adaptation mechanism during split-belt treadmill walking that may have implications for metabolic cost (Selgrade et al., 2017a,b). Therefore, temporal control may be tuned to energetic optima because the main determinant of the metabolic cost of walking with asymmetrical gait parameters is step time asymmetry. In future work it would be interesting to pursue whether our results, that step time asymmetry is energetically optimal while foot placement difference and step length asymmetry is not tuned to optima, is explained from distinctions in temporal and spatial control or from the mechanical consequences of asymmetrical gait parameters.

This study focused on steady-state gait parameters during split-belt treadmill walking and we did not study how gait parameters transiently changed during the adaptation period. We did not study the adaptation periods because our subjects had accumulated extensive experience with split-belt treadmill walking prior to adaptation which influences the adaptation rate of split-belt treadmill walking (Day et al., 2018). Previous work has suggested different time-scales for temporal and spatial gait parameters in which temporal parameters reach steady-state quicker than spatial parameters (Malone et al., 2012). Our data suggest that adaptation of steady-state gait parameters may be driven by energy optimization. The time-scale for an energy optimization process has been suggested to be at least 30 seconds, but could require longer periods with exploration in order to learn a novel cost landscape and to offset convergence towards an optimal gait parameter (Selinger et al., 2015; Snaterse et al., 2011). Our subjects accumulated extensive experience with split-belt treadmill walking from their training visit and their previous data collection visits. The training visit was necessary for subjects to sustain reliable steady-state gait parameters within our feedback-constrained experimental setup. In future work it may be interesting to study the time-course of temporal and spatial gait parameters in order to infer different control mechanisms. For example, it is possible that step time asymmetry adapts quickly because temporal gait parameters are sensitive to energy optimization.

Our main focus has been showing that changes in the values of gait parameters induce changes to energy cost without considering the mechanics of split-belt treadmill walking. However, from a simple cost model we propose that the split-belt treadmill's constraint on the combination of stride length and stride time (Eq. 6.5) influenced the cost landscape in which step time asymmetry and foot placement difference varied (Fig. 6.3A,B): at a constant stride time, there is a linear decrease in stride length with step time asymmetry. This may create a trade-off in stance cost (Eq. 6.6, decreasing with a shorter stride length) and swing cost (Eq. 6.7, increasing with step time asymmetry) that explains the existence of an energetically optimal step time asymmetry (Fig. 6.4). The special mechanics of split-belt treadmill walking provide other opportunities from which walkers can benefit: humans adapt to steady-state walking in which they increase their backwards displacement during single support on the leg on the fast belt and decrease their backwards displacement during single support on the leg on the slow belt (Selgrade et al., 2017b). This is energetically less costly since it is less demanding to generate forward propulsion on the slow leg relative to the fast leg. Another proposed mechanism of split-belt treadmill walking that allows people to decrease their own mechanical work output and take advantage of work provided by the treadmill (Sánchez et al., 2019) may partly explain the cost landscape in which step length asymmetry and foot placement difference varied: the descending portions of the cost landscapes (Fig. 6.3C,D) may be explained by lower metabolic demand as foot placement differences increases. While we limited our analysis to metabolic energy consumption in this study, understanding the mechanical demands and strategies during split-belt treadmill walking may be a fruitful area for understanding neuromechanical control of human walking and the energetics of asymmetrical walking (Selgrade et al., 2017a,b; Sánchez et al., 2019).

We found that subjects adopt asymmetrical step times that are energetically optimal during split-belt treadmill walking. People that have suffered a stroke or amputees that walk with a prosthetic leg often walk asymmetrically. Our data support the idea that asymmetrical gait may be a functional adaptation in order to walk economically. This supports new evidence that suggests that unilateral amputees may walk asymmetrically to optimize energy cost (Handford & Srinivasan, 2018; Wedge, 2019). However, we suspect that whether asymmetry may be beneficial or detrimental depends on many factors, such as joint loading or stability, and may vary from person to person (Sánchez & Finley, 2018). Nonetheless, it is an intriguing idea that people exploit asymmetry to optimize energy cost which warrants further research.

CHAPTER 7

CONCLUSION

Hemiparetic and amputee walking often has asymmetrical step lengths and step times (Roerdink et al., 2007; Isakov et al., 2000), and the gait is metabolically costlier than symmetrical, able-bodied walking (Waters & Mulroy, 1999). Consequently, asymmetry is often attributed to account for the increased energy expenditure. However, the metabolic cost of walking with asymmetrical step lengths or step times is not well understood. Asymmetrical step lengths have been proposed to incur a metabolic cost (Srinivasan, 2011), yet no experimental evidence has shown the cost of step length asymmetry. An experiment of able-bodied people walking with step time asymmetry showed an added cost compared to walking symmetrically (Ellis et al., 2013). However, step lengths were free to vary in this study which makes it difficult to ascribe the added cost of asymmetry to the separate effects of either the cost of asymmetry in step lengths or step times or, alternatively, their additive cost.

We performed experiment 1 in which we devised an experimental setup that allowed us to enforce asymmetry in step lengths and step times during normal treadmill walking and we recruited 10 able-bodied subjects that walked with a range of combinations of asymmetry in step lengths and step times. This allowed us to measure the metabolic cost of walking with asymmetry in either step lengths or step times and to test whether the costs are additive when people walk with concurrent asymmetry in step lengths and step times. We found that the metabolic cost of walking with step time asymmetry was more than twice the cost of step length asymmetry and that the costs were not additive. Rather, the metabolic cost of walking with concurrent asymmetry in step lengths and step times is best explained by the cost of step time asymmetry alone.

Previous studies of hemiparetic and amputee walking (Adamczyk & Kuo, 2015; Farris et al., 2015) and able-bodied people walking asymmetrically (Ellis et al., 2013) have found that total mechanical work performed on the center of mass increased and that the positive work was redistributed from push-off to pendular phases of the stride cycle. In experiment 1 we hypothesized that positive mechanical work would explain the metabolic cost of asymmetrical walking. We found that asymmetry increased total positive work moderately and redistributed positive work so that the percentage of work performed in pendular phases increased. Even though total positive work over the entire stride increased with asymmetry, the rate of total work poorly explained the metabolic cost of asymmetry. Instead, rate of work performed in pendular phases correlated better with metabolic cost which suggests that pendular work may exact a metabolic cost that explains a significant portion of the metabolic cost of asymmetrical walking.

Overall, the results from our experiment 1 show the metabolic cost of walking with asymmetry in step lengths and step times and how the costs interact when walking with concurrent asymmetry in step lengths and step times. Furthermore, our data suggest that a significant portion of the metabolic cost of asymmetrical walking is derived from increased production of positive mechanical work during the pendular phases of the stride cycle. These results have implications for rehabilitation of hemiparetic and amputee walking which often has asymmetrical gait parameters (Patterson et al., 2008; Sanderson & Martin, 1997). For example, our data suggest that changing step time asymmetry is more effective than changing step length asymmetry or foot placement difference in inducing changes to metabolic cost (Sánchez & Finley, 2018; Roemmich et al., 2019).

As stated previously, hemiparetic and amputee walking often has asymmetrical gait parameters (Roerdink et al., 2007; Isakov et al., 2000), and the gait is metabolically costlier than symmetrical, able-bodied walking (Waters & Mulroy, 1999). But even though symmetrical gait parameters are energetically optimal in able-bodied walking (Ellis et al., 2013), asymmetrical gait parameters may be adopted if asymmetry is optimal under imposed constraints on the locomotor system. Adaptability of asymmetry has been demonstrated on a split-belt treadmill: following a short adaptation period in which gait parameters are transiently perturbed, people choose steady-state gait parameters with asymmetrical step times, different foot placements and nearly symmetrical step lengths (Reisman et al., 2005). Energy optimization has been proposed to explain how steady-state gait parameters are adopted following the adaptation period (Finley et al., 2013). However, the effect of changes to step time asymmetry, foot placement difference and step length asymmetry on energetic cost during split-belt treadmill walking has only partly been tested (Sánchez et al., 2017, 2019) and it is therefore unclear if asymmetry is controlled in order to optimize metabolic cost.

We performed experiment 2 to test if able-bodied people adopt steady-state gait parameters to optimize energy cost during split-belt treadmill walking. We recruited 10 subjects that walked with a range of combinations of step time asymmetry, foot placement difference and step length asymmetry around their preferred values during 3 conditions with speed-differences of 0.5 m s^{-1}, 1.0 m s^{-1} and 1.5 m s^{-1}. We found that our subjects preferred asymmetrical step times, different foot placements and nearly symmetrical step lengths; as speed-differences increased, step time asymmetry and foot placement differences increased while step lengths remained nearly symmetrical. We compared the preferred gait parameters to the optimal values of the gait parameters and found that only step time asymmetry optimized metabolic cost, but that neither foot placement difference nor step length asymmetry optimized cost.

Our results of experiment 2 suggest that asymmetry in gait parameters may be preferred if asymmetry is energetically optimal. The finding that step time asymmetry is energetically optimal may reflect that temporal control is tuned to energy optimization; alternatively, this finding may also reflect that the mechanical consequence of changing step time asymmetry has a greater effect on metabolic cost than changing step length asymmetry which does not necessarily imply a distinction between temporal and spatial control of gait parameters.

Our results taken together with recent studies on the mechanics of split-belt treadmill walking (Selgrade et al., 2017a,b) suggest that the metabolic cost of asymmetrical walking on both a normal treadmill and during split-belt treadmill walking may be derived from a redistribution of positive work within the stride cycle. We show that the metabolic cost of asymmetry in normal treadmill walking may be derived from increased positive work during pendular phases of the stride cycle. During the adaptation period to split-belt treadmill walking there is a gradual decrease in pendular positive work (Selgrade et al., 2017a) that tracks the concurrent decrease in metabolic cost (Finley et al., 2013). Following the adaptation period to split-belt treadmill walking, pendular positive work remains elevated compared to normal treadmill walking at the same average speed (Selgrade et al., 2017a) which may explain the added metabolic cost of split-belt treadmill walking compared to normal treadmill walking at the same average speed (Stenum & Choi, 2017). We therefore propose that pendular positive work may explain the metabolic cost of asymmetrical walking that is general for both normal and split-belt treadmill environments.

In our study the increase in pendular positive work with asymmetrical walking appeared to be predominantly driven by an increase in ankle work. This ankle strategy to increase pendular work in asymmetrical walking on a normal treadmill is similar to results of split-belt treadmill walking: during the adaptation period there is a redistribution of work from pendular phases to push-off (Selgrade et al., 2017a) concurrent with a shift in the timing of ankle work from pendular phases to push-off (Selgrade et al., 2017b). This suggests a common mechanism where people may use an ankle strategy to increase pendular positive work in asymmetrical walking on a normal treadmill or during split-belt treadmill. Our study and those reporting an ankle strategy (Selgrade et al., 2017b) included able-bodied participants. Importantly, this ankle strategy may not generalize to other types of asymmetry such as unilateral amputee gait with a prosthesis or hemiparetic gait with weak plantarflexors. Instead, these types of gaits may utilize other joint-level mechanical adaptations when walking asymmetrically.

Overall, the results from experiments 1 and 2 show that preferred step time asymmetry was always energetically optimal: in normal treadmill walking people preferred *symmetrical* step times which were optimal while in split-belt treadmill walking people preferred *asymmetrical* step times that were nonetheless optimal. This supports the idea that preferred asymmetry in gait parameters may not necessarily be more costly and that asymmetrical gait may be a functional adaptation in order to walk economically. This is in support of recent studies that suggest that unilateral amputees may walk asymmetrically to optimize metabolic cost (Handford & Srinivasan, 2018; Wedge, 2019). Whether asymmetry is beneficial or detrimental likely depends on many factors and may vary from person to person (Sánchez & Finley, 2018). Nonetheless, it is an intriguing idea that people exploit gait asymmetry to optimize energy cost which warrants further research.

APPENDIX A

DERIVATION OF SPLIT-BELT TREADMILL'S CONSTRAINT ON THE LOCOMOTOR PATTERN

We will show that the locomotor pattern during split-belt treadmill locomotion depends on the averaged belt speeds, the belt speed-difference and self-selected step time asymmetry.

First, we define foot placement differences between left and right feet (in the global reference frame) at successive bilateral foot contacts. We have 2 differences: first, the difference between the right foot's anterior-posterior position at right foot contact and the left foot's anterior-posterior position at the preceding left foot contact ($\alpha_{\mathrm{L}\rightarrow\mathrm{R}}$); and, second, the difference between the left foot's anterior-posterior position at left foot contact and the right foot's anterior-posterior position at the preceding right foot contact ($\alpha_{\mathrm{R}\rightarrow\mathrm{L}}$). The foot placement differences are equal and opposite:

$$\alpha_{\mathrm{L}\rightarrow\mathrm{R}} = -\alpha_{\mathrm{R}\rightarrow\mathrm{L}} \,. \tag{A.1}$$

Next, we express step lengths as combinations of foot placement differences, belt speeds and step times (Finley et al., 2015). Left-to-right step length is:

$$l_{\mathrm{L}\rightarrow\mathrm{R}} = \alpha_{\mathrm{L}\rightarrow\mathrm{R}} + v_{\mathrm{L}} * t_{\mathrm{L}\rightarrow\mathrm{R}} \,, \tag{A.2}$$

while right-to-left step length is:

$$l_{\mathrm{R}\rightarrow\mathrm{L}} = \alpha_{\mathrm{R}\rightarrow\mathrm{L}} + v_{\mathrm{R}} * t_{\mathrm{R}\rightarrow\mathrm{L}} \,. \tag{A.3}$$

Consequently, stride length is equal to:

$$l_{stride} = v_{\mathrm{L}} * t_{\mathrm{L}\to\mathrm{R}} + v_{\mathrm{R}} * t_{\mathrm{R}\to\mathrm{L}} \,. \tag{A.4}$$

Next, we can express step times as combinations of stride time and step time asymmetry by using Equations 3.1 and 3.4. Left-to-right step time is:

$$\begin{aligned} t_{\mathrm{L}\to\mathrm{R}} &= \frac{1}{2}t_{stride} + \frac{1}{2}t_{stride} * asym_{\mathrm{T}} \\ &= t_{stride} * (\frac{1}{2} + \frac{1}{2}asym_{\mathrm{T}}) \,, \end{aligned} \tag{A.5}$$

while right-to-left step time is:

$$\begin{aligned} t_{\mathrm{R}\to\mathrm{L}} &= \frac{1}{2}t_{stride} - \frac{1}{2}t_{stride} * asym_{\mathrm{T}} \\ &= t_{stride} * (\frac{1}{2} - \frac{1}{2}asym_{\mathrm{T}}) \,. \end{aligned} \tag{A.6}$$

Finally, from Equations A.4 to A.6 we can express stride length using belt speeds, stride time and step time asymmetry:

$$\begin{aligned} l_{stride} &= v_{\mathrm{L}} * t_{stride} * (\frac{1}{2} + \frac{1}{2}asym_{\mathrm{T}}) + v_{\mathrm{R}} * t_{stride} * (\frac{1}{2} - \frac{1}{2}asym_{\mathrm{T}}) \\ &= (\frac{1}{2}(v_{\mathrm{R}} + v_{\mathrm{L}}) - \frac{1}{2}(v_{\mathrm{R}} - v_{\mathrm{L}}) * asym_{\mathrm{T}}) * t_{stride} \,. \end{aligned} \tag{A.7}$$

From Equation A.7 we get that the locomotor pattern is constrained by the averaged belt speeds ($\overline{v} = \frac{1}{2}(v_{\mathrm{R}} + v_{\mathrm{L}})$), the belt speed-difference ($\Delta v = v_{\mathrm{R}} - v_{\mathrm{L}}$) and step time asymmetry:

$$l_{stride} * t_{stride}^{-1} = \overline{v} - \frac{\Delta v}{2} * asym_{\mathrm{T}} \,. \tag{A.8}$$

Equation A.8 can be validated by a data set in which 5 subjects walked on a treadmill at 1.31 m s^{-1} at 5 different stride times (80%, 90%, 100%, 110% and 120% of their preferred stride rate) and walked on a split-belt treadmill with the left belt speed at 0.79 m s^{-1} and the right belt speed at 1.84 m s^{-1} ($\Delta v = 1.05$ m s^{-1}) at the same 5 stride times. Furthermore, 2 of 5 subjects also walked on the split-belt treadmill with the left belt speed at 0.53 m s^{-1} and the right belt speed at 2.10 m s^{-1} ($\Delta v = 1.57$ m s^{-1}) at the same stride times. Stride length and stride time were constrained by treadmill speed during normal treadmill walking, but in split-belt treadmill walking there was considerable variability in the locomotor pattern (Fig. A.1A). However, in split-belt treadmill walking, the locomotor pattern variability is explained by the averaged belt speeds, the belt speed difference and the self-selected step time asymmetry according to Equation A.8 (Fig. A.1B). We contend that Equation A.8 has been verified by the data set and claim that the locomotor pattern during split-belt treadmill locomotion is constrained by the averaged belt speeds, the speed-difference between the belts and the self-selected step time asymmetry.

To interpret Equation A.8, we note that, in split-belt treadmill locomotion like on a normal treadmill, stride length and stride time remain proportional. But in split-belt treadmill locomotion, stride length and stride time are proportional to the averaged belt speeds, the speed-difference between the belts and the self-selected step time asymmetry. Averaged belt speeds and belt speed-difference is set by the experimenter and cannot be changed by the person walking or running on the split-belt treadmill. However, step time asymmetry can be volitionally changed and interacts linearly with the belt speed-difference to change the proportionality of stride length and stride time. At a constant stride time, the effect of volitionally changing step time asymmetry is to change stride length: if step time asymmetry is greater than 0, then stride length decreases; and, if step time asymmetry is less than 0, stride length increases.

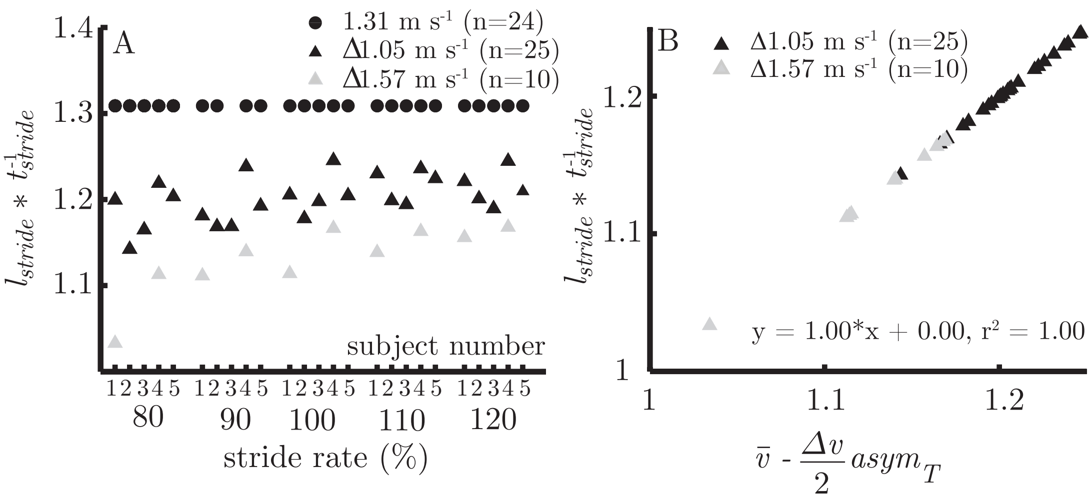

Figure A.1: Validation of split-belt treadmill's constraint on the locomotor pattern. A: In normal treadmill walking (1.31 m s^{-1}), the locomotor pattern is constrained by treadmill speed (combinations of stride length and stride time must be equal to treadmill speed), but in split-belt treadmill walking (Δ1.05 m s^{-1} and Δ1.57 m s^{-1}), there is considerable variability in the locomotor pattern. B: The locomotor pattern variability in split-belt treadmill walking (Δ1.05 m s^{-1} and Δ1.57 m s^{-1}) is explained by the averaged belt speeds, the speed-difference and self-selected step time asymmetry. We performed a linear regression analysis to test if our analytically derived constraint of split-belt treadmill locomotion could explain the variability in measured stride length and stride time during split-belt treadmill walking.

APPENDIX B

TWO METHODS FOR CALCULATING STEP LENGTH

We define step lengths, in accordance with usual definitions (Zatsiorky et al., 1994), as the anterior-posterior distance between the same anatomical marker on either foot between successive bilateral foot contacts with the ground. We calculate step lengths (l) using foot placement differences (α), step times (t) and individual treadmill belt speeds (v) (Donelan et al., 2004; Finley et al., 2015). The left-to-right step length is calculated as:

$$l_{\mathrm{L}\rightarrow\mathrm{R}} = \alpha_{\mathrm{L}\rightarrow\mathrm{R}} + v_{\mathrm{L}} * t_{\mathrm{L}\rightarrow\mathrm{R}}\,, \tag{B.1}$$

and the right-to-left step length is calculated as:

$$l_{\mathrm{R}\rightarrow\mathrm{L}} = \alpha_{\mathrm{R}\rightarrow\mathrm{L}} + v_{\mathrm{R}} * t_{\mathrm{R}\rightarrow\mathrm{L}}\,. \tag{B.2}$$

A modified method to calculate step length is often used in studies on split-belt treadmill locomotion (Finley et al., 2013; Reisman et al., 2005) in which step lengths are calculated as the anterior-posterior distance between the same anatomical marker of each foot at the instant of either foot contact. Using the modified method, step lengths are then calculated at an instant in time. The position of an anatomical marker on the foot, however, changes during the stance phase. For example, as the lateral malleolus marker moves forward when the trailing stance foot plantarflexes, this will lead to a systematic underestimation of the actual step length when calculated at an instant in time using malleolus markers. In our calculation of step lengths, the position of an anatomical marker on the foot is analytically projected, using the duration of the step and the belt speed (that is, the distance that the anatomical position traveled during the step, had it remained in the same place on the treadmill belt), and corrected for differences in foot placements. We thus capture the actual step length according to our definition.

We assessed the effect of implementing either calculation method (our analytical step lengths or the modified, instantaneous step lengths) on step lengths and step length asymmetry by using a pilot data set in which 5 subjects walked on a treadmill at 1.31 m s^{-1} at 5 different stride times (80%, 90%, 100%, 110% and 120% of their preferred stride rate) and walked on a split-belt treadmill with the left belt speed at 0.79 m s^{-1} and the right belt speed at 1.84 m s^{-1} ($\Delta v = 1.05$ m s^{-1}) at the same 5 stride times. Furthermore, 2 of 5 subjects also walked on the split-belt treadmill with the left belt speed at 0.53 m s^{-1} and the right belt speed at 2.10 m s^{-1} ($\Delta v = 1.57$ m s^{-1}) at the same stride times.

Step lengths were highly correlated between methods (Fig. B.1A). However, the instantaneous method underestimated step lengths for longer steps (regression slope is greater than 1). Step length asymmetry calculated from either instantaneous or analytical step lengths agreed well with each other (Fig. B.1B). We conclude that using either method will sufficiently explore step length asymmetry when it is experimentally constrained and will sufficiently capture actual step length asymmetry when used as a variable in further analyses.

Even though the methods for calculating step lengths are highly correlated, we cannot accept the modified, instantaneous method for the treadmill constraint analyses (see sections 3.1.7 and 3.1.8). First, since the instantaneous method underestimates step length, the locomotor pattern, using instantaneous step lengths, fails to satisfy the constraint of normal treadmill walking (instantaneous locomotor pattern does not equal 1.31 m s^{-1}, Fig. B.2A). On the other hand, the locomotor pattern, using analytical step lengths, satisfies the constraint of normal treadmill walking. Second, even though we cannot, a priori, compare the locomotor patterns (using either method) in split-belt treadmill walking to conclude how well the methods perform (Fig. B.2B,C), the locomotor pattern must satisfy the constraint of the split-belt treadmill environment (Equation A.8). Again, the locomotor pattern, using instantaneous step lengths, fails to satisfy the

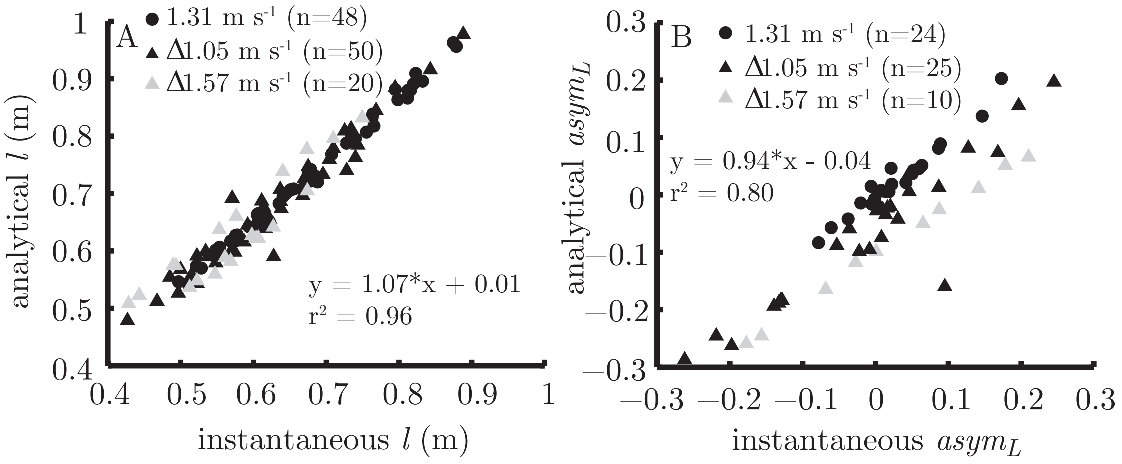

Figure B.1: Comparison of 2 methods for calculating step lengths. Comparison of step lengths calculated using either a modified method at the instant of foot contact (instantaneous step length) or our analytical method (analytical step length) which uses the foot placement difference, step times and individual treadmill belt speeds (A). Comparison of step length asymmetry using the modified instantaneous method and our analytical method (B). For each comparison we performed a linear regression analysis.

constraint of split-belt treadmill locomotion, while the locomotor pattern, using analytical step lengths, satisfies the constraint (Fig. B.2D). We conclude that only analytical step lengths satisfy the locomotor pattern constraints of normal treadmill locomotion and split-belt treadmill locomotion, and, furthermore, that only analytical step lengths are in accordance with our definition of step length. However, since both step lengths and step length asymmetry agree well between methods, we are justified in making comparisons with studies that implement the modified, instantaneous step length method.

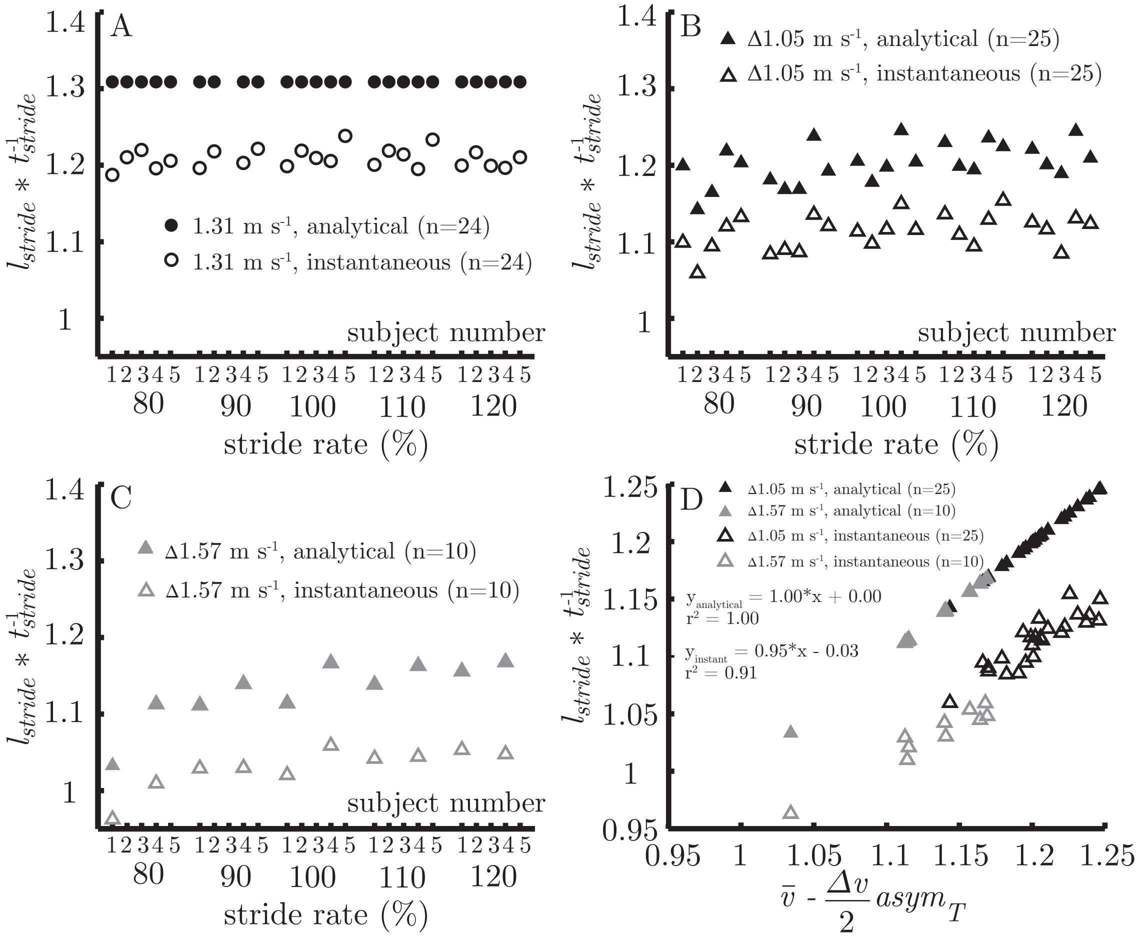

Figure B.2: Comparison of whether 2 methods for calculating step lengths satisfy normal treadmill and split-belt treadmill constraints on the locomotor pattern. Subject-specific comparison of locomotor patterns (combination of stride length and stride time) using step lengths calculated from the analytical and instantaneous methods for normal treadmill walking at 1.31 m s^{-1} (A), split-belt treadmill walking with a speed-difference of 1.05 m s^{-1} (B) and a speed-difference of 1.57 m s^{-1} (C). Comparison of locomotor pattern constraint during split-belt treadmill locomotion using analytical and instantaneous step length calculations (D). We performed a linear regression analysis to test if the locomotor pattern calculated from each method satisfied the constraint of split-belt treadmill locomotion.

APPENDIX C

DERIVATION OF THE RELATIONSHIP BETWEEN FOOT PLACEMENT DIFFERENCE AND ASYMMETRY IN STEP LENGTHS AND STEP TIMES

Derivation of formula of foot placement difference on a normal treadmill

We wish to show how foot placement difference (α) is related to the treadmill's belt speed (v), stride time (t_{stride}), step length asymmetry ($asym_{\text{L}}$) and step time asymmetry ($asym_{\text{T}}$). The combination of stride length and stride time must satisfy belt speed such that:

$$l_{stride} * l_{stride}^{-1} = v \,. \tag{C.1}$$

The stride cycle consist of a step from the left leg's heel-strike to the right leg's heel-strike ($\text{L} \rightarrow \text{R}$) and from the right leg's heel-strike to the left leg's heel-strke ($\text{R} \rightarrow \text{L}$). We define step length asymmetry as:

$$asym_{\text{L}} = \frac{\Delta l}{l_{stride}} = \frac{l_{\text{L}\rightarrow\text{R}} - l_{\text{R}\rightarrow\text{L}}}{l_{\text{L}\rightarrow\text{R}} + l_{\text{R}\rightarrow\text{L}}} \,, \tag{C.2}$$

and step time asymmetry as:

$$asym_{\text{T}} = \frac{\Delta t}{t_{stride}} = \frac{t_{\text{L}\rightarrow\text{R}} - t_{\text{R}\rightarrow\text{L}}}{t_{\text{L}\rightarrow\text{R}} + t_{\text{R}\rightarrow\text{L}}} \,. \tag{C.3}$$

We consider steady-state gait parameters such that:

$$\alpha_{\mathrm{L}\rightarrow\mathrm{R}} = -\alpha_{\mathrm{R}\rightarrow\mathrm{L}} \, . \tag{C.4}$$

Furthermore, we define the left-to-right step length as:

$$l_{\mathrm{L}\rightarrow\mathrm{R}} = t_{\mathrm{L}\rightarrow\mathrm{R}} * v + \alpha_{\mathrm{L}\rightarrow\mathrm{R}} \, , \tag{C.5}$$

and the left-to-right step length as:

$$l_{\mathrm{R}\rightarrow\mathrm{L}} = t_{\mathrm{R}\rightarrow\mathrm{L}} * v + \alpha_{\mathrm{R}\rightarrow\mathrm{L}} \, . \tag{C.6}$$

We first find step length difference using Eqs. C.4, C.5 and C.6:

$$\begin{aligned} \Delta l = l_{\mathrm{L}\rightarrow\mathrm{R}} - l_{\mathrm{R}\rightarrow\mathrm{L}} &= t_{\mathrm{L}\rightarrow\mathrm{R}} * v + \alpha_{\mathrm{L}\rightarrow\mathrm{R}} - (t_{\mathrm{R}\rightarrow\mathrm{L}} * v + \alpha_{\mathrm{R}\rightarrow\mathrm{L}}) \\ &= 2\alpha_{\mathrm{L}\rightarrow\mathrm{R}} + \Delta t * v \, . \end{aligned} \tag{C.7}$$

From here, we, first, express step length difference as the product of step length asymmetry and stride length (Eq. C.2), second, express stride length as the product of stride time and belt speed (Eq. C.1), and, third, express step time difference as the product of step time asymmetry and stride time (Eq. C.3):

$$asym_{\mathrm{L}} * t_{stride} * v = asym_{\mathrm{T}} * t_{stride} * v + 2\alpha_{\mathrm{L}\rightarrow\mathrm{R}} \, . \tag{C.8}$$

Last, we isolate foot placement difference:

$$\alpha_{\mathrm{L}\rightarrow\mathrm{R}} = \frac{1}{2} * t_{stride} * v * (asym_{\mathrm{L}} - asym_{\mathrm{T}}) \, . \tag{C.9}$$

Derivation of formula for foot placement difference on a split-belt treadmill

On a split-belt treadmill we can set one treadmill belt to run slow (v_{S}) and the other belt to run fast (v_{F}). The average belt speed ($\overline{v}$) is $\frac{1}{2}(v_{\mathrm{F}} + v_{\mathrm{S}})$ and the belt speed-difference (Δv) is $v_{\mathrm{F}} - v_{\mathrm{S}}$. The stride cycle consists of a step from heel-strike on the leg on the slow belt to heel-strike on the leg on the fast belt ($\mathrm{S}\rightarrow\mathrm{F}$) and a step from heel-strike on the leg on the fast belt to heel-strike on the leg on the slow belt ($\mathrm{F}\rightarrow\mathrm{S}$). We define step length asymmetry as:

$$asym_{\mathrm{L}} = \frac{\Delta l}{l_{stride}} = \frac{l_{\mathrm{S}\rightarrow\mathrm{F}} - l_{\mathrm{F}\rightarrow\mathrm{S}}}{l_{\mathrm{S}\rightarrow\mathrm{F}} + l_{\mathrm{F}\rightarrow\mathrm{S}}}\,, \tag{C.10}$$

and step time asymmetry as:

$$asym_{\mathrm{T}} = \frac{\Delta t}{t_{stride}} = \frac{t_{\mathrm{S}\rightarrow\mathrm{F}} - t_{\mathrm{F}\rightarrow\mathrm{S}}}{t_{\mathrm{S}\rightarrow\mathrm{F}} + t_{\mathrm{F}\rightarrow\mathrm{S}}}\,. \tag{C.11}$$

In Appendix A we derived the split-belt treadmill constraint on the combination of stride length and stride time:

$$l_{stride} * t_{stride}^{-1} = \overline{v} - \frac{\Delta v}{2} * asym_{\mathrm{T}}\,. \tag{C.12}$$

We consider steady-state gait parameters such that:

$$\alpha_{\mathrm{S}\rightarrow\mathrm{F}} = -\alpha_{\mathrm{F}\rightarrow\mathrm{S}}\,. \tag{C.13}$$

Furthermore, we define the slow-to-fast step length as:

$$l_{\mathrm{S}\rightarrow\mathrm{F}} = t_{\mathrm{S}\rightarrow\mathrm{F}} * v_{\mathrm{S}} + \alpha_{\mathrm{S}\rightarrow\mathrm{F}}\,, \tag{C.14}$$

and the fast-to-slow step length as:

$$l_{\mathrm{F}\rightarrow\mathrm{S}} = t_{\mathrm{F}\rightarrow\mathrm{S}} * v_{\mathrm{F}} + \alpha_{\mathrm{F}\rightarrow\mathrm{S}}\,. \tag{C.15}$$

First, we find step length difference using Eqs. C.13, C.14 and C.15:

$$\begin{aligned}\Delta l = l_{\mathrm{S}\to\mathrm{F}} - l_{\mathrm{F}\to\mathrm{S}} &= t_{\mathrm{S}\to\mathrm{F}} * v_{\mathrm{S}} + \alpha_{\mathrm{S}\to\mathrm{F}} - (t_{\mathrm{F}\to\mathrm{S}} * v_{\mathrm{F}} + \alpha_{\mathrm{F}\to\mathrm{S}}) \\ &= 2\alpha_{\mathrm{S}\to\mathrm{F}} + t_{\mathrm{S}\to\mathrm{F}} * v_{\mathrm{S}} - t_{\mathrm{F}\to\mathrm{S}} * v_{\mathrm{F}}\,. \end{aligned} \tag{C.16}$$

Next, we change the last 2 terms on the right-hand side into the sum of their halves and add a sum of terms $(\frac{1}{2}t_{\mathrm{S}\to\mathrm{F}} * v_{\mathrm{F}} - \frac{1}{2}t_{\mathrm{S}\to\mathrm{F}} * v_{\mathrm{F}} + \frac{1}{2}t_{\mathrm{F}\to\mathrm{S}} * v_{\mathrm{S}} - \frac{1}{2}t_{\mathrm{F}\to\mathrm{S}} * v_{\mathrm{S}})$ to the right-hand side:

$$\begin{aligned}\Delta l = 2\alpha_{\mathrm{S}\to\mathrm{F}} &+ \frac{1}{2}t_{\mathrm{S}\to\mathrm{F}} * v_{\mathrm{S}} + \frac{1}{2}t_{\mathrm{S}\to\mathrm{F}} * v_{\mathrm{S}} - \frac{1}{2}t_{\mathrm{F}\to\mathrm{S}} * v_{\mathrm{F}} - \frac{1}{2}t_{\mathrm{F}\to\mathrm{S}} * v_{\mathrm{F}} \\ &+ \frac{1}{2}t_{\mathrm{S}\to\mathrm{F}} * v_{\mathrm{F}} - \frac{1}{2}t_{\mathrm{S}\to\mathrm{F}} * v_{\mathrm{F}} + \frac{1}{2}t_{\mathrm{F}\to\mathrm{S}} * v_{\mathrm{S}} - \frac{1}{2}t_{\mathrm{F}\to\mathrm{S}} * v_{\mathrm{S}}\,. \end{aligned} \tag{C.17}$$

We convert the sum of terms on the right-hand side:

$$\Delta l = 2\alpha_{\mathrm{S}\to\mathrm{F}} + \frac{1}{2}(v_{\mathrm{F}} + v_{\mathrm{S}})(t_{\mathrm{S}\to\mathrm{F}} - t_{\mathrm{F}\to\mathrm{S}}) + \frac{1}{2}(-v_{\mathrm{F}} + v_{\mathrm{S}})(t_{\mathrm{S}\to\mathrm{F}} + t_{\mathrm{F}\to\mathrm{S}})\,. \tag{C.18}$$

We insert average speed ($\overline{v}$), speed-difference (Δv), step time difference (Δt) and stride time (t_{stride}):

$$\Delta l = 2\alpha_{\mathrm{S}\to\mathrm{F}} + \overline{v} * \Delta t - \frac{\Delta v}{2} * t_{stride}\,. \tag{C.19}$$

At this point, we have obtained a similar expression of step length difference as derived by Finley et al. (2015). From here, we, first, express step length difference as the product of step length asymmetry and stride length (Eq. C.10), second, express stride length using the split-belt treadmill's constraint on stride length and stride time (Eq. C.12) and, third, express step time difference as the product of step time asymmetry and stride time (Eq. C.11):

$$asym_{\mathrm{L}} * (\overline{v} - \frac{\Delta v}{2} * asym_{\mathrm{T}}) * t_{stride} = 2\alpha_{\mathrm{S}\to\mathrm{F}} + \overline{v} * asym_{\mathrm{T}} * t_{stride} - \frac{\Delta v}{2} * t_{stride}\,. \tag{C.20}$$

Last, we isolate foot placement difference:

$$\alpha_{\mathrm{S}\to\mathrm{F}} = \frac{1}{2} * t_{stride} * (\overline{v} * (asym_{\mathrm{L}} - asym_{\mathrm{T}}) + \frac{\Delta v}{2} * (1 - asym_{\mathrm{L}} * asym_{\mathrm{T}}))\,. \tag{C.21}$$

Alternatively, the relationship between foot placement difference, step length asymmetry and step time asymmetry can be expressed as:

$$asym_{\mathrm{T}} = \frac{-2\alpha_{\mathrm{S}\to\mathrm{F}} + (\overline{v} * asym_{\mathrm{L}} + \frac{\Delta v}{2}) * t_{stride}}{(\overline{v} + \frac{\Delta v}{2} * asym_{\mathrm{L}}) * t_{stride}}\,, \tag{C.22}$$

or

$$asym_{\mathrm{L}} = \frac{2\alpha_{\mathrm{S}\to\mathrm{F}} + (\overline{v} * asym_{\mathrm{T}} - \frac{\Delta v}{2}) * t_{stride}}{(\overline{v} - \frac{\Delta v}{2} * asym_{\mathrm{T}}) * t_{stride}}\,. \tag{C.23}$$

APPENDIX D

SUPPLEMENTAL DATA FOR EXPERIMENT 1

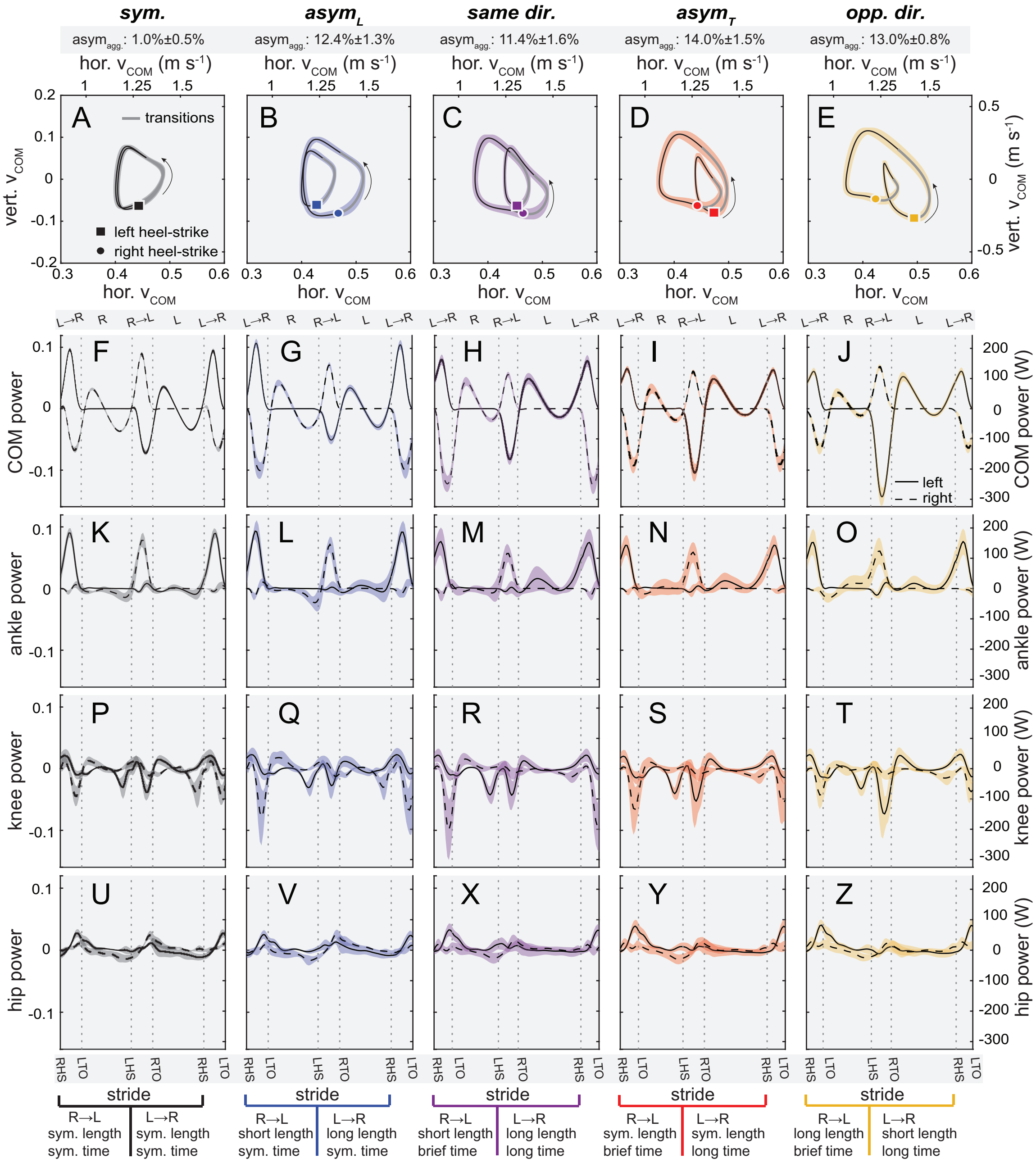

Figure D.1: Example of center of mass velocity and mechanical power for symmetrical and asymmetrical walking. Data is averaged across 10 subjects and trials were chosen to give about equal magnitudes of asymmetry (shading is standard error of the mean). (A–E) Center of mass velocity in anterior-posterior (hor.) and vertical (vert.) directions. Top and right-hand axes display velocity dimensionalized to m s^{-1}. Circles and squares are right and left heel-strikes, respectively. Grey paths are step-to-step transitions (double support). Mechanical power performed on the center of mass (F–J) and at the ankle (K–O), knee (P–T) and hip (U–Z). Solid and dashed lines are left and right legs, respectively. Right-hand Y-axes display power dimensionalized to W.

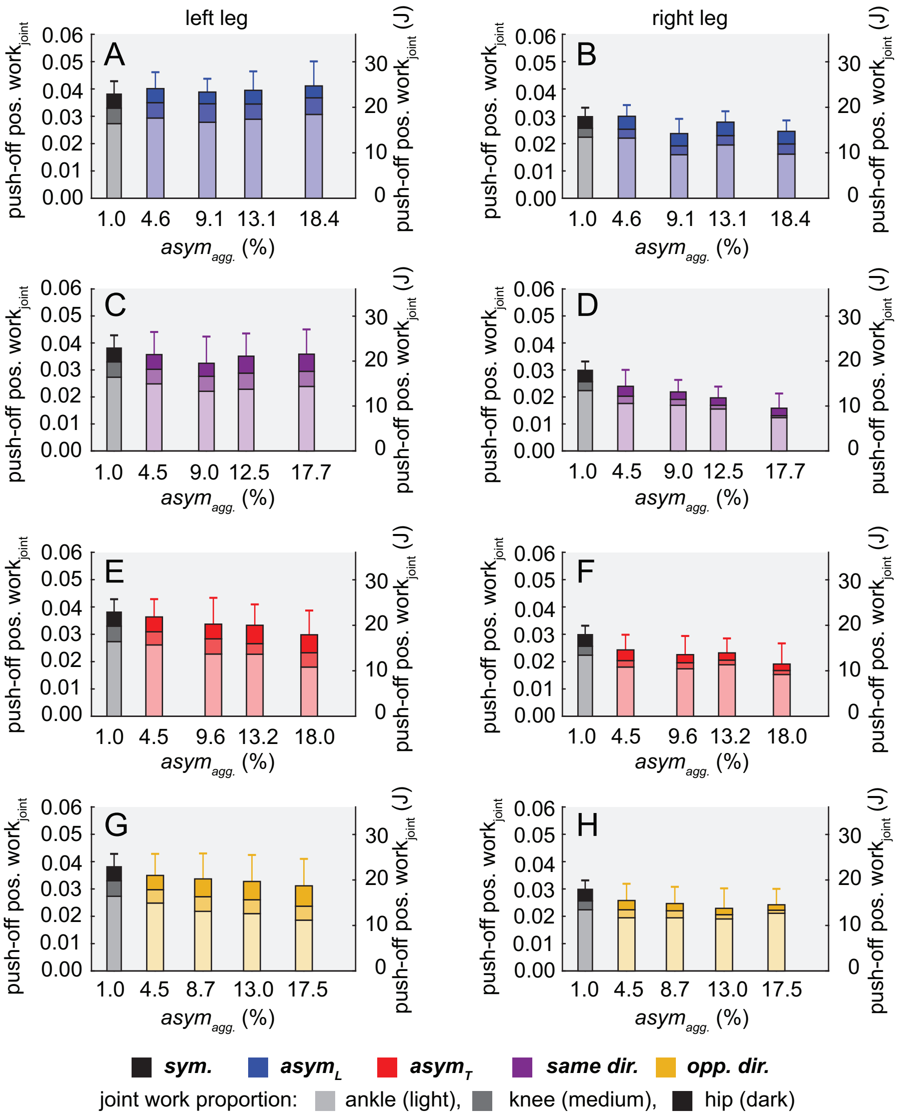

Figure D.2: Push-off joint work in asymmetrical walking. Data are averaged across all trials in each cluster and error bars are standard deviations of summed joint work. Shading shows each joint's contribution to summed joint work: ankle (light), knee (medium) and hip (dark). Right-hand Y-axes display work dimensionalized to J.

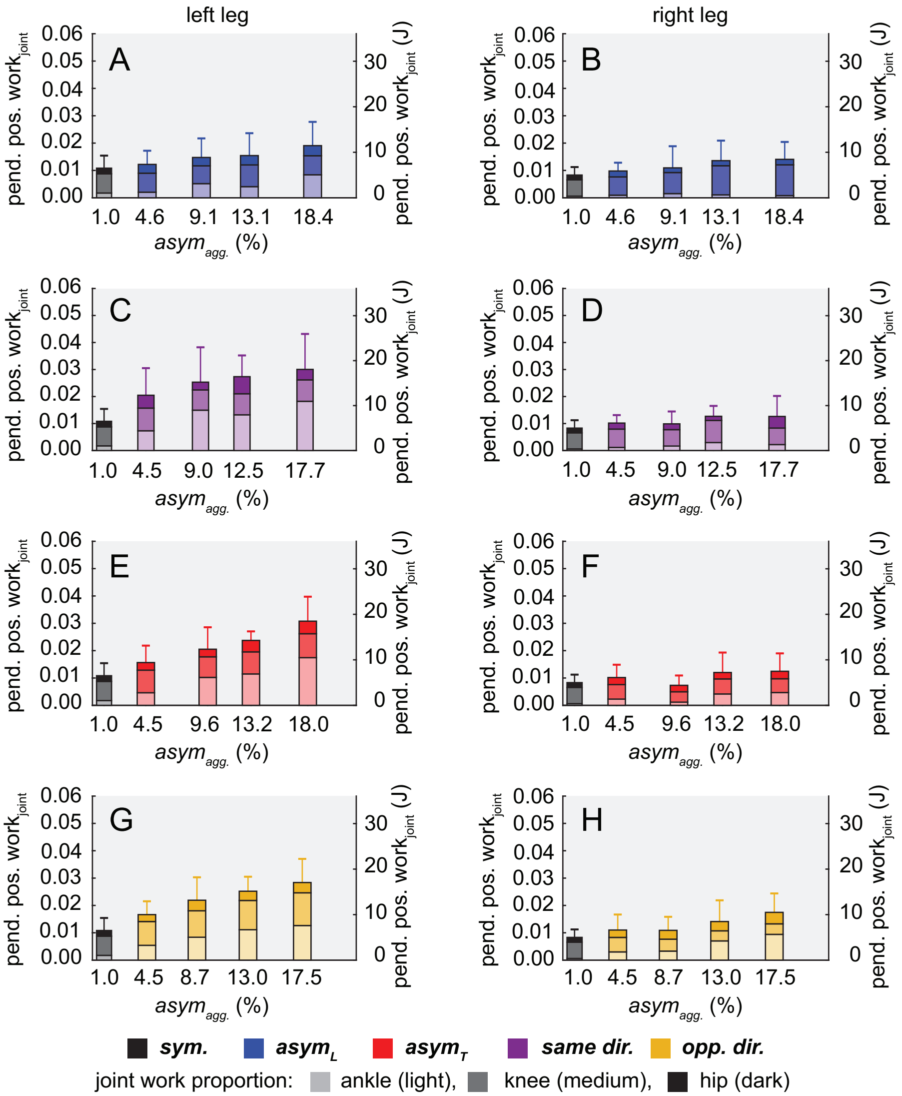

Figure D.3: Positive joint work during the pendular phase in asymmetrical walking. Data are averaged across all trials in each cluster and error bars are standard deviations of summed joint work. Shading shows each joint's contribution to summed joint work: ankle (light), knee (medium) and hip (dark). Right-hand Y-axes display work dimensionalized to J.

Table D.1: Linear regressions of metabolic cost of asymmetry. Regressions refer to data presented in Fig. 5.3 (page 55) and Fig. 5.4 (page 56).

Relation	Condition	Slope	Intercept	r^2	P
met. cost (vs. $asym_{agg.}$)	$\boldsymbol{asym}_{\mathbf{l}}$	1.41	98.2	0.42	<0.001
	$\boldsymbol{asym}_{\mathbf{t}}$	3.65	92.5	0.71	<0.001
	same dir.	3.81	98.7	0.60	<0.001
	opp. dir.	4.03	94.0	0.73	<0.001
residuals (vs. $asym_{agg.}$)	cost of $\boldsymbol{asym}_{\mathbf{l}}$	-2.46	1.6	0.49	<0.001
	cost of $\boldsymbol{asym}_{\mathbf{t}}$	-0.50	-0.8	0.04	0.070
	additive cost	0.99	0.4	0.13	0.001

Table D.2: Linear regressions of center of mass mechanics. Regressions refer to data presented in Fig. 5.5 (page 58) and Fig. 5.6 (page 59). Actual collisional losses of center of mass energy ($W^{-}_{COM,coll.}$), total positive work performed on the center of mass over entire stride ($W^{+}_{COM,stride}$), positive work performed in pendular phases ($W^{+}_{COM,pend.}$), percentage of positive work performed in pendular phases relative to total positive work (%-$W^{+}_{COM,pend.}$).

Relation	Condition	Slope	Intercept	r^2	P
pred. coll. loss (vs. $asym_{agg.}$)	$\boldsymbol{asym}_{\mathbf{l}}$	0.84	97.8	0.60	<0.001
	$\boldsymbol{asym}_{\mathbf{t}}$	0.57	100.3	0.38	<0.001
	same dir.	1.20	98.1	0.72	<0.001
	opp. dir.	1.50	97.0	0.80	<0.001
$W^{-}_{COM,coll.}$ (vs. pred. coll. loss)	ensemble	0.46	-0.1	0.57	<0.001
$W^{+}_{COM,stride}$ (vs. $W^{-}_{COM,coll.}$)	ensemble	0.80	0.0	0.77	<0.001
$W^{+}_{COM,pend.}$ (vs. $W^{-}_{COM,coll.}$)	ensemble	1.02	-0.0	0.85	<0.001
$W^{-}_{COM,coll.}$ (vs. $asym_{agg.}$)	$\boldsymbol{asym}_{\mathbf{l}}$	1.85	98.5	0.32	<0.001
	$\boldsymbol{asym}_{\mathbf{t}}$	2.84	99.1	0.38	<0.001
	same dir.	2.70	106.4	0.27	<0.001
	opp. dir.	3.89	101.2	0.54	<0.001
$W^{+}_{COM,stride}$ (vs. $asym_{agg.}$)	$\boldsymbol{asym}_{\mathbf{l}}$	0.71	99.0	0.15	0.006
	$\boldsymbol{asym}_{\mathbf{t}}$	0.76	95.0	0.16	0.004
	same dir.	0.98	99.2	0.17	0.003
	opp. dir.	0.79	97.7	0.16	0.004
%-$W^{+}_{COM,pend.}$ (vs. $asym_{agg.}$)	$\boldsymbol{asym}_{\mathbf{l}}$	2.01	99.1	0.25	<0.001
	$\boldsymbol{asym}_{\mathbf{t}}$	5.98	94.2	0.61	<0.001
	same dir.	5.49	110.3	0.47	<0.001
	opp. dir.	5.73	98.4	0.57	<0.001

Table D.3: Linear regressions of mechanical work rate and metabolic cost. Regressions refer to data presented in Fig. 5.7 on page 61. Rate of total positive work performed on the center of mass throughout entire stride ($\dot{W}^{+}_{COM,stride}$), rate of total positive work summed across joints throughout entire stride ($\dot{W}^{+}_{\Sigma joint,stride}$), rate of positive work performed on the center of mass in pendular phases ($\dot{W}^{+}_{COM,pend.}$), rate of positive work summed across joints in pendular phases ($\dot{W}^{+}_{\Sigma joint,pend.}$).

Relation	Condition	Slope	Intercept	r^2	P
$\dot{W}^{+}_{COM,stride}$ (vs. met. cost)	ensemble	3.20	0.1	0.26	<0.001
$\dot{W}^{+}_{\Sigma joint,stride}$ (vs. met. cost)	ensemble	0.51	0.1	0.13	<0.001
$\dot{W}^{+}_{COM,pend.}$ (vs. met. cost)	ensemble	3.44	0.1	0.51	<0.001
$\dot{W}^{+}_{\Sigma joint,pend.}$ (vs. met. cost)	ensemble	1.58	0.1	0.63	<0.001

Table D.4: Linear regressions of mechanical adaptations to asymmetrical walking. Regressions refer to data presented in Fig. 5.8 (page 62) and Fig. 5.9 (page 63). Push-off work performed on the center of mass ($W^{+}_{COM,push-off}$), positive work performed on the center of mass during the pendular phase ($W^{+}_{COM,pend.}$), positive work in pendular phases at ankle ($W^{+}_{ankle,pend.}$), knee ($W^{+}_{knee,pend.}$) and hip ($W^{+}_{hip,pend.}$) and summed across joints ($W^{+}_{\Sigma joint,pend.}$).

Relation	Condition	Slope	Intercept	r^2	P
left $W^{+}_{COM,push-off}$ (vs. $asym_{agg.}$)	$\boldsymbol{asym}_{\mathbf{l}}$	0.0004	0.026	0.16	0.004
	$\boldsymbol{asym}_{\mathbf{t}}$	−0.0006	0.027	0.36	<0.001
	same dir.	−0.0002	0.025	0.03	0.267
	opp. dir.	−0.0008	0.027	0.55	<0.001
right $W^{+}_{COM,push-off}$ (vs. $asym_{agg.}$)	$\boldsymbol{asym}_{\mathbf{l}}$	−0.0005	0.024	0.35	<0.001
	$\boldsymbol{asym}_{\mathbf{t}}$	−0.0006	0.024	0.49	<0.001
	same dir.	−0.0009	0.024	0.72	<0.001
	opp. dir.	−0.0003	0.024	0.10	0.023
left $W^{+}_{COM,pend.}$ (vs. $asym_{agg.}$)	$\boldsymbol{asym}_{\mathbf{l}}$	0.0003	0.012	0.06	0.080
	$\boldsymbol{asym}_{\mathbf{t}}$	0.0015	0.011	0.52	<0.001
	same dir.	0.0013	0.014	0.37	<0.001
	opp. dir.	0.0015	0.012	0.47	<0.001
right $W^{+}_{COM,pend.}$ (vs. $asym_{agg.}$)	$\boldsymbol{asym}_{\mathbf{l}}$	0.0006	0.010	0.23	<0.001
	$\boldsymbol{asym}_{\mathbf{t}}$	0.0005	0.009	0.11	0.017
	same dir.	0.0007	0.009	0.20	0.001
	opp. dir.	0.0002	0.010	0.02	0.315
$W^{+}_{\Sigma joint,pend.}$ (vs. $W^{+}_{ankle,pend.}$)	ensemble	1.16	0.0	0.71	<0.001
$W^{+}_{\Sigma joint,pend.}$ (vs. $W^{+}_{knee,pend.}$)	ensemble	0.70	0.0	0.12	<0.001
$W^{+}_{\Sigma joint,pend.}$ (vs. $W^{+}_{hip,pend.}$)	ensemble	1.01	0.0	0.21	<0.001

BIBLIOGRAPHY

Abbott, B. C., Bigland, B., & Ritchie, J. M. (1952). The physiological cost of negative work. *J Physiol*, 117(3), 380–90.

Adamczyk, P. G. & Kuo, A. D. (2009). Redirection of center-of-mass velocity during the step-to-step transition of human walking. *J Exp Biol*, 212(16), 2668–78.

Adamczyk, P. G. & Kuo, A. D. (2015). Mechanisms of gait asymmetry due to push-off deficiency in unilateral amputees. *IEEE T Neur Sys Reh*, 23(5), 776–85.

Alexander, R. M. (2001). Design by numbers. *Nature*, 412(6847), 591.

Anderson, F. C. & Pandy, M. G. (2001). Dynamic optimization of human walking. *J Biomech Eng*, 123(5), 381–90.

Ankaralı, M. M., Sefati, S., Madhav, M. S., Long, A., Bastian, A. J., & Cowan, N. J. (2015). Walking dynamics are symmetric (enough). *J R Soc Interface*, 12(108), 20150209.

Arsenault, A. B., Winter, D. A., & Marteniuk, R. G. (1986). Bilateralism of emg profiles in human locomotion. *Am J Phys Med*, 65(1), 1–16.

Awad, L. N., Palmer, J. A., Pohlig, R. T., Binder-Macleod, S. A., & Reisman, D. S. (2015). Walking speed and step length asymmetry modify the energy cost of walking after stroke. *Neurorehab Neural Re*, 29(5), 416–23.

Bastian, A. J. (2008). Understanding sensorimotor adaptation and learning for rehabilitation. *Curr Opin Neurol*, 21(6), 628–33.

Bauby, C. E. & Kuo, A. D. (2000). Active control of lateral balance in human walking. *J Biomech*, 33(11), 1433–40.

Bellanca, J. L., Lowry, K. A., Vanswearingen, J. M., Brach, J. S., & Redfern, M. S. (2013). Harmonic ratios: a quantification of step to step symmetry. *J Biomech*, 46(4), 828–31.

Bernstein, N. A. (1967). *The co-ordination and regulation of movements*. Oxford: Pergamon Press.

Bertram, J. E. (2005). Constrained optimization in human walking: cost minimization and gait plasticity. *J Exp Biol*, 208(6), 979–91.

Bertram, J. E. & Ruina, A. (2001). Multiple walking speed-frequency relations are predicted by constrained optimization. *J Theor Biol*, 209(4), 445–53.

Bertram, J. E. A. & Hasaneini, S. J. (2013). Neglected losses and key costs: tracking the energetics of walking and running. *J Exp Biol*, 216(6), 933–38.

Beyaert, C., Grumillier, C., Martinet, N., Paysant, J., & André, J.-M. (2008). Compensatory mechanism involving the knee joint of the intact limb during gait in unilateral below-knee amputees. *Gait Posture*, 28(2), 278–84.

Bornstein, M. H. & Bornstein, H. G. (1976). The pace of life. *Nature*, 259, 557–9.

Brockway, J. M. (1987). Derivation of formulae used to calculate energy expenditure in man. *Hum Nutr Clin Nutr*, 41(6), 463–71.

Brown, A. M., Zifchock, R. A., & Hillstrom, H. J. (2014). The effects of limb dominance and fatigue on running biomechanics. *Gait Posture*, 39(3), 915–9.

Bruijn, S. M., Meijer, O. G., Beek, P. J., & van Dieën, J. H. (2013). Assessing the stability of human locomotion: a review of current measures. *J R Soc Interface*, 10(83), 20120999.

Bruijn, S. M., van Dieën, J. H., Meijer, O. G., & Beek, P. J. (2009). Is slow walking more stable? *J Biomech*, 42(10), 1506–12.

Bussel, B., Roby-Brami, A., Neris, O. R., & Yakovleff, A. (1996). Evidence for a spinal stepping generator in man. *Paraplegia*, 34(2), 91–2.

Calancie, B., Needham-Shropshire, B., Jacobs, P., Willer, K., Zych, G., & Green, B. A. (1994). Involuntary stepping after chronic spinal cord injury. evidence for a central rhythm generator for locomotion in man. *Brain*, 117(5), 1143–59.

Capaday, C., Lavoie, B. A., Barbeau, H., Schneider, C., & Bonnard, M. (1999). Studies on the corticospinal control of human walking. i. responses to focal transcranial magnetic stimulation of the motor cortex. *J Neurophysiol*, 81(1), 129–39.

Cavagna, G. A. (1975). Force platforms as ergometers. *J Appl Physiol*, 39(1), 174–9.

Cavagna, G. A., Heglund, N. C., & Taylor, C. R. (1977). Mechanical work in terrestrial locomotion: two basic mechanisms for minimizing energy expenditure. *Am J Physiol*, 233(5), R243–61.

Cavagna, G. A. & Margaria, R. (1966). Mechanics of walking. *J Appl Physiol*, 21(1), 271–8.

Cavanagh, P. R. & Williams, K. R. (1982). The effect of stride length variation on oxygen uptake during distance running. *Med Sci Sports Exerc*, 14(1), 30–5.

Chen, G., Patten, C., Kothari, D. H., & Zajac, F. E. (2005). Gait differences between individuals with post-stroke hemiparesis and non-disabled controls at matched speeds. *Gait Posture*, 22(1), 51–6.

Cher, P. H., Stewart, I. B., & Worringham, C. J. (2015). Minimum cost of transport in human running is not ubiquitous. *Med Sci Sports Exerc*, 47(2), 307–14.

Chodera, J. D. (1974). Analysis of gait from footprints. *Physiotherapy*, 60(6), 179–81.

Choi, J. T. & Bastian, A. J. (2007). Adaptation reveals independent control networks for human walking. *Nat Neurosci*, 10(8), 1055–62.

Choi, J. T., Jensen, P., Nielsen, J. B., & Bouyer, L. J. (2016). Error signals driving locomotor adaptation: cutaneous feedback from the foot is used to adapt movement during perturbed walking. *J Physiol*, 594(19), 5673–84.

Choi, J. T., Vining, E. P., Reisman, D. S., & Bastian, A. J. (2009). Walking flexibility after hemispherectomy: split-belt treadmill adaptation and feedback control. *Brain*, 132(3), 722–33.

Christensen, L. O., Johannsen, P., Sinkjær, T., Petersen, N., Pyndt, H. S., & Nielsen, J. B. (2000). Cerebral activation during bicycle movements in man. *Exp Brain Res*, 135(1), 66–72.

Collins, A. G. & Valentine, J. W. (2001). Defining phyla: evolutionary pathways to metazoan body plans. *Evol Dev*, 3(6), 432–42.

Collins, J. J. & Stewart, I. B. (1993). Coupled nonlinear oscillators and the symmetries of animal gaits. *J Nonlinear Sci*, 3(1), 349–92.

Cotes, J. E. & Meade, F. (1960). The energy expenditure and mechanical energy demand in walking. *Ergonomics*, 3(2), 97–119.

Croft, J. L., Schroeder, R. T., & Bertram, J. E. A. (2019). The landscape of movement control in locomotion: Cost, strategy, and solution. *Front Psychol*, 10, 716.

Crone, C., Hultborn, H., Jespersen, B., & Nielsen, J. (1987). Reciprocal ia inhibition between ankle flexors and extensors in man. *J Physiol*, 389(1), 163–85.

Darmohray, D. M., Jacobs, J. R., Marques, H. G., & Carey, M. R. (2019). Spatial and temporal locomotor learning in mouse cerebellum. *Neuron*, 102(1), 217–31.

Day, K. A., Leech, K. A., Roemmich, R. T., & Bastian, A. J. (2018). Accelerating locomotor savings in learning: compressing four training days to one. *J Neurophysiol*, 119(6), 2100–13.

Diedrich, F. J. & Warren, W. H., J. (1995). Why change gaits? dynamics of the walk-run transition. *J Exp Psychol Hum Percept Perform*, 21(1), 183–202.

Dimitrijevic, M. R., Gerasimenko, Y., & Pinter, M. M. (1998). Evidence for a spinal central pattern generator in humans. *Ann N Y Acad Sci*, 860(1), 360–76.

Dingwell, J. B. & Marin, L. C. (2006). Kinematic variability and local dynamic stability of upper body motions when walking at different speeds. *J Biomech*, 39(3), 444–52.

Doke, J., Donelan, J. M., & Kuo, A. D. (2005). Mechanics and energetics of swinging the human leg. *J Exp Biol*, 208(3), 439–45.

Doke, J. & Kuo, A. D. (2007). Energetic cost of producing cyclic muscle force, rather than work, to swing the human leg. *J Exp Biol*, 210(13), 2390–8.

Donelan, J. M., Kram, R., & Kuo, A. D. (2001). Mechanical and metabolic determinants of the preferred step width in human walking. *Proc Biol Sci*, 268(1480), 1985–92.

Donelan, J. M., Kram, R., & Kuo, A. D. (2002a). Mechanical work for step-to-step transitions is a major determinant of the metabolic cost of human walking. *J Exp Biol*, 205(23), 3717–27.

Donelan, J. M., Kram, R., & Kuo, A. D. (2002b). Simultaneous positive and negative external mechanical work in human walking. *J Biomech*, 35(1), 117–24.

Donelan, J. M., Shipman, D. W., Kram, R., & Kuo, A. D. (2004). Mechanical and metabolic requirements for active lateral stabilization in human walking. *J Biomech*, 37(6), 827–35.

Du Chatinier, K. & Rozendal, R. H. (1970). Temporal symmetry of gait of selected normal human subjects. *Proc K Ned Akad Wet C*, 73(4), 353–61.

Eccles, J. C., Fatt, P., & Landgren, S. (1956). Central pathway for direct inhibitory action of impulses in largest afferent nerve fibres to muscle. *J Neurophysiol*, 19(1), 75–98.

Ellis, R. G., Howard, K. C., & Kram, R. (2013). The metabolic and mechanical costs of step time asymmetry in walking. *Proc Biol Sci*, 280(1756), 20122784.

England, S. A. & Granata, K. P. (2007). The influence of gait speed on local dynamic stability of walking. *Gait Posture*, 25(2), 172–178.

Exell, T. A., Gittoes, M. J., Irwin, G., & Kerwin, D. G. (2012). Gait asymmetry: composite scores for mechanical analyses of sprint running. *J Biomech*, 45(6), 1108–11.

Farris, D. J., Hampton, A., Lewek, M. D., & Sawicki, G. S. (2015). Revisiting the mechanics and energetics of walking in individuals with chronic hemiparesis following stroke: from individual limbs to lower limb joints. *J Neuroeng Rehabil*, 12, 24.

Farris, D. J. & Sawicki, G. S. (2012). The mechanics and energetics of human walking and running: a joint level perspective. *J R Soc Interface*, 9(66), 110–8.

Finley, J. M. & Bastian, A. J. (2017). Associations between foot placement asymmetries and metabolic cost of transport in hemiparetic gait. *Neurorehab Neural Re*, 31(2), 168–77.

Finley, J. M., Bastian, A. J., & Gottschall, J. S. (2013). Learning to be economical: the energy cost of walking tracks motor adaptation. *J Physiol*, 591(4), 1081–95.

Finley, J. M., Long, A., Bastian, A. J., & Torres-Oviedo, G. (2015). Spatial and temporal control contribute to step length asymmetry during split-belt adaptation and hemiparetic gait. *Neurorehab Neural Re*, 29(8), 786–95.

Finnerty, J. R., Pang, K., Burton, P., Paulson, D., & Martindale, M. Q. (2004). Origins of bilateral symmetry: Hox and dpp expression in a sea anemone. *Science*, 304(5675), 1335–7.

Forczek, W. & Staszkiewicz, R. (2012). An evaluation of symmetry in the lower limb joints during the able-bodied gait of women and men. *J Hum Kinet*, 35(1), 47–57.

Franklin, D. W. & Wolpert, D. M. (2011). Computational mechanisms of sensorimotor control. *Neuron*, 72(3), 425–42.

Garcia, M., Chatterjee, A., Ruina, A., & Coleman, M. (1998). The simplest walking model: Stability, complexity, and scaling. *J Biomech Eng-T ASME*, 120(2), 281–8.

Gonzalez-Rubio, M., Velasquez, N., & Torres-Oviedo, G. (2019). Explicit control of step timing during split-belt walking reveals interdependent recalibration of movements in space and time. *Front Hum Neurosci*, 13, 207.

Gottschall, J. S. & Kram, R. (2005). Energy cost and muscular activity required for leg swing during walking. *J Appl Physiol*, 99(1), 23–30.

Gregg, R. D., Dhaher, Y. Y., Degani, A., & Lynch, K. M. (2012). On the mechanics of functional asymmetry in bipedal walking. *IEEE T Bio-Med Eng*, 59(5), 1310–8.

Gundersen, L. A., Valle, D. R., Barr, A. E., Danoff, J. V., Stanhope, S. J., & Snyder-Mackler, L. (1989). Bilateral analysis of the knee and ankle during gait: an examination of the relationship between lateral dominance and symmetry. *Phys Ther*, 69(8), 640–50.

Gurney, B. (2002). Leg length discrepancy. *Gait Posture*, 15(2), 195–206.

Gutmann, A. K., Jacobi, B., Butcher, M. T., & Bertram, J. E. (2006). Constrained optimization in human running. *J Exp Biol*, 209(4), 622–32.

Haddad, J. M., van Emmerik, R. E., Whittlesey, S. N., & Hamill, J. (2006). Adaptations in interlimb and intralimb coordination to asymmetrical loading in human walking. *Gait Posture*, 23(4), 429–34.

Hak, L., Houdijk, H., Beek, P. J., & van Dieën, J. H. (2013). Steps to take to enhance gait stability: the effect of stride frequency, stride length, and walking speed on local dynamic stability and margins of stability. *PLoS One*, 8(12), e82842.

Hamill, J., Bates, B., & Knutzen, K. (1984). Ground reaction force symmetry during walking and running. *Res Q Exerc Sport*, 55(3), 289–93.

Hamill, J., Bates, B., Knutzen, K., & Sawhill, J. (1983). Variations in ground reaction force parameters at different running speeds. *Hum Mov Sci*, 2, 47–56.

Handford, M. L. & Srinivasan, M. (2018). Energy-optimal human walking with feedback-controlled robotic prostheses: A computational study. *IEEE T Neur Sys Reh*, 26(9), 1773–82.

Hannah, R. E., Morrison, J. B., & Chapman, A. E. (1984). Kinematic symmetry of the lower limbs. *Arch Phys Med Rehabil*, 65(4), 155–8.

Harris, C. M. & Wolpert, D. M. (1998). Signal-dependent noise determines motor planning. *Nature*, 394(6695), 780–4.

Herzog, W., Nigg, B. M., Read, L. J., & Olsson, E. (1989). Asymmetries in ground reaction force patterns in normal human gait. *Med Sci Sports Exerc*, 21(1), 110–4.

Hill, A. V. (1938). The heat of shortening and the dynamic constants of muscle. *Proc R Soc Lond B Biol Sci*, 126(843), 136–95.

Hill, A. V. (1958). The relation between force developed and energy liberated in an isometric twitch. *Proc R Soc Lond B Biol Sci*, 149(934), 58–62.

Hodges, P. W. & Tucker, K. (2011). Moving differently in pain: a new theory to explain the adaptation to pain. *Pain*, 152(3 Suppl), S90–8.

Högberg, P. (1952). How do stride length and stride frequency influence the energy-output during running? *Arbeitsphysiologie*, 14(6), 437–41.

Holt, K. G., Hamill, J., & Andres, R. O. (1991). Predicting the minimal energy costs of human walking. *Med Sci Sports Exerc*, 23(4), 491–8.

Holt, K. G., Jeng, S. F., Ratcliffe, R., & Hamill, J. (1995). Energetic cost and stability during human walking at the preferred stride frequency. *J Mot Behav*, 27(2), 164–78.

Hoogkamer, W., Bruijn, S. M., & Duysens, J. (2014). Stride length asymmetry in split-belt locomotion. *Gait Posture*, 39(1), 652–4.

Houdijk, H., Pollmann, E., Groenewold, M., Wiggerts, H., & Polomski, W. (2009). The energy cost for the step-to-step transition in amputee walking. *Gait Posture*, 30(1), 35–40.

Hreljac, A. (1993). Preferred and energetically optimal gait transition speeds in human locomotion. *Med Sci Sports Exerc*, 25(10), 1158–62.

Hsiao-Wecksler, E. T., Polk, J. D., Rosengren, K. S., Sosnoff, J. J., & Hong, S. (2010). A review of new analytic techniques for quantifying symmetry in locomotion. *Symmetry*, 2(2), 1135–55.

Huang, T. W., Shorter, K. A., Adamczyk, P. G., & Kuo, A. D. (2015). Mechanical and energetic consequences of reduced ankle plantar-flexion in human walking. *J Exp Biol*, 218(22), 3541–50.

Hunter, L. C., Hendrix, E. C., & Dean, J. C. (2010). The cost of walking downhill: is the preferred gait energetically optimal? *J Biomech*, 43(10), 1910–5.

Isakov, E., Keren, O., & Benjuya, N. (2000). Trans-tibial amputee gait: time-distance parameters and emg activity. *Prosthet Orthot Int*, 24(3), 216–20.

Kang, H. G. & Dingwell, J. B. (2008). Effects of walking speed, strength and range of motion on gait stability in healthy older adults. *J Biomech*, 41(14), 2899–905.

Kiehn, O. (2016). Decoding the organization of spinal circuits that control locomotion. *Nat Rev Neurosci*, 17(4), 224–38.

Kodesh, E., Kafri, M., Dar, G., & Dickstein, R. (2012). Walking speed, unilateral leg loading, and step symmetry in young adults. *Gait Posture*, 35(1), 66–9.

Kuo, A. D. (1999). Stabilization of lateral motion in passive dynamic walking. *Int J Robot Res*, 18(9), 917–30.

Kuo, A. D. (2001). A simple model of bipedal walking predicts the preferred speed-step length relationship. *J Biomech Eng-T ASME*, 123(3), 264–9.

Kuo, A. D. (2002). Energetics of actively powered locomotion using the simplest walking model. *J Biomech Eng-T ASME*, 124(1), 113–20.

Kuo, A. D. (2007). The six determinants of gait and the inverted pendulum analogy: A dynamic walking perspective. *Hum Mov Sci*, 26(4), 617–56.

Kuo, A. D. & Donelan, J. M. (2010). Dynamic principles of gait and their clinical implications. *Phys Ther*, 90(2), 157–74.

Kuo, A. D., Donelan, J. M., & Ruina, A. (2005). Energetic consequences of walking like an inverted pendulum: step-to-step transitions. *Exerc Sport Sci Rev*, 33(2), 88–97.

Lai, K. A., Lin, C. J., Jou, I. M., & Su, F. C. (2001). Gait analysis after total hip arthroplasty with leg-length equalization in women with unilateral congenital complete dislocation of the hip—comparison with untreated patients. *J Orthop Res*, 19(6), 1147–52.

Lisberger, S. G. & Thach, W. T. (2013). *The cerebellum*, (pp. 960–981). McGraw-Hill: New York, 5th edition.

Lockhart, D. B. & Ting, L. H. (2007). Optimal sensorimotor transformations for balance. *Nat Neurosci*, 10(10), 1329–36.

Malone, L. A., Bastian, A. J., & Torres-Oviedo, G. (2012). How does the motor system correct for errors in time and space during locomotor adaptation? *J Neurophysiol*, 108(2), 672–83.

Margaria, R., Cerretelli, P., Aghemo, P., & Sassi, G. (1963). Energy cost of running. *J Appl Physiol*, 18(2), 367–70.

Marsh, R. L., Ellerby, D. J., Carr, J. A., Henry, H. T., & Buchanan, C. I. (2004). Partitioning the energetics of walking and running: swinging the limbs is expensive. *Science*, 303(5654), 80–3.

Martin, P. E., Royer, T. D., & Mattes, S. J. (1997). Effect of symmetrical and asymmetrical lower extremity inertia changes on walking economy. *Med Sci Sport Exer*, 29(5), 86.

Martin, T. A., Keating, J. G., Goodkin, H. P., Bastian, A. J., & Thach, W. T. (1996). Throwing while looking through prisms. ii. specificity and storage of multiple gaze-throw calibrations. *Brain*, 119(4), 1199–211.

Mattes, S. J., Martin, P. E., & Royer, T. D. (2000). Walking symmetry and energy cost in persons with unilateral transtibial amputations: Matching prosthetic and intact limb inertial properties. *Arch Phys Med Rehabil*, 81(5), 561–8.

Matthis, J. S., Barton, S. L., & Fajen, B. R. (2017). The critical phase for visual control of human walking over complex terrain. *Proc Natl Acad Sci USA*, 114(32), E6720–E6729.

McCrea, D. A. & Rybak, I. A. (2008). Organization of mammalian locomotor rhythm and pattern generation. *Brain Res Rev*, 57(1), 134–46.

McGeer, T. (1990). Passive dynamic walking. *Int J Robot Res*, 9(2), 62–82.

McLean, D. L., Masino, M. A., Koh, I. Y., Lindquist, W. B., & Fetcho, J. R. (2008). Continuous shifts in the active set of spinal interneurons during changes in locomotor speed. *Nat Neurosci*, 11(12), 1419–29.

Mero, A., Komi, P. V., & Gregor, R. J. (1992). Biomechanics of sprint running. a review. *Sports Med*, 13(6), 376–92.

Miller, R. H., Umberger, B. R., Hamill, J., & Caldwell, G. E. (2012). Evaluation of the minimum energy hypothesis and other potential optimality criteria for human running. *Proc Biol Sci*, 279(1733), 1498–505.

Minetti, A. E. (1998). The biomechanics of skipping gaits: a third locomotion paradigm? *Proc Biol Sci*, 265(1402), 1227–35.

Minetti, A. E., Ardigo, L. P., & Saibene, F. (1994). The transition between walking and running in humans: metabolic and mechanical aspects at different gradients. *Acta Physiol Scand*, 150(3), 315–23.

Mochon, S. & McMahon, T. A. (1980). Ballistic walking. *J Biomech*, 13(1), 49–57.

Monsch, E. D., Franz, C. O., & Dean, J. C. (2012). The effects of gait strategy on metabolic rate and indicators of stability during downhill walking. *J Biomech*, 45(11), 1928–33.

Morton, S. M. & Bastian, A. J. (2006). Cerebellar contributions to locomotor adaptations during splitbelt treadmill walking. *J Neurosci*, 26(36), 9107–16.

Neptune, R. R., Zajac, F. E., & Kautz, S. A. (2004). Muscle mechanical work requirements during normal walking: the energetic cost of raising the body's center-of-mass is significant. *J Biomech*, 37(6), 817–25.

Nielsen, J. B. (2003). How we walk: central control of muscle activity during human walking. *Neuroscientist*, 9(3), 195–204.

Nubar, Y. & Contini, R. (1961). A minimal principle in biomechanics. *Bull Math Biophys*, 23(4), 377–91.

Pagliara, R., Snaterse, M., & Donelan, J. M. (2014). Fast and slow processes underlie the selection of both step frequency and walking speed. *J Exp Biol*, 217(16), 2939–46.

Park, S. & Finley, J. M. (2017). Characterizing dynamic balance during adaptive locomotor learning. In *39th Annual International Conference of the IEEE Engineering in Medicine and Biology Society (EMBC)* (pp. 50–3).

Passmore, R. & Durnin, J. V. (1955). Human energy expenditure. *Physiol Rev*, 35(4), 801–40.

Patterson, K. K., Parafianowicz, I., Danells, C. J., Closson, V., Verrier, M. C., Staines, W. R., Black, S. E., & McIlroy, W. E. (2008). Gait asymmetry in community-ambulating stroke survivors. *Arch Phys Med Rehab*, 89(2), 304–10.

Pearson, K. G. (2004). Generating the walking gait: role of sensory feedback. *Prog Brain Res*, 143, 123–9.

Perry, J. & Burnfield, J. M. (2010). *Gait Analysis: Normal and Pathological Function.* Thorofare, NJ: SLACK Inc.

Petersen, N., Christensen, L. O., & Nielsen, J. (1998). The effect of transcranial magnetic stimulation on the soleus h reflex during human walking. *J Physiol*, 513(2), 599–610.

Petersen, N., Morita, H., & Nielsen, J. (1999). Modulation of reciprocal inhibition between ankle extensors and flexors during walking in man. *J Physiol*, 520(2), 605–19.

Petersen, N. T., Butler, J. E., Marchand-Pauvert, V., Fisher, R., Ledebt, A., Pyndt, H. S., Hansen, N. L., & Nielsen, J. B. (2001). Suppression of emg activity by transcranial magnetic stimulation in human subjects during walking. *J Physiol*, 537(2), 651–6.

Polk, J. D., Stumpf, R. M., & Rosengren, K. S. (2017). Limb dominance, foot orientation and functional asymmetry during walking gait. *Gait Posture*, 52, 140–146.

Prokop, T., Berger, W., Zijlstra, W., & Dietz, V. (1995). Adaptational and learning processes during human split-belt locomotion: interaction between central mechanisms and afferent input. *Exp Brain Res*, 106(3), 449–56.

Ralston, H. J. (1958). Energy-speed relation and optimal speed during level walking. *Int Z Angew Physiol*, 17(4), 277–83.

Rankin, B. L., Buffo, S. K., & Dean, J. C. (2014). A neuromechanical strategy for mediolateral foot placement in walking humans. *J Neurophysiol*, 112(2), 374–83.

Rathkey, J. K. & Wall-Scheffler, C. M. (2017). People choose to run at their optimal speed. *Am J Phys Anthropol*, 163(1), 85–93.

Reisman, D. S., Bastian, A. J., & Morton, S. M. (2010). Neurophysiologic and rehabilitation insights from the split-belt and other locomotor adaptation paradigms. *Phys Ther*, 90(2), 187–95.

Reisman, D. S., Block, H. J., & Bastian, A. J. (2005). Interlimb coordination during locomotion: what can be adapted and stored? *J Neurophysiol*, 94(4), 2403–15.

Roemmich, R. T. & Bastian, A. J. (2018). Closing the loop: From motor neuroscience to neurorehabilitation. *Annu Rev Neurosci*, 41(1), 415–29.

Roemmich, R. T., Leech, K. A., Gonzalez, A. J., & Bastian, A. J. (2019). Trading symmetry for energy cost during walking in healthy adults and persons poststroke. *Neurorehab Neural Re*, 33(8), 602–13.

Roemmich, R. T., Long, A. W., & Bastian, A. J. (2016). Seeing the errors you feel enhances locomotor performance but not learning. *Curr Biol*, 26(20), 2707–16.

Roerdink, M. & Beek, P. J. (2011). Understanding inconsistent step-length asymmetries across hemiplegic stroke patients: Impairments and compensatory gait. *Neurorehab Neural Re*, 25(3), 253–8.

Roerdink, M., Lamoth, C. J., Kwakkel, G., van Wieringen, P. C., & Beek, P. J. (2007). Gait coordination after stroke: Benefits of acoustically paced treadmill walking. *Phys Ther*, 87(8), 1009–22.

Roerdink, M., Roeles, S., van der Pas, S. C., Bosboom, O., & Beek, P. J. (2012). Evaluating asymmetry in prosthetic gait with step-length asymmetry alone is flawed. *Gait Posture*, 35(3), 446–51.

Ruina, A., Bertram, J. E., & Srinivasan, M. (2005). A collisional model of the energetic cost of support work qualitatively explains leg sequencing in walking and galloping, pseudo-elastic leg behavior in running and the walk-to-run transition. *J Theor Biol*, 237(2), 170–92.

Russell, D. M. & Haworth, J. L. (2014). Walking at the preferred stride frequency maximizes local dynamic stability of knee motion. *J Biomech*, 47(1), 102–8.

Sadeghi, H., Allard, P., Prince, F., & Labelle, H. (2000). Symmetry and limb dominance in able-bodied gait: a review. *Gait Posture*, 12(1), 34–45.

Sánchez, N. & Finley, J. M. (2018). Individual differences in locomotor function predict the capacity to reduce asymmetry and modify the energetic cost of walking poststroke. *Neurorehab Neural Re*, 32(8), 701–13.

Sánchez, N., Park, S., & Finley, J. M. (2017). Evidence of energetic optimization during adaptation differs for metabolic, mechanical, and perceptual estimates of energetic cost. *Sci Rep*, 7(1), 7682.

Sánchez, N., Simha, S. N., Donelan, J. M., & Finley, J. M. (2019). Taking adavantage of external mechanical work to reduce metabolic cost: the mechanics and energetics of split-belt treadmill walking. *J Physiol*, 597(15), 4053–68.

Sanderson, D. J. & Martin, P. E. (1997). Lower extremity kinematic and kinetic adaptations in unilateral below-knee amputees during walking. *Gait Posture*, 6(2), 126–36.

Sasaki, K., Neptune, R. R., & Kautz, S. A. (2009). The relationships between muscle, external, internal and joint mechanical work during normal walking. *J Exp Biol*, 212(5), 738–44.

Saunders, J. B., Inman, V. T., & Eberhart, H. D. (1953). The major determinants in normal and pathological gait. *J Bone Joint Surg Am*, 35-A(3), 543–58.

Sawicki, G. S. & Ferris, D. P. (2009). Powered ankle exoskeletons reveal the metabolic cost of plantar flexor mechanical work during walking with longer steps at constant step frequency. *J Exp Biol*, 212(1), 21–31.

Sawicki, G. S., Lewis, C. L., & Ferris, D. P. (2009). It pays to have a spring in your step. *Exerc Sport Sci Rev*, 37(3), 130–8.

Scott, S. H. (2004). Optimal feedback control and the neural basis of volitional motor control. *Nat Rev Neurosci*, 5(7), 532–46.

Seeley, M. K., Umberger, B. R., Clasey, J. L., & Shapiro, R. (2010). The relation between mild leg-length inequality and able-bodied gait asymmetry. *J Sports Sci Med*, 9(4), 572–9.

Seeley, M. K., Umberger, B. R., & Shapiro, R. (2008). A test of the functional asymmetry hypothesis in walking. *Gait Posture*, 28(1), 24–8.

Selgrade, B. P., Thajchayapong, M., Lee, G. E., Toney, M. E., & Chang, Y. H. (2017a). Changes in mechanical work during neural adaptation to asymmetric locomotion. *J Exp Biol*, 220(16), 2993–3000.

Selgrade, B. P., Toney, M. E., & Chang, Y. H. (2017b). Two biomechanical strategies for locomotor adaptation to split-belt treadmill walking in subjects with and without transtibial amputation. *J Biomech*, 53(28), 136–43.

Selinger, J. C., O'Connor, S. M., Wong, J. D., & Donelan, J. M. (2015). Humans can continuously optimize energetic cost during walking. *Curr Biol*, 25(18), 2452–6.

Seminati, E., Nardello, F., Zamparo, P., Ardigo, L. P., Faccioli, N., & Minetti, A. E. (2013). Anatomically asymmetrical runners move more asymmetrically at the same metabolic cost. *PLoS One*, 8(9), e74134.

Shadmehr, R., Huang, H. J., & Ahmed, A. A. (2016). A representation of effort in decision-making and motor control. *Curr Biol*, 26(14), 1929–34.

Sinkjær, T., Andersen, J. B., Ladouceur, M., Christensen, L. O., & Nielsen, J. B. (2000). Major role for sensory feedback in soleus emg activity in the stance phase of walking in man. *J Physiol*, 523(3), 817–27.

Snaterse, M., Ton, R., Kuo, A. D., & Donelan, J. M. (2011). Distinct fast and slow processes contribute to the selection of preferred step frequency during human walking. *J Appl Physiol*, 110(6), 1682–90.

Snyder, K. L. & Farley, C. T. (2011). Energetically optimal stride frequency in running: the effects of incline and decline. *J Exp Biol*, 214(12), 2089–95.

Snyder, K. L., Snaterse, M., & Donelan, J. M. (2012). Running perturbations reveal general strategies for step frequency selection. *J Appl Physiol*, 112(8), 1239–47.

Soo, C. H. & Donelan, J. M. (2012). Coordination of push-off and collision determine the mechanical work of step-to-step transitions when isolated from human walking. *Gait Posture*, 35(2), 292–7.

Sparrow, W. A. & Newell, K. M. (1998). Metabolic energy expenditure and the regulation of movement economy. *Psychon B Rev*, 5(2), 173–96.

Srinivasan, M. (2011). Fifteen observations on the structure of energy-minimizing gaits in many simple biped models. *J R Soc Interface*, 8(54), 74–98.

Srinivasan, M. & Ruina, A. (2006). Computer optimization of a minimal biped model discovers walking and running. *Nature*, 439(7072), 72–5.

Stenum, J., Bruijn, S. M., & Jensen, B. R. (2014). The effect of walking speed on local dynamic stability is sensitive to calculation methods. *J Biomech*, 47(15), 3776–9.

Stenum, J. & Choi, J. T. (2016). Neuromuscular effort predicts walk-run transition speed in normal and adapted human gaits. *J Exp Biol*, 219(18), 2809–13.

Stenum, J. & Choi, J. T. (2017). Metabolic and mechanical demands of symmetrical and asymmetrical walking on a split-belt treadmill. In *Proceedings of the 41st Annual Meeting of the American Society of Biomechanics, Boulder, CO, USA, August 8th - August 11th, 2017*.

Steudel-Numbers, K. L. & Wall-Scheffler, C. M. (2009). Optimal running speed and the evolution of hominin hunting strategies. *J Hum Evol*, 56(4), 355–60.

Stoquart, G., Detrembleur, C., & Lejeune, T. (2012). The reasons why stroke patients expend so much energy to walk slowly. *Gait Posture*, 36(3), 409–13.

Strike, S. C. & Taylor, M. J. (2009). The temporal-spatial and ground reaction impulses of turning gait: is turning symmetrical? *Gait Posture*, 29(4), 597–602.

Talpalar, A. E., Bouvier, J., Borgius, L., Fortin, G., Pierani, A., & Kiehn, O. (2013). Dual-mode operation of neuronal networks involved in left-right alternation. *Nature*, 500(7460), 85–8.

Thorstensson, A. & Roberthson, H. (1987). Adaptations to changing speed in human locomotion: speed of transition between walking and running. *Acta Physiol Scand*, 131(2), 211–4.

Todorov, E. (2004). Optimality principles in sensorimotor control. *Nat Neurosci*, 7(9), 907–15.

Todorov, E. & Jordan, M. I. (2002). Optimal feedback control as a theory of motor coordination. *Nat Neurosci*, 5(11), 1226–35.

Umberger, B. R. (2010). Stance and swing phase costs in human walking. *J R Soc Interface*, 7(50), 1329–40.

Umberger, B. R. & Martin, P. E. (2007). Mechanical power and efficiency of level walking with different stride rates. *J Exp Biol*, 210(18), 3255–65.

van Ingen Schenau, G. (1980). Some fundamental aspects of the biomechanics of overground versus treadmill locomotion. *Med Sci Sports Exerc*, 12(4), 257–61.

Wang, Y. & Watanabe, K. (2012). Limb dominance related to the variability and symmetry of the vertical ground reaction force and center of pressure. *J Appl Biomech*, 28(4), 473–8.

Waters, R. L. & Mulroy, S. (1999). The energy expenditure of normal and pathologic gait. *Gait Posture*, 9(3), 207–31.

Wedge, R. (2019). *Metabolic cost and stability of locomotion in people with lower limb amputation*. PhD thesis, University of Massachusetts Amherst.

Whitall, J. & Caldwell, G. E. (1992). Coordination of symmetrical and asymmetrical human gait. *J Mot Behav*, 24(4), 339–53.

Whittlesey, S. N., van Emmerik, R. E., & Hamill, J. (2000). The swing phase of human walking is not a passive movement. *Motor Control*, 4(3), 273–92.

Winter, D. A. (1990). *Biomechanics and motor control of human movement.* Hoboken, NJ: Wiley.

Wolpert, D. M., Pearson, K. G., & Ghez, C. P. (2013). *The organization and planning of movement*, (pp. 741–767). McGraw-Hill: New York, 5th edition.

Wong, J. D., O'Connor, S. M., Selinger, J. C., & Donelan, J. M. (2017). Contribution of blood oxygen and carbon dioxide sensing to the energetic optimization of human walking. *J Neurophysiol*, 118(2), 1425–33.

Yanagihara, D. & Kondo, I. (1996). Nitric oxide plays a key role in adaptive control of locomotion in cat. *Proc Natl Acad Sci USA*, 93(23), 13292–7.

Yang, J. F., Lamont, E. V., & Pang, M. Y. (2005). Split-belt treadmill stepping in infants suggests autonomous pattern generators for the left and right leg in humans. *J Neurosci*, 25(29), 6869–76.

Zarrugh, M. Y. & Radcliffe, C. W. (1978). Predicting metabolic cost of level walking. *Eur J Appl Physiol Occup Physiol*, 38(3), 215–23.

Zatsiorky, V. M., Werner, S. L., & Kaimin, M. A. (1994). Basic kinematics of walking. step length and step frequency. a review. *J Sports Med Phys Fitness*, 34(2), 109–34.

Zelik, K. E. & Kuo, A. D. (2010). Human walking isn't all hard work: evidence of soft tissue contributions to energy dissipation and return. *J Exp Biol*, 213(24), 4257–64.